Comparative study of steam injection modes for a proposed biomass-driven cogeneration cycle: Performance improvement and CO2 emission reduction

(Article begins on next page)

21 December 2024

Comparative study of steam injection modes for a proposed biomass-driven cogeneration cycle: Performance improvement and CO₂ emission reduction

Simin Anvari[a], Andrzej Szlęk[a], Alessia Arteconi[b], Umberto Desideri[c,*], Marc A. Rosen[d]

[a]Silesian University of Technology, Institute of Thermal Technology, Konarskiego 22A Gliwice, Poland

[b]Department of Mechanical Engineering, KU Leuven, B-3000 Leuven, Belgium

[c,*]Department of Energy, Systems, Territory and Constructions Engineering, University of Pisa, Italy

[d]Faculty of Engineering and Applied Science, University of Ontario Institute of Technology, 2000 Simcoe Street North, Oshawa, Ontario, L1G 0C5, Canada

Abstract

Biomass fuel energy can be utilized in cogeneration cycles through the gasification process. This reduces pollution and increases the efficiency of conventional cycles, and makes use of renewable energy instead of fossil fuels. In this paper, in order to generate both electricity and cooling, a cogeneration system has been proposed using biomass fuels. Then, various ways of injecting steam into each proposed cycle are proposed in order to improve its efficiency and performance. The following cycles are suggested and modeled: CHP with the steam injection into the combustion chamber, CHP with the steam injection into gasifier, and CHP with the steam injection into the gasifier and combustion chamber simultaneously. All proposed cycles are initially analyzed from energy, exergy, exergo-economic, and environmental perspectives. Following analyses of the cycles, results are compared and discussed to select the cycle with the best balance in terms of thermodynamics, economics and pollutant emissions. Then, a parametric study is discussed in which, along with determining the influence of changing an important thermodynamic parameter on cycle performance, the simultaneous influence of two parameters

---
* Corresponding author: umberto.desideri@unipi.it

is calculated and verified. The results show that the steam-injected gasifier cycle is about 5.43% more efficient than the steam-injected combustion chamber cycle, and its carbon dioxide emissions are about 5.2% lower. Also, the cycle by simultaneous injection of steam into both the gasifier and combustion chamber offers the highest efficiency and pollution reduction. Additionally, by simultaneously increasing the mass flow rates of steam injection into the proposed system with simultaneous steam injection into both the gasifier and combustion chamber, the exergy efficiency and costs are increased by 11.2% and 3.5% respectively, and CO_2 emission are reduced by 12.5%.

Keywords: Biomass, gasification, exergy, exergoeconomic, steam injection, gas turbine, CO_2 emissions

NOMENCLATURE

c	exergy unit cost ($/GJ)	Con	condenser
$\dot{E}$	exergy (kJ)	CFW	close feed water
$\dot{E}_D$	exergy destruction rate (MW)	D	destruction
h	specific enthalpy (kJ/kg)	e	exit condition
$\dot{m}$	mass flow rate (kg/s)	Eva	evaporator
P	pressure (bar)	g	gas
PEC	equipment purchase cost ($)	Gen	generator
r_{AC}	compressor pressure ratio	GT	gas turbine
T	temperature (K)	HRSG	heat recovery steam generator
$\dot{W}$	power output (kW)	HPST	high pressure steam turbine
$\dot{Z}$	rate of capital cost ($/h)	i	inlet condition
Greek Symbols		k	component
Δ	difference	LPST	low pressure steam turbine
ε	exergy efficiency	OFW	open feed water
η	energy efficiency	p	product
Subscripts		PP	pinch point
ABS	absorber	SHX	solution heat exchanger
AC	air compressor	tot	total
CC	combustion chamber	0	reference state for exergy

1 Introduction

Concerns over increasing global energy demand, economic growth and environmental pollutant emissions have driven up fossil fuel prices [1]. Using renewable energy can diversify the primary energy portfolio and provide an alternative energy sources to the fossil fuels. Biomass energy is a kind of renewables which is derived from living or dead organisms (such as plants and animals). Biomass is used as an alternative fuel because, unlike fossil fuels, it is reproduced in a time frame of the same order of magnitude as its utilization [2]. Different power generation cycles can be set up to use the biomass energy produced during gasification processes, namely internal combustion engines, steam power plants, gas turbines and combined cycles and ORCs to cite the most studied and applied. In this paper the attention will be focused on power generation systems based on gas turbines.

CHP (combined heat and power), or CCHP cycle (combined heat, power, and cooling) production can be developed from power generation cycles, such as Brayton cycles, to recover the heat rejected by the cycle through other thermodynamic cycles, such as steam turbine or refrigeration systems [3]. Due to waste heat recovery, CHP/CCHP cycles are more efficient, produce fewer pollutants, and are more economically viable compared to power cycles. Performing exergy and exergoeconomic analyses on CHP/CCHP systems can be effective for improving their efficiencies [4]. Exergy and exergoeconomic analyses reveal the components of thermodynamic cycle with the highest rates of the exergy destruction and highest associated costs, while optimization methods can be used to enhance system performance and reduce losses.

Researchers have often tried to determine how to make CHP/CCHP cycles more efficient and more effective. Steam injection in combustion chamber is one method proposed in Brayton cycles. The Cheng cycle is an example of these cycles [5]. With this cycle, the Brayton cycle's waste heat is employed to heat the water and then the generated steam at a heat recovery boiler is

3

transferred to combustion chamber using. The cycle becomes more efficient and NO_x emissions are reduced as well. Furthermore, biomass gasification processes that inject steam into the gasifier can enhancement the efficiency of the gasification process and reduce pollution as well [6]. An overview of some of the articles in these fields is provided below.

In a biomass gasification simulation, Habibollahzade et al. [6] considered a variety of feedstocks in different mediums including steam, air, CO_2, oxygen, oxygen-enriched air, and a combination of these. They performed a parametric analysis to consider how the main parameters affected the gasifier's performance. Furthermore, a tri-objective optimization was used to optimize the system. The researchers found that biomass gasification using CO_2 and steam provides higher energy efficiencies, at about 93.7% and 94.7%, respectively.

Using both the first and second laws of thermodynamic, Fagbenle et al. [7] modeled a gas turbine system that burns biogas and uses steam injection. It was reported that, by introducing steam into the combustion chamber, a significant share of the exergy destruction rate in it was reduced, which accounted for 79% of the total exergy destruction rate in total. Barreto et al. [8] studied an advanced exergy and exergo-economic study for a power generation cycle with a steam injection to the combustion chamber and gas turbine components of investigated system. Authors reported that their methodology can be applied to all steam injected power plants that have air cooling and compression refrigeration, and all combined-cycle power plants. As a result of applying their methodologies to the mentioned cycles, their performances improved economically and environmentally.

Several combinations of gas turbine power enhancement technologies have been compared by Shukla and Singh [9]: a gas turbine cycle with the steam injection, a gas turbine cycle with the

inlet air cooling, and a gas turbine with both inlet air cooling and steam injection. They reported that, with steam injection only, the power production increases by 7.2%, while with the steam injection and an air cooling the power production increases about 9.5%.

A CHP plant was retrofitted by Ziółkowski et al. [10] considering two approaches: injecting steam into gas turbine and combined steam-injected gas turbines. Using energy and exergy studies of these cycles, the authors reported that modernizing the combined steam-injected gas turbine improves the electric and system efficiencies compared to steam-injected gas turbines alone. The steam injection also reduces emissions of NO_x.

Moradi et al. [11] developed the combination of a steam-injected micro turbine using biomass fuel and an Organic Rankine system. For steam production for a gasification process as well as for the steam injection for the micro turbine, a heat recovery steam generator was used. They reported that, for a syngas-fueled integrated system, 127.6 kW_{el} was produced with a 23.6% electrical efficiency by injecting 25 g/s of the steam to the combustion chamber.

A validated thermoenvironmental model was used by Kayadelen and Ust [12] to evaluate a simple, an intercooled, a steam injected Brayton cycle and a steam injected intercooled gas turbine cycle from the perspectives of the pollutant emissions, economics, efficiency, and network output. They also investigated the optimal parameters for the cycles and found that, as a consequence of injected steam, in the simple gas turbine system and an intercooled gas turbine cycle, the specific fuel consumption values were reduced by 6.7% and 4.5%, respectively. Furthermore, the intercooled steam injected to gas turbine cycles and the steam injected into gas turbine system emits less pollution than the simple cycle. Renzi et al. [13] proposed the use of a steam injection micro gas turbine in conjunction with a gasifier. A comparison was made

between the system that burns syngas and one that burns natural gas. To study the impact of injected steam on emissions, the researchers created a one-dimensional combustion chamber model. The analysis results indicated that the rate of fuel mass flow increases with rising steam mass flow rates when the gas turbine output temperature is defined at its design point. In addition, a higher rate of steam mass flow (56 g/s) led to both a higher net power generation and a higher electrical efficiency for an investigated system. Camporeale et al. [14] conducted a technical-economic analysis of the organic Rankine cycles that use biomass as an external fuel source. The thermodynamic study determined that the output electrical power as well as the overall efficiency of a 1.3 MW biofuel externally fired gas turbine increased by 50% while the produced thermal power decreased by 74%. Furthermore, they found that a combination of biofuel externally fired a gas turbines and an organic Rankine cycle maximizes profitability over a simple biofuel externally fired gas turbine unless there is a high thermal energy demand.

Pio et al. [15] considered the effects of superheated steam injection on mixture of producer gas and gasification efficiency in a pilot-scale experiment using an auto thermal process at during direct air gasification of biomass to generate a bubbling fluidized bed. The results indicated that, for high-density biomass air gasification, steam injection's potential for improving the producer gas quality is high. However, for the biomass by the low density, it has been restricted to adjusting the H_2/CO mole ratio and has limited potential. Using a micro gas turbine plant fed with methane fuel enhanced with hydrogen and a humidifying of the system, Reale and Sannino [16] examined the performance of the plant from energetic and environmental perspectives. A major outcome reported in this research is that injecting hydrogen up to 30% by volume into the combustor of the suggested micro gas turbine achieves regular and safe combustion mainly due to steam injection up to 125% of fuel flow. Xiao et al. [17] suggested a solar microgas turbine by

steam injection to the gas turbine and an organic Rankine cycle. Addition of steam injection and an organic Rankine cycle can increase the output power around 8.3 kW and 30.4 kW respectively, which results in an addition by 37.7% in net power production and an improvement in its efficiency and flexibility of the cycle.

Regarding the studies reviewed, it can be concluded that the steam injection into the gas turbine cycles can enhance cycle efficiency while simultaneously reducing pollutants. Furthermore, the addition of steam to gasification processes also is effective in reducing pollutant production and improving the gasification process. Thus, in order to consider the positive effects of steam injection into these components on the performance of thermodynamic systems, it is interesting to be able to analysis and compare their results in a cogeneration system. This article proposes a biomass driven CHP cycle that uses gasification. The proposed CHP system consists of a combination of a Brayton cycle, a two-pressure steam turbine cycle, and the (Li-Br) absorption refrigeration system to generate power and cooling. With this cycle, biomass is used instead of fossil fuels and the Brayton cycle's waste heat is used recycled to steam turbine and refrigeration cycles, leading to a CHP cycle that has a higher efficiency and lower pollution emissions. For the proposed CHP system, different modes of steam injection are studied and modeled. The four considered cycles are: basic CHP cycle, CHP cycle with a steam injection to the combustion chamber, CHP cycle with the steam injection to gasifier, and CHP cycle with simultaneous steam injection to gasifier and combustion chamber. By considering this the most credible comparative study is one that incorporates energy, exergy, economic and environmental factors in modeling a combined system. Proposed cycles are subject to comprehensive analyses from energy, exergy, exergoeconomic, and environmental viewpoints. Results are compared, and a cycle with lower carbon dioxide emissions and higher efficiency which is also justified from an economic

viewpoint is selected as a cycle with better performance. In next step, the parametric studies are investigated to consider the impact of either one critical thermodynamics parameter, or the simultaneous effect of two critical thermodynamic parameters, on the general performance of selected CHP system. It is well known that parametric studies are important since they can show how thermodynamic parameters affect system performance. The results of these studies can be used to improve the system's performance. The parameters considered are exergy efficiency, cycle costs including investment costs, and costs of exergy destruction rate, and the amount of CO_2 emissions.

2 Description of proposed biomass-driven CHP cycles for electricity and cooling

Fig. 1 shows the basic CHP cycle considered in this paper. This CHP cycle combines a Brayton cycle, a two-pressure steam turbine cycle and (Li-Br) absorption refrigeration cycle to produce electricity and cooling. The CHP cycle uses biomass as the input fuel; that fuel provides the cycle's energy through the gasification process. In general, the cycle operates as follows. Biomass fuel at point 3 along with ambient air is fed to gasifier where gasification happens, and the produced gases at 850 °C (point 5) enter the combustion chamber. The gases from the gasification process react with compressed air from point 2 to hot gases production in combustion chamber. After leaving the combustion chamber at point 6, the hot gases expand to generate electrical power in the gas turbine component. The hot gases at point 7 leave the Brayton cycle and are recycled by heat recovery steam generator 1 to heat the passing steam. Using heat from hot gases, steam reaches the superheated steam state and enters the high pressure steam turbine in point a13. The expanded steam at point a16 enters heat recovery steam generator 2, which receives heat from the hot gases circulating in this component, and then the superheated steam at point a17 enters the low pressure steam turbine, which generates electrical

power. After leaving heat recovery steam generator 2, the hot gases enter generator at point 9 and are used to provide cooling via the Li-Br absorption refrigeration cycle. Thus, biomass energy is used to electricity and cooling generation in the proposed basic CHP cycle.

As mentioned previously, this paper's main purpose is to propose a CHP cycle that is optimally effective from a thermodynamic, economic, and environmental standpoint. Injecting steam into combustion chamber can improve the performance of Brayton cycles [18]. Furthermore, injecting steam into the gasifier as an agent can also improve the gasification process and ultimately improve performance of the power cycle [19]. Gasification involves partial thermal decomposition, which results in production of gases containing mostly CO and hydrogen. However, in combustion chamber, due to reaction of the gasification gases with oxygen provided by the air compressor, the combustion process is completed and the gasification plant converts CO and hydrogen to carbon dioxide and water. In this respect, steam injection to the combustion chamber as well as gasifier can be regarded as an important parameter in studying power generation cycles. Therefore, in this article, we examine and compare different types of steam injection into the proposed basic CHP cycle. This is done to achieve the most efficient performance of proposed basic CHP cycle.

The different types of steam injection that are considered in the basic CHP cycle follow:

1- Injecting steam into the combustion chamber: In this case, which is called the CHP cycle with the steam injection into combustion chamber or second proposed CHP cycle, steam enters combustion chamber at point 5 and reacts with gases generated by the gasification process and compressed inlet air from point 2. A schematic of this cycle is drawn in Fig. 2a.

2- Injecting steam into the gasifier: In this case, which is called the CHP cycle with steam injection into the gasifier or third proposed CHP cycle, steam enters the gasifier and reacts with the biomass fuel and incoming air. A schematic of this cycle is drawn in Fig. 2b.

3- Injecting steam into the gasifier and the combustion chamber: In this case, which is called the CHP cycle with the steam injection to the gasifier and the combustion chamber or fourth proposed CHP cycle, steam enters both the gasifier and the combustion chamber. The schematic of this cycle is drawn in Fig. 2c.

All four CHP cycles are examined in this paper from thermodynamic, exergoeconomic, and environmental perspectives. To determine the relative effects of the three steam injected CHPs, they are compared with each other and with the basic CHP cycle. Then, the most suitable CHP cycle is selected for further examination. EES engineering software is used to model and analyze the proposed CHP cycles. The model assumptions for the gasification process, Brayton cycle and Li-Br absorption refrigeration cycle follow those in references [20, 21, 22]. The assumptions applied in the steam turbine cycle modeling for the proposed CHP cycle are mentioned in Table 1.

Table 1 Data input for steam turbine cycle modeling and the injection steam modes for the proposed biomass-driven CHP cycle

Parameter	Assumed value
Heat recovery steam generators 1 and 2 pinch point temperature	$5 < \Delta T_{PP} < 25$
Superheat temperature difference in steam turbine cycle	$\Delta T_{superheat} = 3$
Isentropic efficiencies of high and low pressure steam turbines (%)	$\eta_{ST} = 80$
Isentropic efficiencies of pumps (%)	$\eta_P = 75$
Condenser outlet pressure of steam turbine (bar)	$P_{a1} = 0.1$

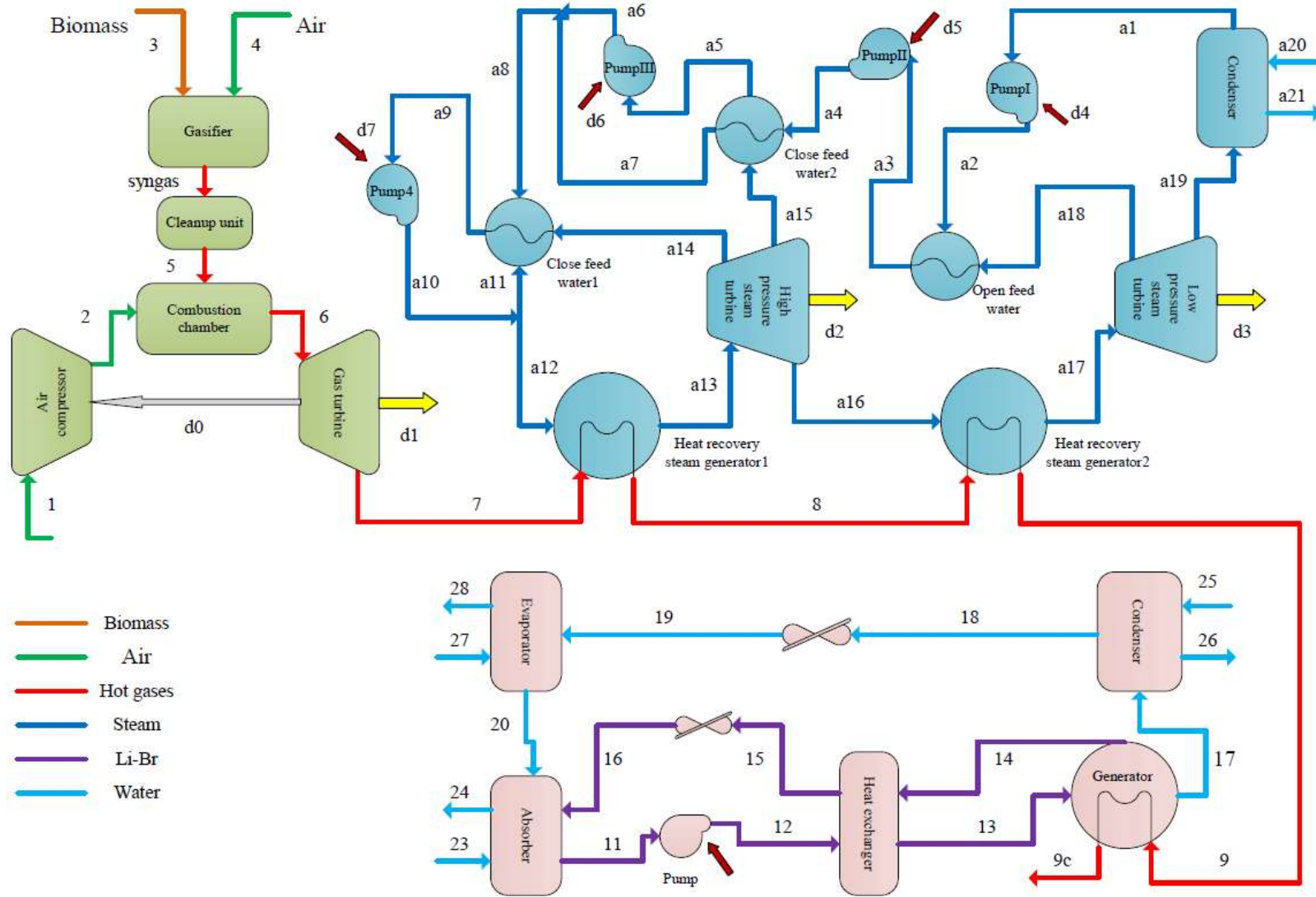|	
Cooling water temperature at condenser inlet (K)	$T_{a20} = 298.15$
Flow rate range for steam injection into combustion chamber (kg/s)	$0 < \left(\dot{m}_{steamCC} / \dot{m}_{air} \right) \times 100 < 5$

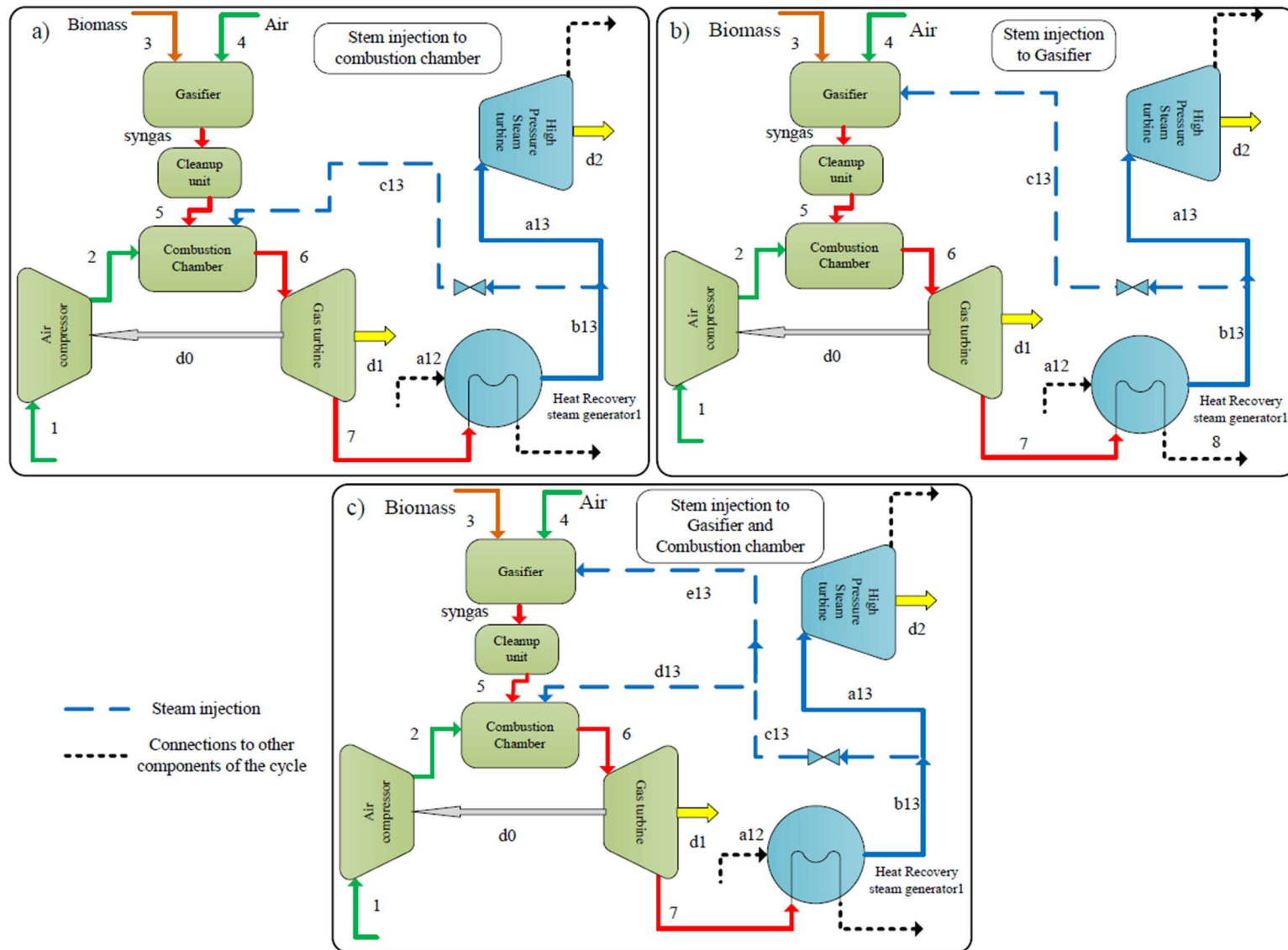**Fig. 1.** Schematic of proposed basic biomass-driven CHP cycle for electricity and cooling

Fig. 2. Variations on proposed basic biomass-driven CHP cycle. **a)** CHP cycle with steam injection to combustion chamber, **b)** CHP cycle with steam injection to gasifier, **c)** CHP cycle with steam injection to combustion chamber and gasifier

3 Energy analyses

According to the first law of thermodynamic, energy is neither produced nor destroyed, but preferably transformed from one form into another. For a control volume in the steady state condition, the balance equations for mass and energy rate follows:

$$\sum \dot{m}_i - \sum \dot{m}_o = 0 \tag{1}$$

$$\sum \left[\dot{Q}_i - \dot{Q}_o \right] + \sum \left[(\dot{m}h)_i - (\dot{m}h)_o \right] + \dot{W} = 0 \tag{2}$$

Here, subscripts i and o respectively denote input and output of states, while $\dot{m}$, h, $\dot{W}$ and $\dot{Q}$ demonstrate mass flow rate, enthalpy , work rate, and heat rate , respectively.

As a biomass fuel, wood is considered in the present study. Models of thermodynamic equilibrium are applied for simulating the process of gasification. All of reactions are supposed to be in thermodynamics equilibrium in an equilibrium model, and the pyrolysis products burns and reach equilibrium before leaving the reduction zone [2]. Details of reduction zone reactions can be found in Ref. [20]. The reaction of biomass fuel with ambient air is as follows:

$$CH_aO_bN_c + wH_2O + m(O_2 + 3.76N_2)$$
$$\rightarrow n_1H_2 + n_2CO + n_3CO_2 + n_4H_2O + n_5CH_4 + n_6N_2 \tag{3}$$
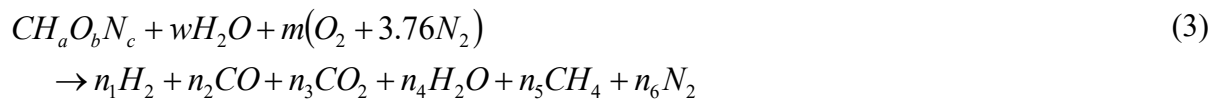
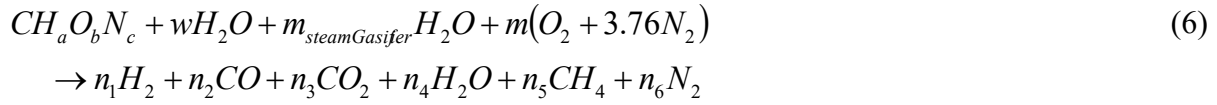where w is the content of biomass fuel moisture and m is amount of inlet air to the gasifier. Wood typically has the chemical formula $CH_{1.44}O_{0.66}$ [23]. With the mass conservation principle applied to H, C, N, and O, it is possible to determine the values for n1 to n6. They differ for each of the four cycles studied. The moisture content of the biomass can be obtained as follows:

$$w = \frac{M_{Biomass}MC}{18(1 - MC)} \tag{4}$$

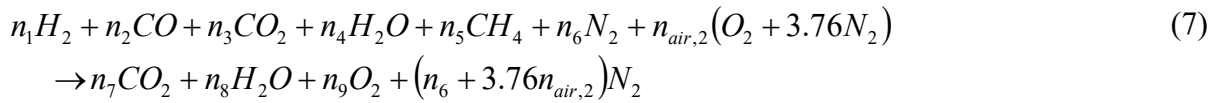Here, MC represents the moisture content of wood per mole, expressible as:

MC = (mass of water/mass of wet biomass) (5)

Note that the gasification process in both the basic and second CHP cycles is described by equation (3). But for the proposed third and fourth CHP cycles that include steam injection into the gasifier, the biomass fuel reaction in the gasifier is as follows [24]:

$$CH_aO_bN_c + wH_2O + m_{steamGasifer}H_2O + m(O_2 + 3.76N_2)$$
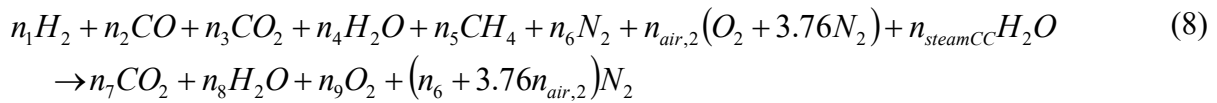$$\rightarrow n_1H_2 + n_2CO + n_3CO_2 + n_4H_2O + n_5CH_4 + n_6N_2$$
(6)

Based on 1 kg of biomass injected into the gasifier, $m_{steamGasifier}$ is the amount of steam injected into the gasifier. Steam is injected to the gasifier based on the steam to carbon ratio [24].

In the basic and third CHP cycles, the gas created by the gasification process enters the combustion chamber, and reacts by incoming air from air compressor, according to the following equation [25]:

$$n_1H_2 + n_2CO + n_3CO_2 + n_4H_2O + n_5CH_4 + n_6N_2 + n_{air,2}(O_2 + 3.76N_2)$$
$$\rightarrow n_7CO_2 + n_8H_2O + n_9O_2 + (n_6 + 3.76n_{air,2})N_2$$
(7)

However, for the second and fourth CHP cycles, which include steam injection into the CC, equation (7) is modified as follows [24]:

$$n_1H_2 + n_2CO + n_3CO_2 + n_4H_2O + n_5CH_4 + n_6N_2 + n_{air,2}(O_2 + 3.76N_2) + n_{steamCC}H_2O$$
$$\rightarrow n_7CO_2 + n_8H_2O + n_9O_2 + (n_6 + 3.76n_{air,2})N_2$$
(8)

where $n_{steamCC}$ is the amount of steam injected to the CC. Rate of steam injection mass flow into the CC is given in Table 1 [26].

For adiabatic combustion, in the combustion chamber of the first and third CHP cycles, equation (9) is used as the energy balance equation and for the combustion chamber of the second and fourth CHP cycles the equation (10) is used as energy balance equation [27]:

$$\sum_j X_j \left(\overline{h}_{fj}^0 + \Delta \overline{h} \right)_{produced\ gas} + \sum_j X_j \left(\overline{h}_{fj}^0 + \Delta \overline{h} \right)_{air,2} = \sum_j X_j \left(\overline{h}_{fj}^0 + \Delta \overline{h} \right)_{products} \tag{9}$$

$$\sum_j X_j \left(\overline{h}_{fj}^0 + \Delta \overline{h} \right)_{produced\ gas} + \sum_j X_j \left(\overline{h}_{fj}^0 + \Delta \overline{h} \right)_{air,2} + \sum_j X_j \left(\overline{h}_{fj}^0 + \Delta \overline{h} \right)_{steamCC} = \sum_j X_j \left(\overline{h}_{fj}^0 + \Delta \overline{h} \right)_{products} \tag{10}$$

A ratio of the produced energy to the input energy is expressed as the total energy efficiency of the CHP cycles [21]:

$$\eta_{CHP} = \frac{\dot{W}_{net} + \dot{Q}_{Cooling}}{\dot{Q}_{in}} \tag{11}$$

Here, $\dot{W}_{net}$ denotes the total power generated by the CHP, $\dot{Q}_{Cooling}$ the cooling rate generated by the CHP, and $\dot{Q}_{in}$ the total rate of the input heat to CHP. These terms can be described as follows:

$$\dot{W}_{net} = \dot{W}_{GT} + \dot{W}_{HPST} - \dot{W}_{AC} + \dot{W}_{LPST} - \dot{W}_{pI} - \dot{W}_{pII} - \dot{W}_{pIII} - \dot{W}_{p4} - \dot{W}_p \tag{12}$$

$$\dot{Q}_{Cooling} = \dot{m}_{20} \left(h_{19} - h_{20} \right) \tag{13}$$

$$\dot{Q}_{in} = \dot{m}_{biomass} \times LHV_{biomass} \tag{14}$$

Here, $LHV_{biomass}$ and $\dot{m}_{biomass}$ denote the biomass lower heating value and the mass flow rate, respectively.

4 Exergy analyses

Thermodynamically, exergy is the maximum value of useful work that can be created by the flow during a process as it comes to thermal, chemical, and mechanical equilibrium with a reference environment. In other words, exergy indicates the amount of usable work. For a kth component of a thermodynamic cycle at steady state conditions, an exergy rate balance equation follows [28]:

$$\dot{E}_{F,k} = \dot{E}_{D,k} + \dot{E}_{P,k} \tag{15}$$

Here, the F, P and D denote input, output and destruction, respectively. Each component of the fourth CHP cycle is analyzed with the exergy rate balance equation, and the resulting equations for the exergy destruction rate of all components are listed in Appendix A.

A ratio of the total useful exergy product to total input exergy is specified as exergy efficiency. The total exergy efficiency for the novel CHP cycles can be written as [29]:

$$\varepsilon_{CHP} = \frac{\left(\dot{W}_{net} + \dot{E}_{Cooling}\right)}{\left(\dot{E}_{in}\right)} \tag{16}$$

Here, $\dot{E}_{Cooling}$ and $\dot{E}_{in}$ are the exergy rates of the produced cooling and inlet biomass fuel, expressible as follows [30]:

$$\dot{E}_{Cooling} = \dot{Q}_{Eva}\left(1 - \frac{T_0}{T_{Eva}}\right) \tag{17}$$

$$\dot{E}_{in} = \dot{m}_{Biomass} \times \beta \times LHV_{Biomass} \tag{18}$$

where β is the ratio between chemical exergy and the lower heating value of biomass fuels' organic fraction. β is approximated as [20]:

$$\beta = \frac{1.044 + 0.16\dfrac{Z_H}{Z_C} - 0.34493\dfrac{Z_O}{Z_C}\left(1 + 0.0531\dfrac{Z_H}{Z_C}\right)}{1 - 0.4142\dfrac{Z_O}{Z_C}} \qquad (19)$$

where Z_O, Z_C and Z_H represent the oxygen, carbon, and hydrogen weight fractions of biomass, respectively.

4 Exergoeconomic analyses

Through the combination of thermo-economics and exergy analysis principles, exergoeconomics provides a valuable tool for improving a thermodynamic cycle's operation. The components with the greatest thermodynamic irreversibilities are identified through exergy analysis, while exergoeconomic analyses determine the cost of irreversibilities. In fact, from an exergoeconomic standpoint, a system is properly optimized when the costs associated with its thermodynamic inefficiencies can justify the extent of the inefficiencies.

In the proposed CHP cycles, for the kth component, an exergoeconomic balance equation is described [31]:

$$\dot{C}_{i,k} - \dot{C}_{o,k} = \dot{Z}_k \qquad (20)$$

$\dot{C}_{i,k}$ and $\dot{C}_{o,k}$ denote the input and output costs respectively for the kth component and $\dot{Z}_k$ is investment cost resulting from operating and maintenance costs, that are determined as [28]:

$$\dot{C}_{i,k} = c_{i,k}\dot{E}_{i,k} \qquad (21)$$

$$\dot{C}_{e,k} = c_{e,k}\dot{E}_{e,k} \qquad (22)$$

$$\dot{Z}_K = \dot{Z}_K^{CL} + \dot{Z}_K^{OM} = CRF \times (\varphi_r / N \times 3600) \times PEC_K \qquad (23)$$

18

Here, $c_{i,k}$, CRF, φ_r, N and PEC_K are the unit cost of exergy, capital recovery factor, maintenance factor (assumed here to be 1.06), annual number of operation hours (assumed here to be 5446 h/year), and purchase equipment cost, respectively. To specify the equipment purchase cost for the presented cycle, expressions are used based on references [4, 20, 28]. CRF can be expressed as

$$CRF = \frac{i_{eff}\left(1+i_{eff}\right)^n}{\left(1+i_{eff}\right)^n -1}$$

(24)

where i_{eff} is the average annual rate of the cost of money. Its value may differ between countries due to different inflation rates. In some countries with high inflation may be high, whereas in most industrialized countries may be low. To consider the effect of inflation on the exergoeconomic calculation, the investment cost and the fuel and product unit costs of all components of the system for the two different inflations included 4% and 12% are determined and compared in the results section.

Interestingly, the exergy destruction costs for kth component are not derived from the exergoeconomic balance equation, but rather by multiplying the unit cost of fuel ($c_{F,k}$) by the rate of exergy destruction to kth component [32]. That is,

$$\dot{C}_{D,k} = c_{F,k}\dot{E}_{D,k}$$

(25)

In this paper, total cycle cost rate is indicated as the sum of total cost of exergy destruction rate, total investment cost, and input fuel cost.

$$\dot{C}_{CHP} = \dot{C}_{D,tot} + \dot{Z}_{tot} + \dot{C}_f$$

(26)

The cost of input biomass fuel ($\dot{C}_f$) can be calculated as [20]:

$$\dot{C}_{fuel} = \left(\frac{\cos t \, / \, metric \quad ton}{1000} \right) \times \left(\frac{3.6}{LHV} \right) \tag{27}$$

The biomass fuel cost is primarily dependent on the type of raw material, as well as the method of collection and processing. Purchasing forest waste, for example, is more expensive than processing it. On the other hand, industrial and municipal wastes have much lower and even negative costs, but higher processing costs. Other factors that affect the finished cost include collection methods, transportation distance, and feedstock type. Therefore, the cost of fuel depends on the conditions in each country.

In an exergoeconomic analysis, the exergoeconomic factor is the important parameter. It can be achived as [21]:

$$f_k = \frac{\dot{Z}_k}{\dot{Z}_k + \dot{C}_{D,k}} \tag{28}$$

As this factor is calculated by dividing investment cost by the total of total investment cost and the cost rate of exergy destruction, the value of factor can determine which of the components in a cycle can be improved by reducing which of the costs.

5 Environmental considerations

Environmental pollutants, including CO_2, are causing many problems for the environment and humans today [33]. Efforts are ongoing to find ways to reduce anthropogenic emissions. Among the proposed options there is the utilization of the renewable energy sources at power plants. Biomass is used as a fuel input to the proposed CHP cycles in this paper in line with this goal. However, carbon dioxide is produced as a result of the gasification reactions in the gasifier. Consequently, this paper aims to reduce carbon dioxide emissions by providing and examining

various options for steam injection into the basic CHP cycle. The following expression is employed to calculate cycle carbon dioxide emissions [20]:

$$\xi_{CO_2-CHP} = \frac{\dot{m}_{CO_2}}{\dot{W}_{net}} \qquad (29)$$

with $\dot{m}_{CO_2}$ the mass flow rate of emitted CO_2 for a CHP cycle. The CO_2 emissions for all considered CHP cycles are calculated and presented in the results section, where they are examined and compared.

6 Results and discussion

In this section, results of the energy, exergy, exergoeconomic and environmental studies of the presented biomass-driven CHP cycles are reported. Then, the results of a parametric analysis are described to define the effects of modifying one parameter or simultaneously changing two parameters on important thermodynamic performance parameters.

6.1 Results of energy, exergy, exergoeconomic and environmental analyses

As mentioned in the introduction section, in this article, we aim to compare how different modes of steam injection affect the performance of the proposed cycles. Steam is injected into the combustion chamber and gasifier of the Brayton cycle in the proposed CHPs. Accordingly, Fig. 3(a) shows the T-S diagram for the gasifier, combustion chamber, and gas turbine in the proposed cycles. It is important to note that in the modeling of the cycles, assumptions such as the gasifier and gas turbine inlet temperatures have been assumed to be the same, in order to better compare the effects of steam injection on the performance of the cycles. Therefore, it can be seen that in point 5 there is a significant difference between the modeled cycles in terms of

entropy produced by gasifier gases. Since steam is injected into the gasifier and combustion chamber, the molar ratios of combustion reactions and mass flow rates of combustion gases are different in all three investigations cycles. Therefore, the hot gases flow at different rates in the combustion chamber, resulting in different Brayton cycles power production. In this figure, a table reports this result.

Due to the steam injection from the steam turbine cycle to the Brayton cycle, a T-S diagram for this cycle is also illustrated in Fig. 3(b). It is assumed that all CHP cycles have the same superheat temperature difference in order to compare the effects of steam injection on their performance. Thus, the T-S diagram of steam turbine cycle for all CHP cycles is almost the same, and the main difference is the mass flow rate of steam entering the turbines, consequently affecting their production power. A table in this diagram shows the mass flow rate of the input steam to the high pressure steam turbine as well as the net power produced by the steam turbine cycle in the studied CHPs. It can be seen that the amount of power produced in the fourth cycle also increases due to the increased mass flow rate of steam entering the steam turbines.
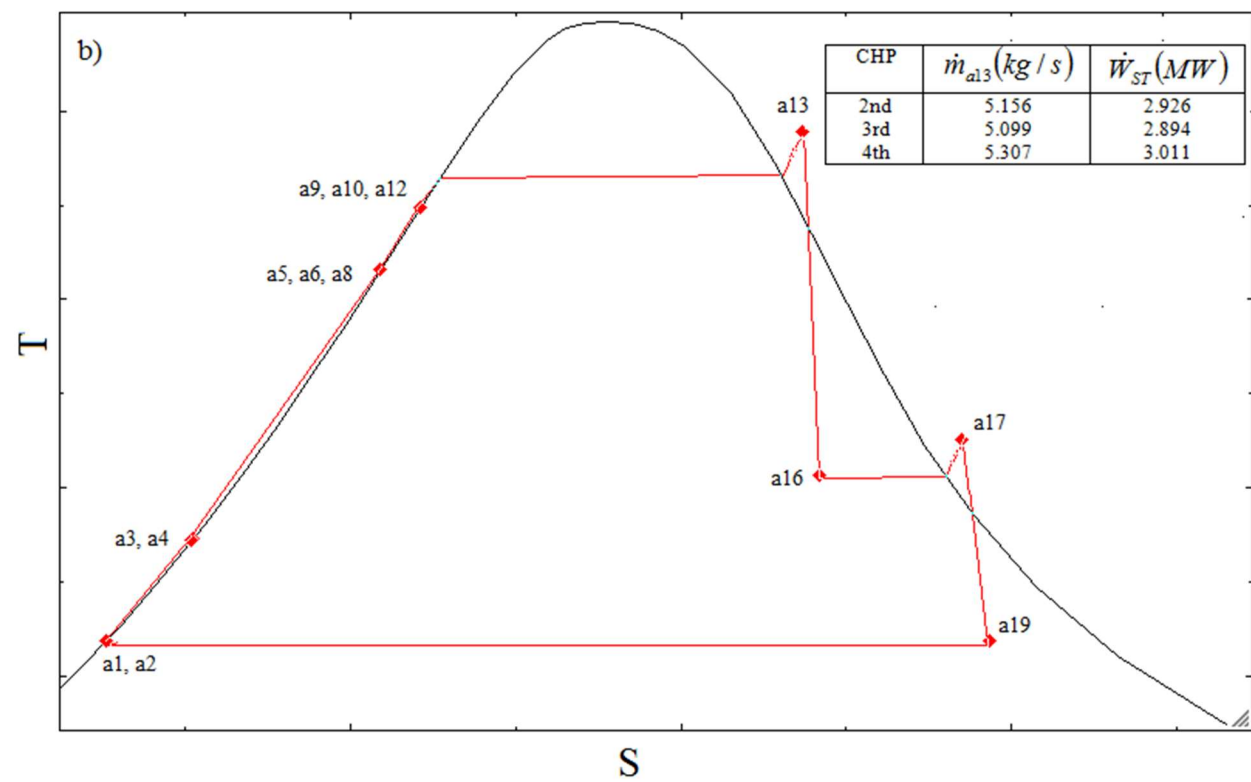
a)

CHP	$\dot{m}_6\left(kg/s\right)$	$\dot{W}_{nst,GT}\left(MW\right)$
2nd	26.06	7.235
3rd	29.04	7.821
4th	30.58	8.189

b)

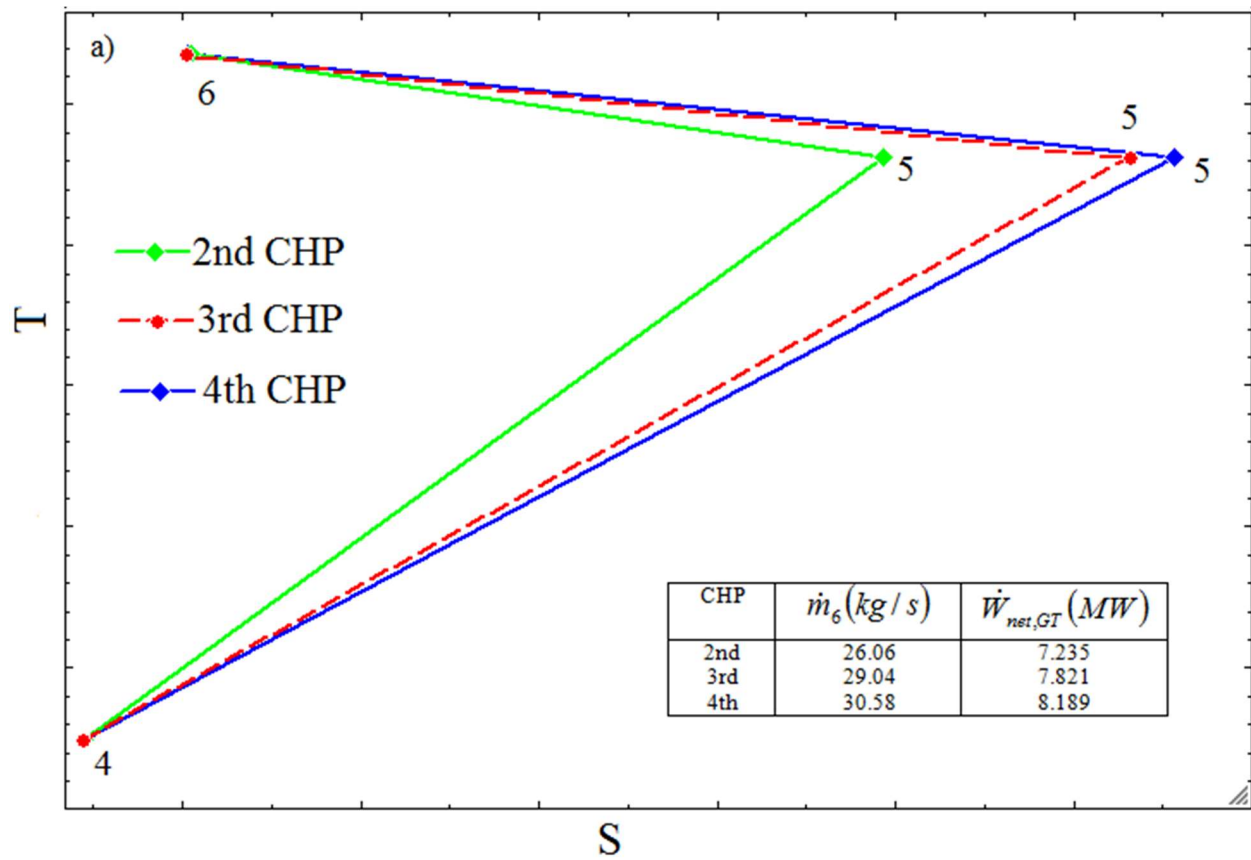| CHP	$\dot{m}_{a13}\left(kg/s\right)$	$\dot{W}_{ST}\left(MW\right)$
2nd	5.156	2.926
3rd	5.099	2.894
4th	5.307	3.011

Fig. 3. T-S diagram for different steam injection modes in, a) the gasifier, combustion chamber and gas turbine components of Brayton cycle of the proposed CHPs, b) the steam turbine cycle of the proposed CHPs

Since one of primary goals of this paper is to develop a CHP system with better performance in subjects of thermodynamics, economics, and environmental impact, various types of steam injection are investigated for the basic CHP system (1- steam injected into the combustion chamber, 2- steam injected into the gasifier and 3- steam injected in both of the combustion chamber and gasifier). In the Figs. 4(a), 5(a), 6(a) and 7(a), resulting performance parameters of the four CHP systems are presented and compared. In Figs. 4(b), 5(b), 6(b) and 7(b), the percentage increase or decrease of the performance parameters of the CHP cycles for different injection modes are presented relative to the basic CHP system.

The performance parameters considered are total cost associated by exergy destructions and the total investment cost rate, CO_2 emissions, net power production, total exergy destruction rate, total exergy and energy efficiencies. As drawn in Figs. 4 to 7, compared to the base CHP cycle, the steam-injection CHP cycles have higher power production and higher efficiencies, as well as lower rates of exergy destruction, lower costs associated with exergy destruction, and lower CO_2 emissions. Through steam injection into the proposed CHP cycles in the investigated states, the mass flow rate of hot gases exiting of the combustion chamber increases, which leads to an increase in production power and efficiencies. Additionally, injecting steam into the combustion chamber or gasifier improves the combustion reaction process, and therefore reduces the amount of exergy destruction in this component, as well as the total amount of exergy destruction. Furthermore, since the costs associated with exergy destruction are calculated with equation (25), by reducing exergy destruction in these components the total amount of costs associated with exergy destruction will also be reduced. The higher investment costs for the proposed cycles in

24

the steam injection modes can be justified by the increased value of mass flow rate in the PEC equations of the components of cycles.

Also in Fig. 4(a) it can be seen that the third CHP cycle (CHP cycle with the steam injection to the gasifier) has a higher efficiency than the second proposed CHP system (CHP with steam injection into the CC). It can be explained by the fact that the total moles of gases produced by the gasifier when steam is injected into the gasifier are more reduced than when steam is injected into the chamber, which is the reason for the 3rd CHP's high efficiency. As a result, the amount of moles of air entering the air compressor in the steam injection to the gasifier has increased more than in the steam injection to the combustion chamber, which leads to a higher mass flow rate of hot gases produced in the combustion chamber, thereby increasing the 3rd cycle's power output. In Fig. 4(b), it is seen that injecting steam into the CC for the second cycle leads to energy and exergy efficiencies enhanced by 3.64% and 3.97% compared to the basic CHP cycle. For the third cycle, energy and exergy efficiencies raised by 8.79% and 9.62% compared to basic CHP cycle, when injecting steam into the gasifier.

Fig. 4(a) shows that the fourth cycle, which involves injecting steam into both the gasifier and CC components, the both energy and exergy efficiencies are highest among four CHP cycles. In Figs. 4, 5, 6 and 7 it can be observed that the both energy and exergy efficiencies increase by 13.3% and 14.6% for the fourth CHP cycle compared to the basic CHP cycle, while the exergy destruction rates, the cost of exergy destruction and CO_2 emissions decrease by about 19.53%, 16% and 12.8% respectively. Note that the total investment cost rate increases about 16% for the fourth CHP cycle compared to the basic CHP cycle. Note that the differences in CO_2 emission between the studied systems are also due to different molar ratios of CO_2 produced in combustion reactions. As a result of steam injection into the gasifier, a lower molar ratio of

carbon dioxide has been produced in the gasifier compared with steam injection into the combustion chamber, so there is less carbon dioxide released in this case. For the 3rd CHP, the gasifier and combustion chamber produce a lower molar ratio of carbon dioxide, so this system produces the lowest amount of carbon dioxide emissions. Thus Figs. 4 and 7 indicates that fourth proposed CHP cycle has the highest efficiencies and the lowest CO_2 emission rates and is also likely the most economically viable compared to the other investigated CHP cycles. In the following, therefore, the thermodynamic and exergoeconomic results for the fourth proposed CHP cycle are investigated in more detail.
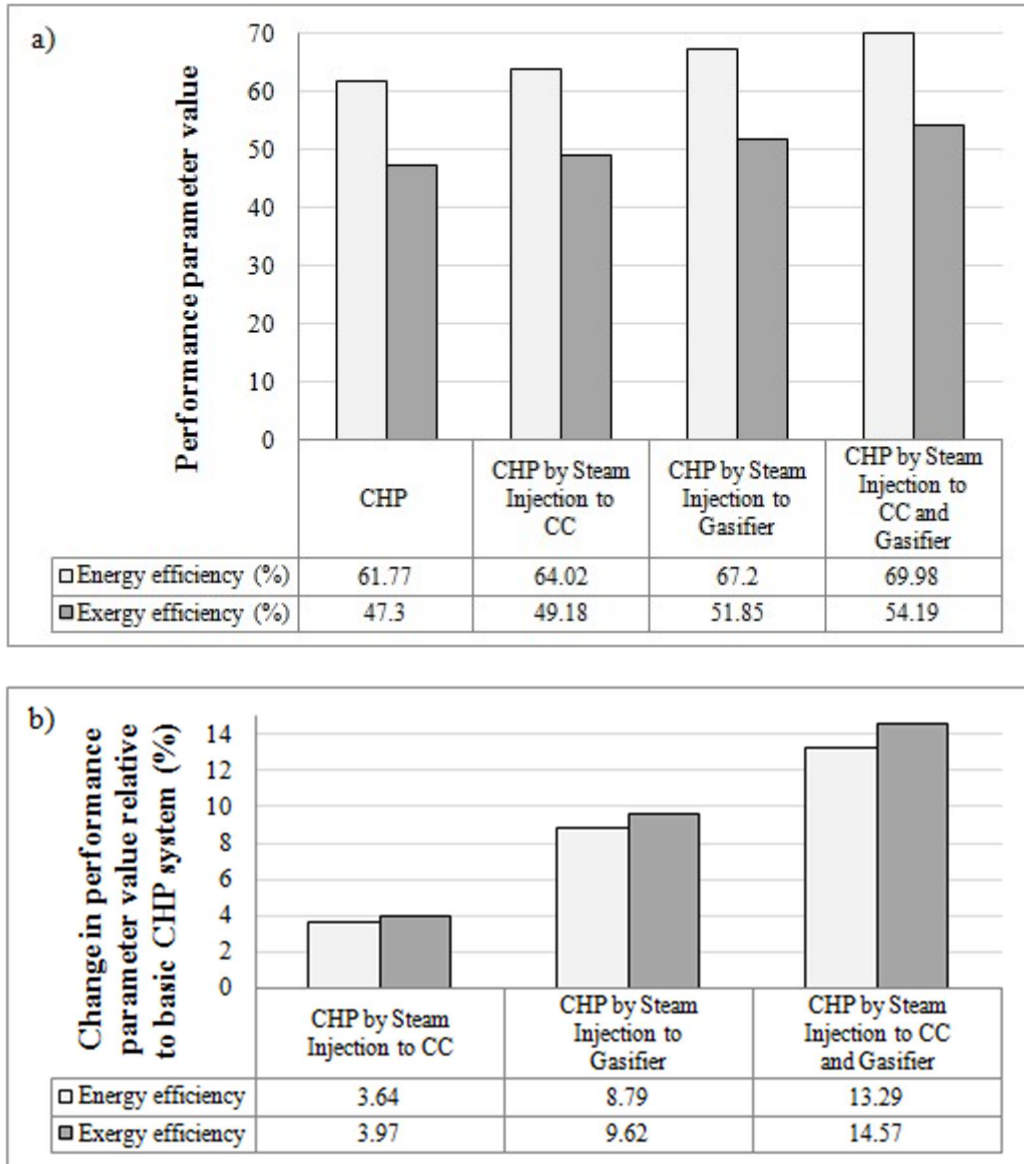
a)

	CHP	CHP by Steam Injection to CC	CHP by Steam Injection to Gasifier	CHP by Steam Injection to CC and Gasifier
▢ Energy efficiency (%)	61.77	64.02	67.2	69.98
▣ Exergy efficiency (%)	47.3	49.18	51.85	54.19

b)

	CHP by Steam Injection to CC	CHP by Steam Injection to Gasifier	CHP by Steam Injection to CC and Gasifier
▢ Energy efficiency	3.64	8.79	13.29
▣ Exergy efficiency	3.97	9.62	14.57

Fig. 4. a) Comparison of total energy and exergy efficiencies between the basic and modified CHP cycles. b) Comparison of percentage change relative to the basic CHP cycle total energy and exergy efficiencies of the cycles for different types of steam injection.
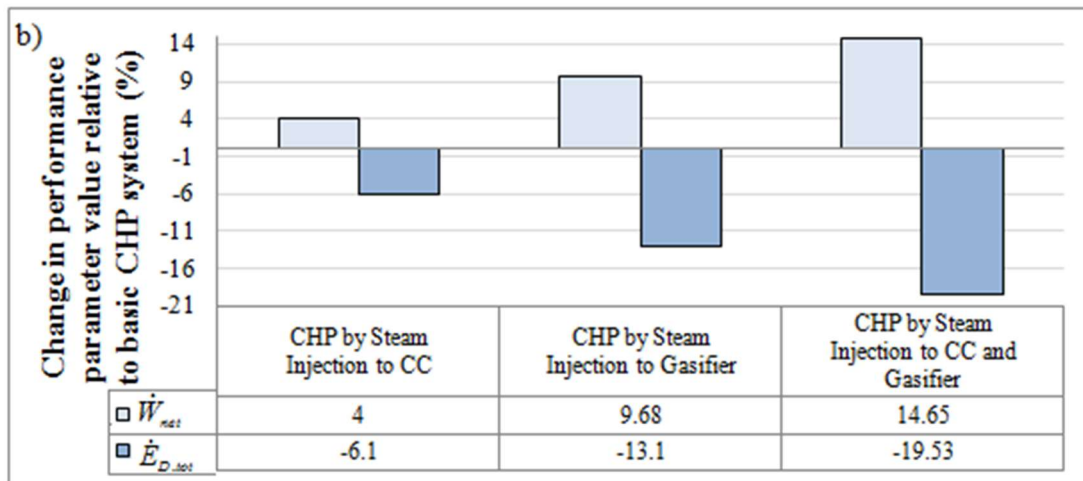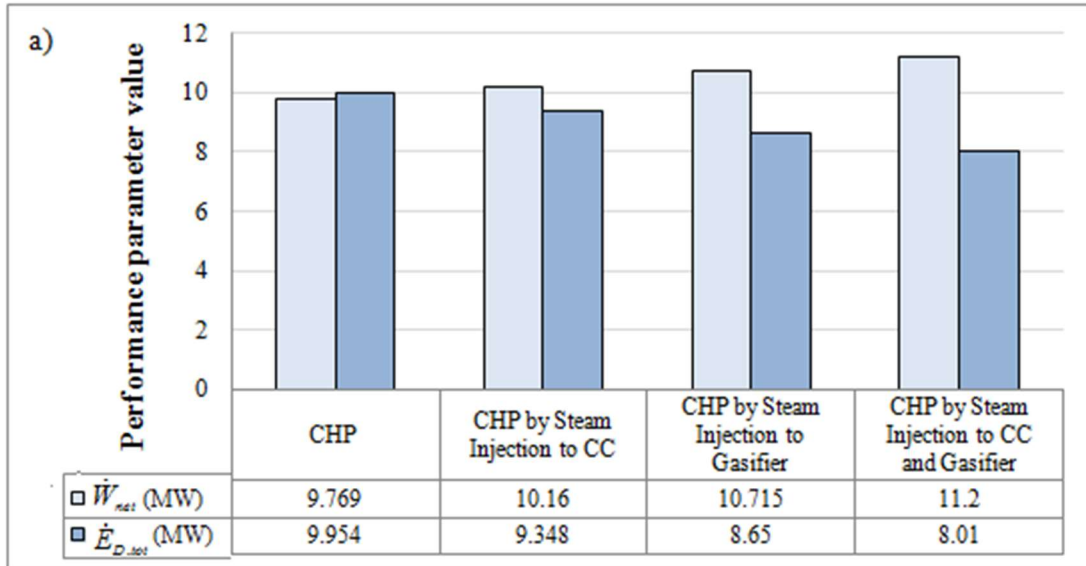
a)

	CHP	CHP by Steam Injection to CC	CHP by Steam Injection to Gasifier	CHP by Steam Injection to CC and Gasifier
$\dot{W}_{net}$ (MW)	9.769	10.16	10.715	11.2
$\dot{E}_{D,tot}$ (MW)	9.954	9.348	8.65	8.01

b)

	CHP by Steam Injection to CC	CHP by Steam Injection to Gasifier	CHP by Steam Injection to CC and Gasifier
$\dot{W}_{net}$	4	9.68	14.65
$\dot{E}_{D,tot}$	-6.1	-13.1	-19.53

Fig. 5. a) Comparison of net power production and total exergy destruction rate between the basic and modified CHP cycles. b) Comparison of percentage change relative to the basic CHP cycle in net power production and total exergy destruction rate of the cycles for different types of steam injection.
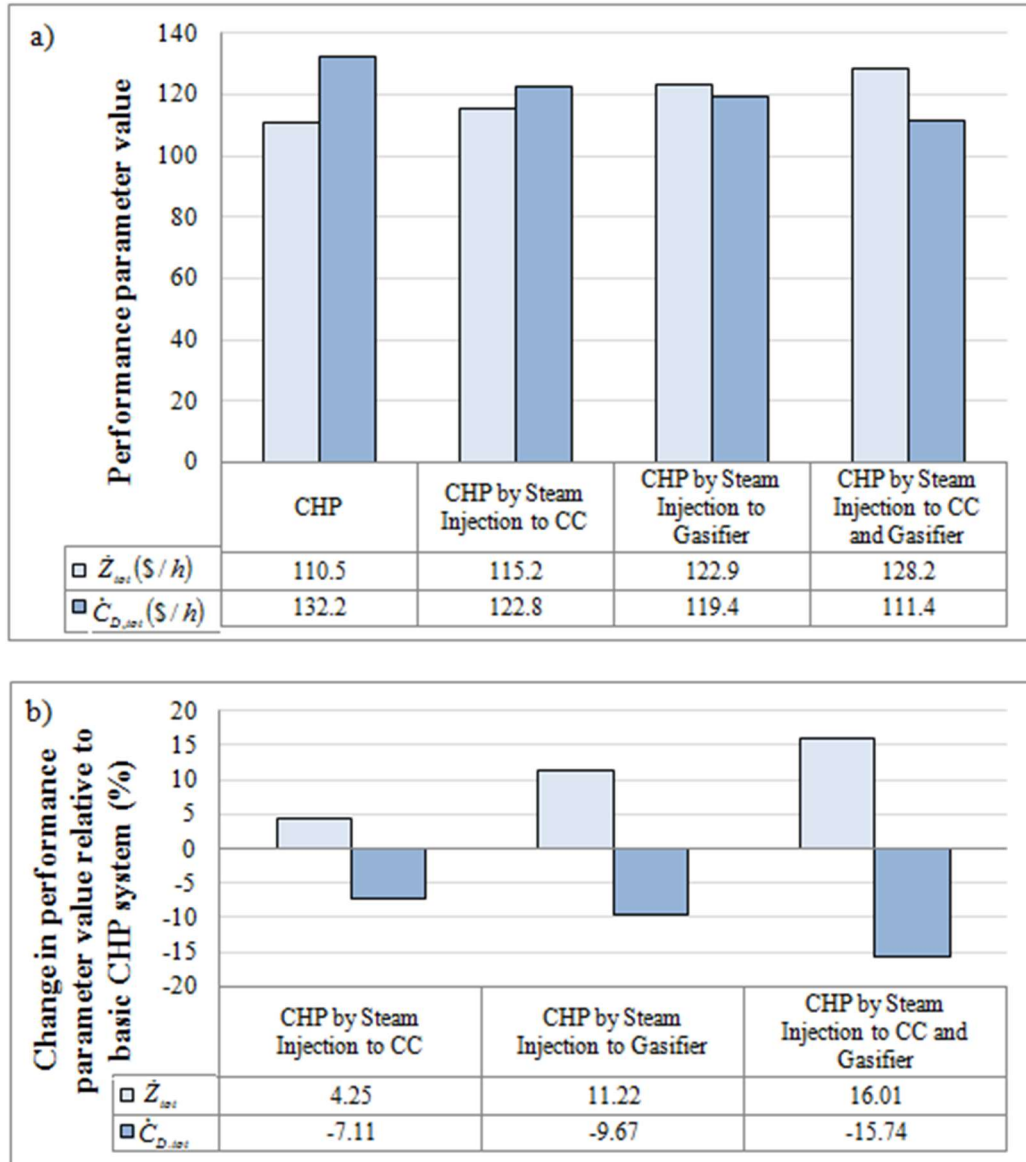
28

a)

	CHP	CHP by Steam Injection to CC	CHP by Steam Injection to Gasifier	CHP by Steam Injection to CC and Gasifier
$\dot{Z}_{tot}$ ($/h)	110.5	115.2	122.9	128.2
$\dot{C}_{D,tot}$ ($/h)	132.2	122.8	119.4	111.4

b)

	CHP by Steam Injection to CC	CHP by Steam Injection to Gasifier	CHP by Steam Injection to CC and Gasifier
$\dot{Z}_{tot}$	4.25	11.22	16.01
$\dot{C}_{D,tot}$	-7.11	-9.67	-15.74

Fig. 6. a) Comparison of total cost associated with exergy destructions and total investment costs between the basic and modified CHP cycles. b) Comparison of percentage change relative to the basic CHP cycle in total cost associated with exergy destructions and total investment costs of the cycles for different types of steam injection.
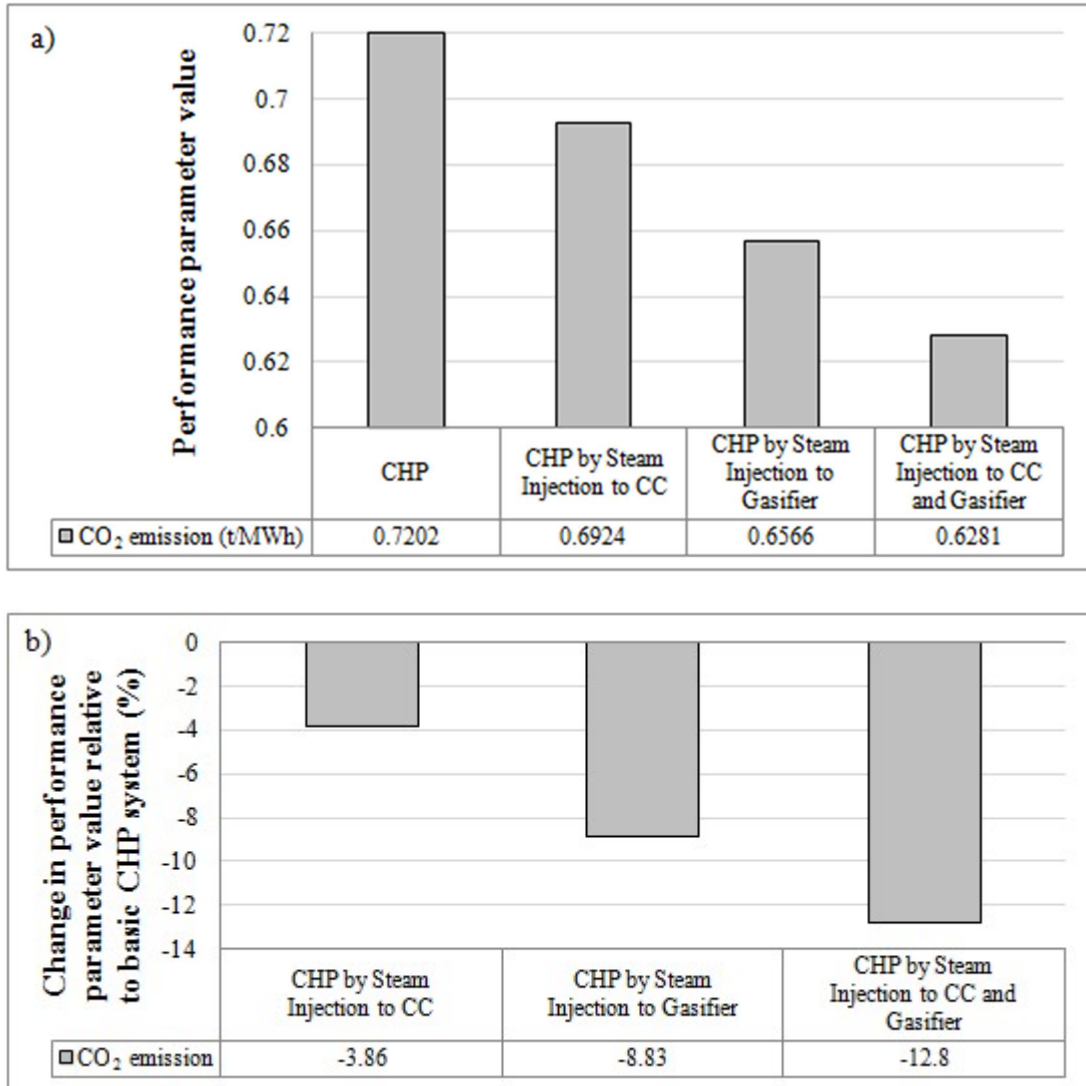
Fig. 7. a) Comparison of CO_2 emission between the basic and modified CHP cycles. b) Comparison of percentage change relative to the basic CHP cycle in CO_2 emission of the cycles for different types of steam injection.

In Table 2, thermodynamic values are listed including temperature, pressure, rate of mass flow, rate of chemical and physical exergy, and the cost rate for all point of the proposed CHP cycle with the steam injection in the CC and Gasifier.

Table 2 Results obtained of thermodynamic analysis of the biomass-driven CHP with the steam injection in combustion chamber and gasifier

Point	Fluid	T (K)	P (bar)	$\dot{m}(kg/s)$	$\dot{E}_{ph}(kW)$	$\dot{E}_{ch}(kW)$	$\dot{E}(kW)$	$\dot{C}(\$/h)$
1	air	298.2	1.013	25.66	0	0	0	0
2	air	612.5	10.13	25.66	7756	0	7756	168.7
3	biomass	298.2	1.013	1	0	20788	20788	171.7
4	air	298.2	1.013	3.192	0	0	0	0
5	produced gas	1073	10	4.872	7042	11849	18891	172
6	comb.gases	1270	9.927	30.58	25575	183.8	25759	342.2
7	comb.gases	826.3	1.154	30.58	8021	183.8	8205	109
8	comb.gases	554.6	1.119	30.58	2624	183.8	2808	37.3
9	comb.gases	492.3	1.086	30.58	1648	183.8	1832	24.34
9c	comb.gases	447	1.013	30.58	1219	183.8	1403	21.43
11	Li-Br Solution	305.2	0.00999	5.207	66.61	6.598	73.21	5.108
12	Li-Br Solution	305.2	0.04812	5.207	66.61	6.597	73.21	5.189
13	Li-Br Solution	337.6	0.04812	5.207	92.75	6.597	99.35	7.4
14	Li-Br Solution	343	0.04812	4.787	204.6	5.478	210.1	14.5
15	Li-Br Solution	305.4	0.04812	4.787	176.2	5.478	181.7	12.54
16	Li-Br Solution	305.4	0.00999	4.787	176.2	5.478	181.7	12.54
17	water	340.3	0.04812	0.42	26.21	1.119	27.33	1.848
18	water	305.4	0.04812	0.42	0.1097	1.119	1.229	0.0831
19	water	280.1	0.00999	0.42	-1.901	1.119	-0.7818	-0.05287
20	water	280.1	0.00999	0.42	-66.27	1.119	-65.15	-4.406
23	water	302.6	1	101.4	13.64	270.2	283.8	0
24	water	305.2	1	101.4	34.32	270.2	304.5	3.24
25	water	302.6	1	96.36	12.96	256.7	269.7	0
26	water	305.2	1	96.36	32.61	256.7	289.4	2.017
27	water	284.9	1	52.99	67.8	141.2	209	0
28	water	280.4	1	52.99	122.8	141.2	264	4.7
a1	steam	319	0.1	3.112	8.713	0	8.713	0.2153
a2	steam	318.9	1	3.112	9.005	0	9.005	0.2226
a3	steam	372.8	1	3.437	115.6	0	115.6	7.463
a4	steam	372.2	35	3.437	125.4	0	125.4	7.487
a5	steam	515.7	35	1.355	327.6	0	327.6	8.596
a6	steam	515.7	60	1.355	330.1	0	330.1	8.622
a7	steam	515.7	60	3.437	837.3	0	837.3	36.42
a8	steam	515.7	60	4.792	1167	0	1167	45.04
a9	steam	548.7	60	0.5147	162.5	0	162.5	4.263
a10	steam	548.9	80	0.5147	163.2	0	163.2	4.287
a11	steam	548.7	80	4.792	1518	0	1518	59.8
a12	steam	548.7	80	5.307	1681	0	1681	64.09

a13	steam	571.2	80	5.307	5618	0	5618	147.4
b13	steam	571.2	80	6.038	6392	0	6392	136.8
c13	steam	571.2	50	0.7313	774.1	0	774.1	19.66
d13	steam	571.2	33	0.05135	54.33	0	54.33	1.051
e13	steam	571.2	33	0.68	719.8	0	719.8	11.41
a14	steam	548.7	60	0.517	519.5	0	519.5	13.63
a15	steam	515.7	35	1.355	1245	0	1245	32.65
a16	steam	406.7	3	3.437	1863	0	1863	48.87
a17	steam	409.7	3	3.437	2223	0	2223	54.92
a18	steam	372.8	1	0.3245	151.5	0	151.5	3.744
a19	steam	319	0.1	3.112	441.3	0	441.3	10.9
a20	water	298.2	1.013	160.9	0	0	0	0
a21	water	308	1.013	160.9	107.2	0	107.2	18.12

As mentioned previously, the proposed CHP cycle in this paper is a combination of Brayton, the absorption refrigeration and steam turbine cycles. In order to reach a better understanding of impacts and contributions of each of these cycles on performance of the fourth CHP cycle, Figs. 8-10 are drawn. In Fig. 8(a), the rates of exergy destruction for each cycle and components of fourth presented CHP are shown. The pie chart in Fig. 8(b) shows the percentage contributions of Brayton cycle, steam turbine cycle, and Li-Br absorption refrigeration to the total exergy destruction of the fourth CHP system. The total exergy destruction of Brayton, steam turbine and absorption refrigeration cycles are marked by red, yellow and gray, respectively. Among the components of the fourth CHP cycle, the gasifier at 2.62 MW has highest rate of exergy destruction, while absorption components have lowest. Since the Brayton cycle consists of a combustion chamber and a gasifier, these are the components by high exergy destruction due to chemical reactions combustion; thus the Brayton cycle at 65% is responsible for the highest percentage of the rate of exergy destruction of fourth CHP. Since the steam turbine and refrigeration cycles utilize the waste heat of the Brayton cycle to produce energy and they do not involve combustion, they contribute less (about 31% and 4% respectively) to the total rate of

exergy destruction of the fourth CHP system. Heat recovery steam generator 1 and 2 are responsible for the most exergy destruction in the steam turbine cycle due to the heat exchange between passing hot gases and steam. As well, the generator with 0.3 MW of exergy destruction has the largest share of exergy destruction among absorption refrigeration components, which is caused by the heat exchange between hot gases and the fluid. Thus, improving the performance of Brayton cycle components provides good potential to significantly enhance the efficiency and decrease the exergy destruction of the fourth CHP cycle.
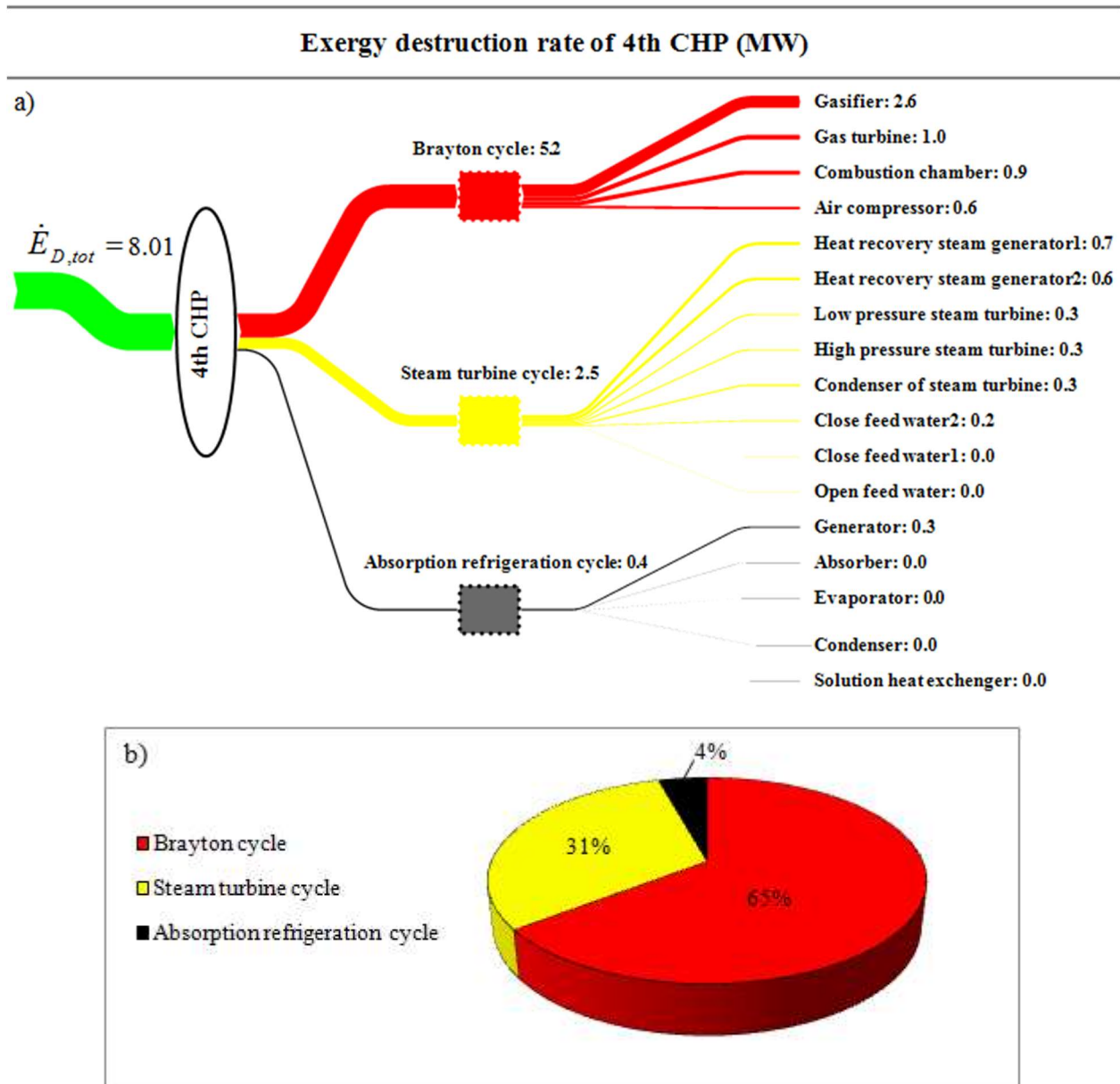
Fig. 8. Exergy destruction results for CHP cycle with steam injection into the CC and gasifier. a) Exergy destruction rate for each cycle and component. b) Breakdown of total exergy destruction rate by cycle section.

Fig. 9(a) shows the costs rate associated by exergy destruction for each cycle and component of fourth CHP cycle. The pie chart in Fig. 9(b) indicates a percentage contribution of the Brayton, steam turbine and absorption refrigeration cycles to the total costs associated with rate of exergy destruction of fourth CHP cycle. Since these costs are associated by exergy destruction (they have been determined using Equation (25) for all components), the cost associated by exergy destruction rate for the fourth CHP cycle components exhibit a similar pattern to the exergy destruction rates. Gasifier is responsible for the largest share of exergy destruction costs in the Brayton cycle, with 20.3 $/h. The steam turbine cycle also has the highest exergy destruction costs for heat recovery steam generators 1 and 2. Further, the generator with 4.9 $/h is the largest cost component in the refrigeration cycle due to exergy destruction. That is at about 50% of total cost associated by the fourth CHP cycle (components of Brayton cycle have the highest cost by exergy destruction). This is followed by the steam turbine cycle and absorption refrigeration cycle, contributing about 44% and 6% respectively of total exergy destruction cost rate in fourth CHP.
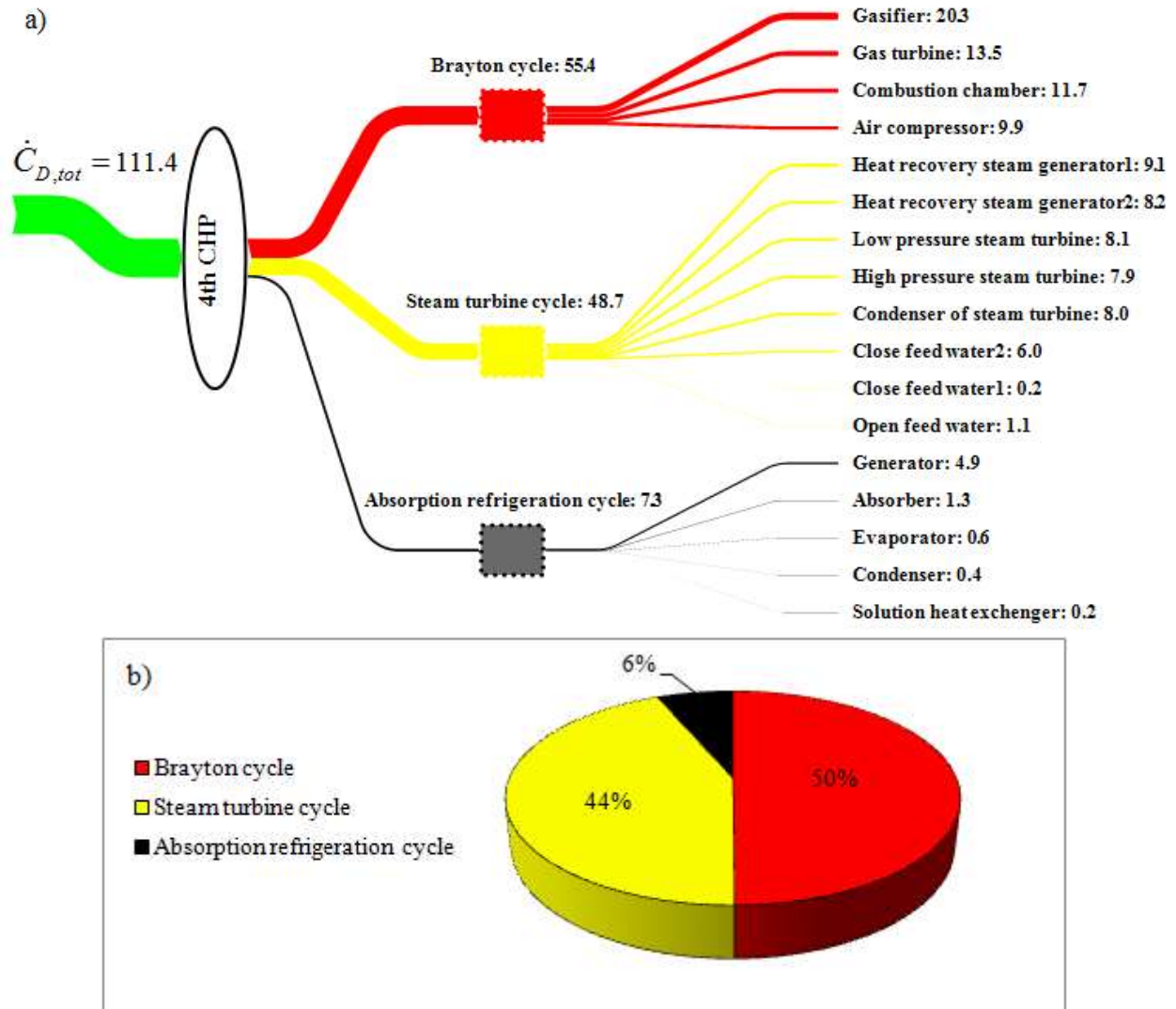
Fig. 9. Cost associated by exergy destruction results for CHP cycle with steam injection into the CC and gasifier. a) Cost rate associated by exergy destruction for each cycle and component. b) Breakdown of the total cost associated by exergy destruction by cycle section.

The investment cost rate for the each cycle and component of the fourth CHP are presented in the Fig. 10(a). The pie chart in Fig. 10(b) shows the percentage contribution of the Brayton, Steam turbine and the absorption refrigeration cycles to the investment cost rate of the fourth CHP cycle. About 67% of total investment cost of the fourth CHP system is associated with the Brayton cycle components, while the steam turbine cycle and the absorption refrigeration cycle

contribute approximately 32% and 1% respectively. Among the components of the fourth CHP cycle, the gas turbine (GT) exhibits the highest investment cost rate at 44 $/h, and in the steam turbine cycle, high pressure steam turbine and low pressure steam turbine have the largest share of investment costs, 10.5 $/h and 8.8 $/h, respectively. The investment cost of absorption refrigeration cycle components is the lowest. The generator, absorber and condenser are the most expensive in the refrigeration cycle with about 0.3 $/h each.

Investment cost rate of 4th CHP (S/h)

a)

Brayton cycle: 85.1	
Gasifier: 10.1	
Gas turbine: 43.9	
Combustion chamber: 2.3	
Air compressor: 28.9	

$\dot{Z}_{tot} = 128.3$

4th CHP

Steam turbine cycle: 41.8

Heat recovery steam generator1: 0.6
Heat recovery steam generator2: 0.3
Low pressure steam turbine: 8.8
High pressure steam turbine: 10.5
Condenser of steam turbine: 7.4
Close feed water2: 4.9
Close feed water1: 5.4
Open feed water: 3.5

Absorption refrigeration cycle: 1.4

Generator: 0.3
Absorber: 0.3
Evaporator: 0.0
Condenser: 0.3
Solution heat exchenger: 0.3

b)

■ Brayton cycle
□ Steam turbine cycle
■ Absorption refrigeration cycle

1%
32%
67%

Fig. 10. Investment cost rate results for CHP cycle with steam injection into the CC and gasifier. a) Investment cost rate for each cycle and component, b) Breakdown of total investment cost by cycle section.

As mentioned in exergoeconomic analysis segment, the value of cost of money due of different inflation in different countries can be different. So, to understand the effect of this difference on the exergoeconomic results, a comparison for the different values of cost of money for the fourth CHP system are presented by Table 3, which contains the unit costs of the fuel and product, and the exergo-economic factor for each component. Note that the exergo-economic factor links the cost associated by exergy destruction and investment cost of the component, and therefore is a useful parameter. A lower value suggests better performance of the cycle is attained by reducing of exergy destruction of the component, and a higher amount suggests better performance by reducing of the component's investment cost. By comparing the obtained exergoeconomic values for the i_{eff}=4% and i_{eff}=12%, it can be seen that the components of the fourth CHP cycle with lower cost of money have the lower values of exergoeconomic factors. It is due the fact that when the cost of money is low, the amount of investment costs is reduced significantly, while the costs of exergy destruction are reduced slightly. Thus, the exergoeconomic factor of the components per small values of cost of money is lower than that in case of high values of the cost of money.

Generally it is observed in Table 3 that higher exergoeconomic factor values are associated with the following components: air compressor (AC), gas turbine (GT), open feed water (OFW) and closed feed water (CFW1). Consequently, for these components it is beneficial to decrease of the exergy destruction rate of components in order to lower cost of the overall cycle. For components such as the gasifier, heat recovery steam generator 2 (HRSG2) and absorber, a focus

38

on reducing the investment cost of components is reasonable in attain the lowest cycle cost. The exergy efficiencies for components of the fourth CHP cycle are also listed at Table 3. It can be indicated that the combustion chamber (CC), GT and AC have the highest component efficiencies, at 96.5%, 94.2% and 92.9%, respectively.

Table 3 Fuel and product unit costs, exergy efficiency and exergoeconomic factor for each component of CHP with the steam injection into the gasifier and combustion chamber for different value of the average annual rate of the cost of money

	i_{eff}= 4%			i_{eff}= 12%			
	c_f	c_p	f	c_f	c_p	f	ε
Component	$(\$/GJ)$	$(\$/GJ)$	$(\%)$	$(\$/GJ)$	$(\$/GJ)$	$(\%)$	$(\%)$
AC	3.945	4.813	65.45	4.655	6.043	74.49	92.93
Gasifier	2.245	2.556	20.73	2.153	2.529	33.16	87.83
CC	3.122	3.334	10.37	3.451	3.69	16	96.47
GT	3.334	3.945	66.38	3.69	4.655	76.44	94.2
HRSG1	3.334	3.853	6.359	3.69	4.288	10.04	87.28
HRSG2	3.334	4.185	2.17	3.69	4.673	3.514	36.86
HPST	6.216	8.274	45.97	7.288	10.31	56.9	84.83
LPST	5.887	8.274	41.33	6.864	10.31	52.23	81.14
Con_ST	5.887	34.35	37.21	6.864	46.97	48.04	24.8
OFW	5.884	16.56	78.61	6.864	17.93	75.92	72.04
CFW1	8.443	9.366	96.55	9.661	10.59	96.08	99.6
CFW2	7.048	9.449	48.35	8.139	10.73	44.8	85
Gen	4.185	13.27	3.1	4.673	15.02	4.897	32.2
Con_ABS	13.78	20.25	30.23	15.75	24.48	40.81	75
Eva	13.78	16.83	23.06	15.75	19.72	32.29	85.43
ABS	14.15	31.53	10.83	16.3	37.57	16.09	47.74
SHX	14.02	16.7	54.9	16.1	20.18	65.84	92.04

6.2 Parametric study of the biomass-driven CHP systems

A parametric study of the investigated CHP cycles is presented in this section. As a key novelty of this paper is the consideration of various types of steam injection into the basic CHP cycle, the impacts of key thermodynamic parameters on general performance of the proposed CHP systems are studied in the parametric investigation. The first investigation examines the effect of the mass flow rate of biomass ($\dot{m}_g$), the mass flow rate of steam injection into the gasifier ($\dot{m}_{SteamInjec tion\_g}$

), mass flow rate of the steam injection in CC ($\dot{m}_{SteamInjection\_CC}$), inlet temperature of steam injection (T_{a13}), and inlet temperature of biomass gasification (T_g), on the general performance of the proposed CHP cycles, including energy and exergy efficiencies (η_{tot} and ε_{tot}), costs of exergy destruction, investment cost and CO_2 emissions. Then effects of two parameters on overall performance of fourth CHP system are examined.

Fig. 11 displays the impact of varying biomass mass flow rate on gasifier performance for second, third and the fourth CHP cycles. Increasing the biomass mass flow rate to gasifier is seen to decrease the energy efficiency of all three cycles, by 6.1%, 4.6% and 4.3% for the second, third and fourth CHP cycles, respectively. This trend occurs because, with increasing biomass mass flow rate, both input energy to cycle and the power production of cycle increase, but the percentage increase in input energy is greater than the percentage increase in power production. As also display by Fig. 11 (a), the exergy efficiency reduces slightly as biomass mass flow rate increments to second cycle, from 49.48% to 49.26%, while it increases for the third and fourth cycles, by 0.94% and 1.02%, respectively. The process may be explained as follows: in the third and fourth cycles, resulting from the increase in biomass mass flow, the total amount of production power increases more than in the second case (while the energy and exergy input to the cycles increases similarly); accordingly, the efficiencies increases. In addition, with biomass mass flow rate increase from 0.7 to 1.35 kg/s, the CO_2 emission decreases slightly in the second and third cycles. This is explained by equation (29), because, as biomass mass flow rates increase, the net power production of the cycles increases; therefore, CO_2 emissions decrease.

The exergy destruction costs and the investment costs exhibit an increasing trend with raising biomass mass flow rate. Due to the increased exergy destruction rate of components, the cost of

exergy destruction has increased. Moreover, as biomass flow rates increase in the combustion chamber, investment costs for components such as gas turbine and air compressor increase significantly, which explains why total investment costs are increasing. As the biomass flow rate raises from 0.7 kg/s to 1.4 kg/s for the fourth CHP cycle, the exergy destruction cost is seen to increase of 80.19 $/h to 148.4 $/h and investment costs from 93 $/h to 172.5 $/h.
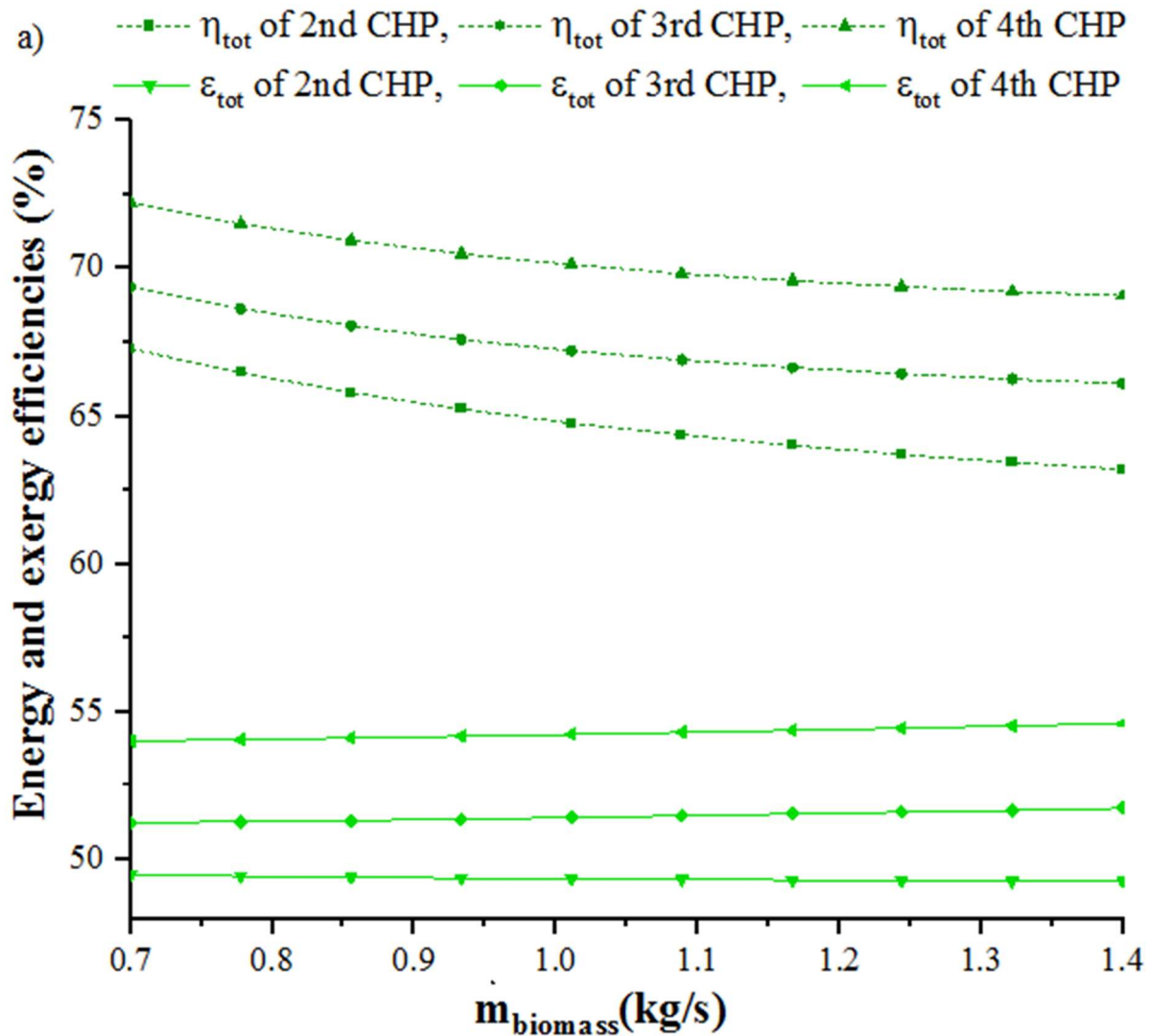
a)

η_{tot} of 2nd CHP, η_{tot} of 3rd CHP, η_{tot} of 4th CHP
ε_{tot} of 2nd CHP, ε_{tot} of 3rd CHP, ε_{tot} of 4th CHP

Energy and exergy efficiencies (%)

$\dot{m}_{biomass}$(kg/s)

b)

Legend:
- $\dot{Z}_{tot}$ of 2nd CHP,
- $\dot{Z}_{tot}$ of 3rd CHP,
- $\dot{Z}_{tot}$ of 4th CHP
- $\dot{C}_{D,tot}$ of 2nd CHP,
- $\dot{C}_{D,tot}$ of 3rd CHP,
- $\dot{C}_{D,tot}$ of 4th CHP

Y-axis: $\dot{Z}_{tot}$ and $\dot{C}_{D,tot}$ (\$/h)

X-axis: $m_{biomass}$ (kg/s)
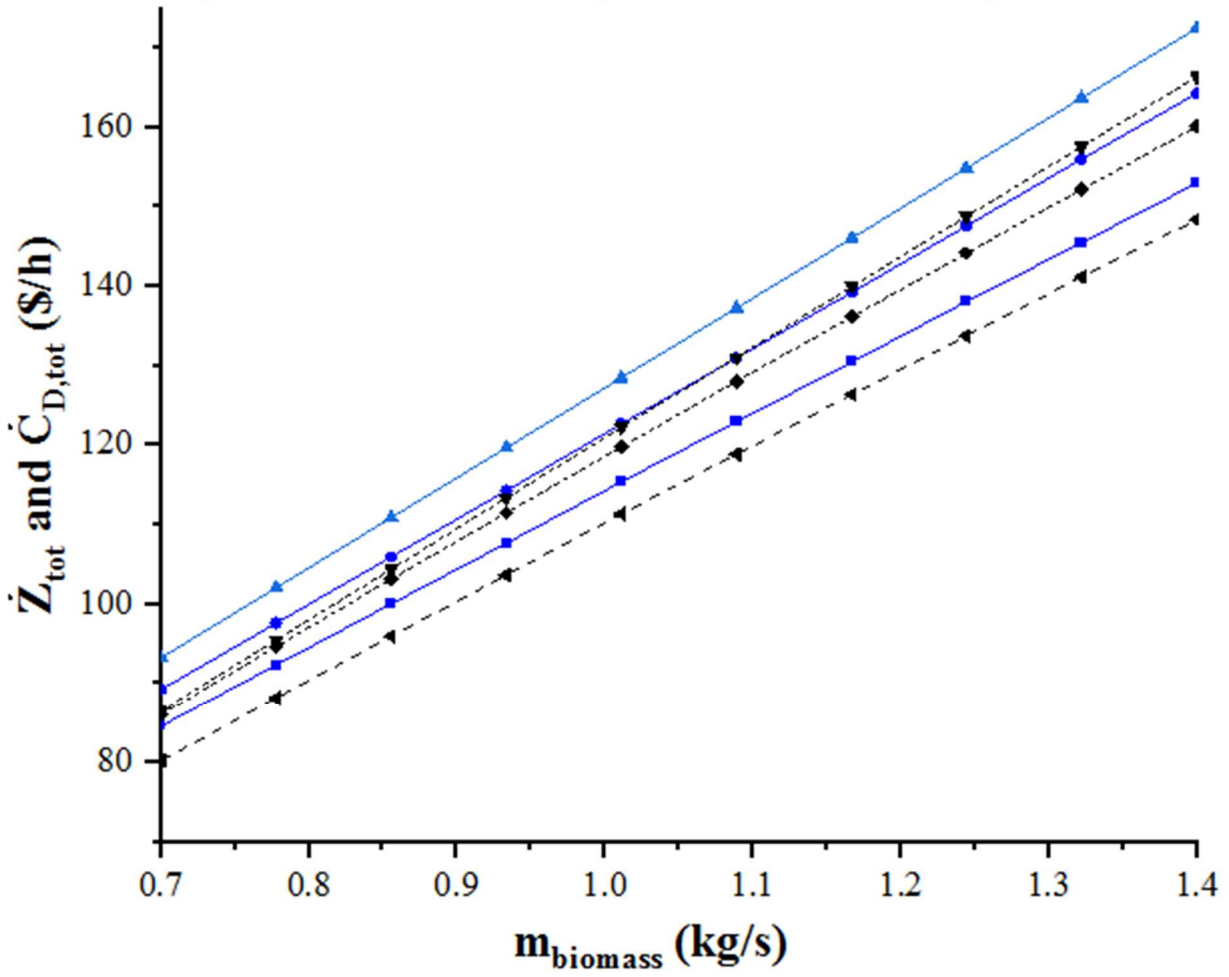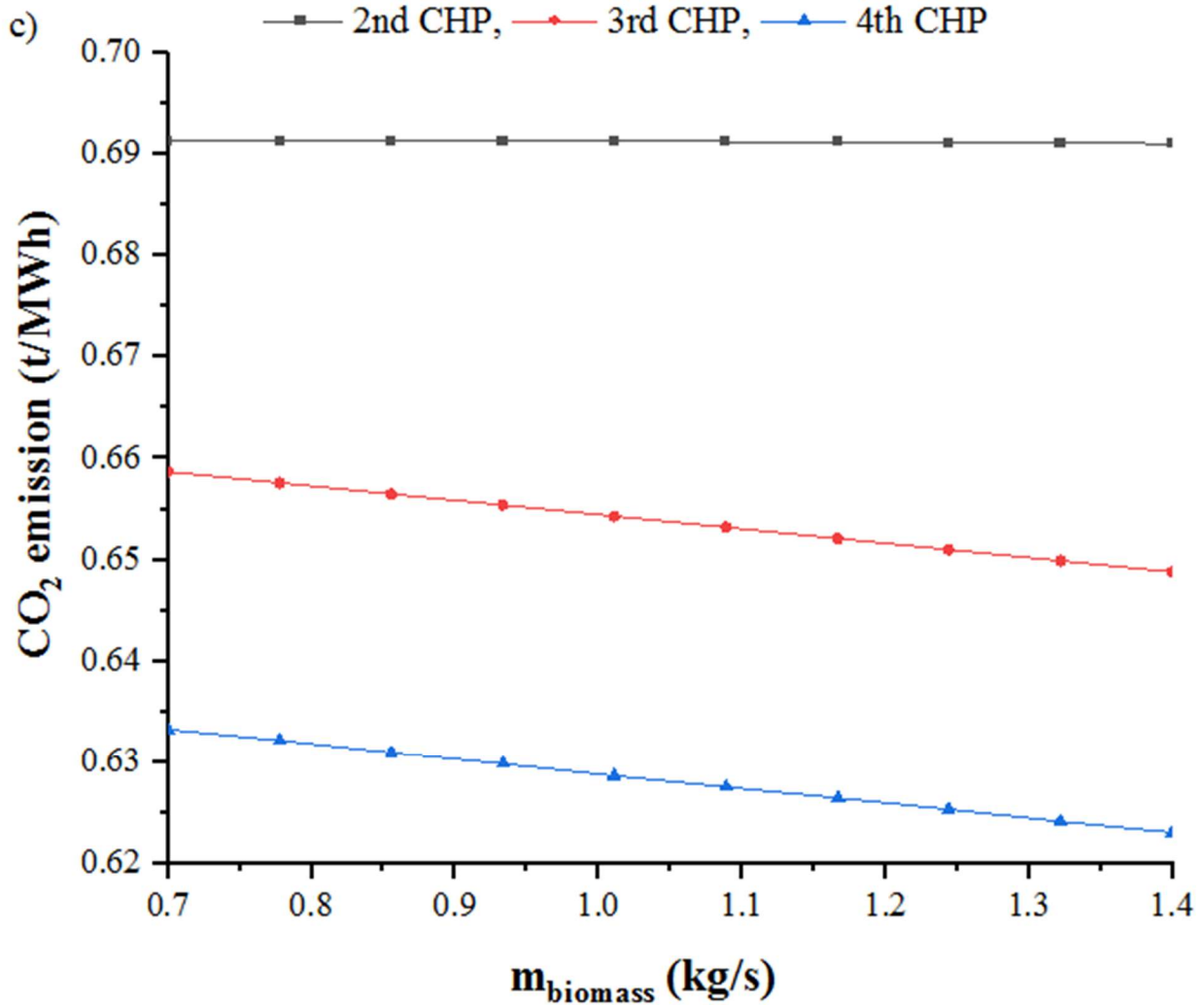
Fig. 11. The effect of varying biomass mass flow rate on: a) the energy and exergy efficiencies, b) total investment cost rate and cost rate associated by exergy destruction, c) CO_2 emission, for the three modified CHP cycles: 2nd CHP (CHP with steam injection to CC), 3rd CHP (CHP with steam injection to gasifier), and 4th CHP (CHP with steam injection to gasifier and CC).

In this paper, wet biomass is considered as input fuel for CHP cycles. Because of this, the moisture content of the inlet biomass fuel (wood), can be considered as a parameter to determine the cycle performance. Fig. 12 shows the effect of biomass gasification temperature, for several moisture percentages of input biomass fuel (10%, 20%, and 30% moisture), on performance of the fourth CHP. The energy and exergy efficiencies of fourth CHP increment slightly as the gasification temperature increments from 1073 K to 1173 K, with varying biomass fuel moisture percentages. For instance, the exergy efficiency of fourth CHP for biomass fuel with 10%, 20%,

43

and 30% moisture contents increases by about 0.57%, 0.53%, and 0.49%, respectively. However, it can be determined in Fig. 12 that increasing the moisture content of biomass fuel increments the both energy and exergy efficiencies of the fourth CHP cycle. For biomass fuel moisture contents of 10%, 20%, and 30%, the exergy efficiency of fourth CHP system rises from 48.55% to 48.84%, 54.29% to 54.58% and 61.05% to 61.35%, respectively. A slight decrease in carbon dioxide emissions is observed with increasing T_g for the fourth CHP cycle. Additionally, as the biomass fuel moisture percentage increases, carbon dioxide emissions decrease. When increasing T_g from 1073 to 1173 K, for input biomass moisture contents of 10%, 20%, and 30%, the CO_2 emissions decrease from 0.6788 to 0.6745 t/MWh, from 0.6287 to 0.625 t/MWh and from 0.5652 to 0.5621 t/MWh, respectively. Moreover, as the biomass gasification temperature increases, the investment costs as well as the costs of the exergy destruction rate, decreases slightly. For increasing moisture contents of biomass fuel, the costs of exergy destruction decrease and investment costs increase. Also, when increasing T_g, for input biomass moisture contents of 10, 20 and 30 percent, the investment cost of the fourth CHP cycle declines from 115.8 to 114.8 $/h, 128.8 to 127.7 $/h, and 147.6 to 146.5 $/h, respectively, also the costs of exergy destruction rate of cycle declines from 130.2 to 127.9 $/h, 112.2 to 110.5 $/h, and 90.2 to 89.03 $/h, respectively.

The results indicate that increasing the moisture content of the gasifier generally has a positive effect on the performance of the cycle as it increases efficiencies and reduces carbon dioxide emissions. Furthermore, increasing the temperature of the gasifier due to an increase in the cycle's production power could improve its performance.
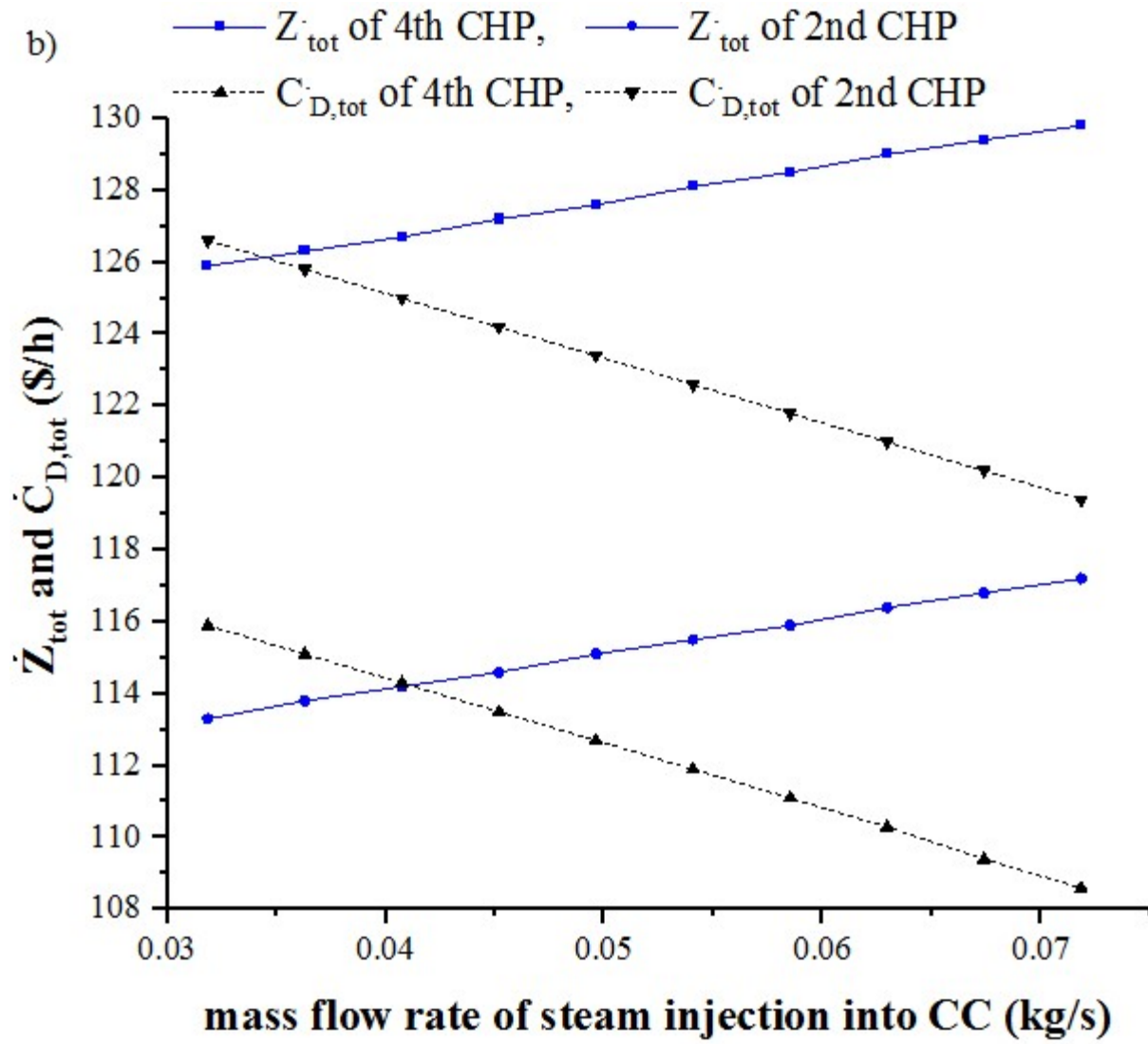
a)

b)
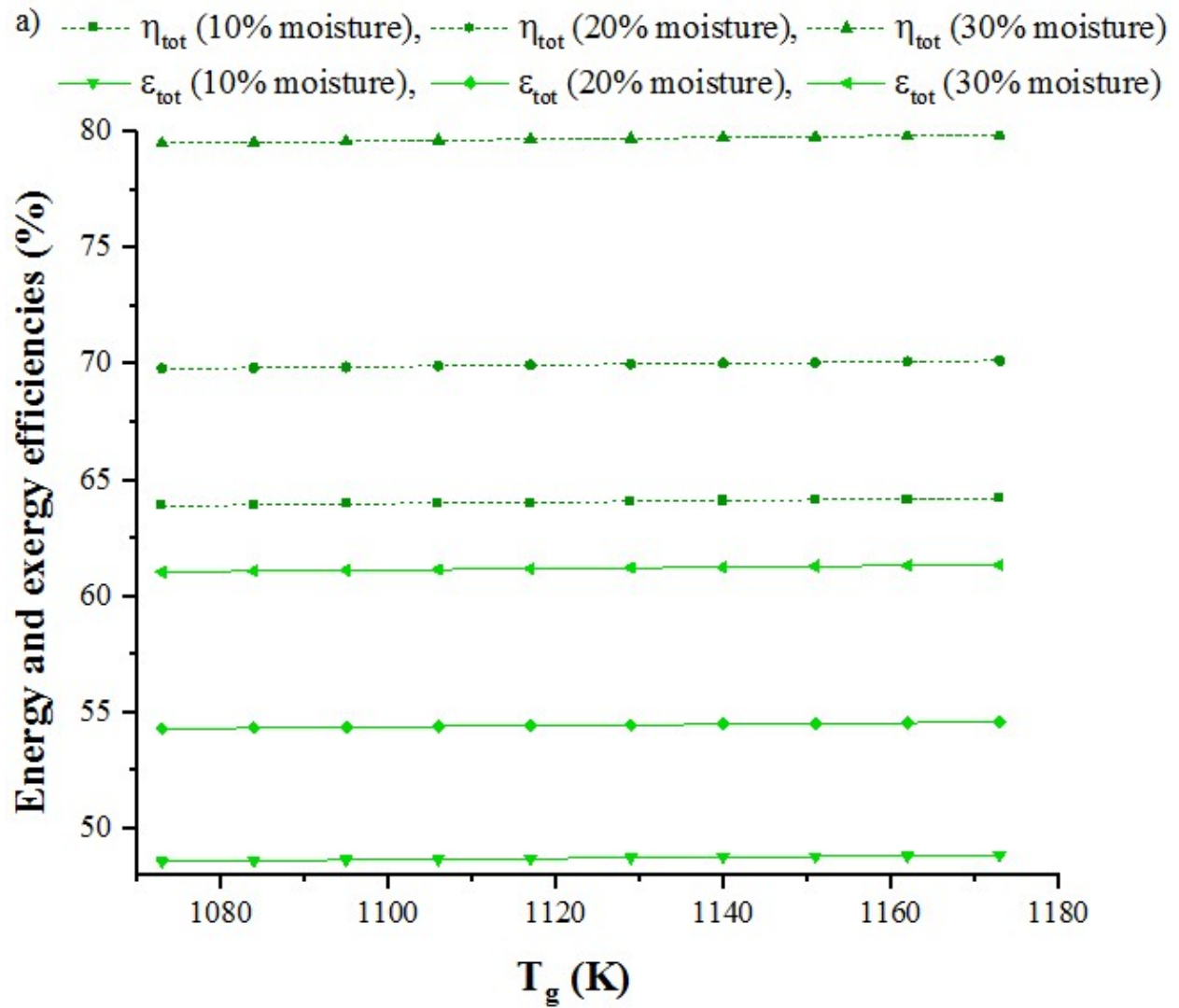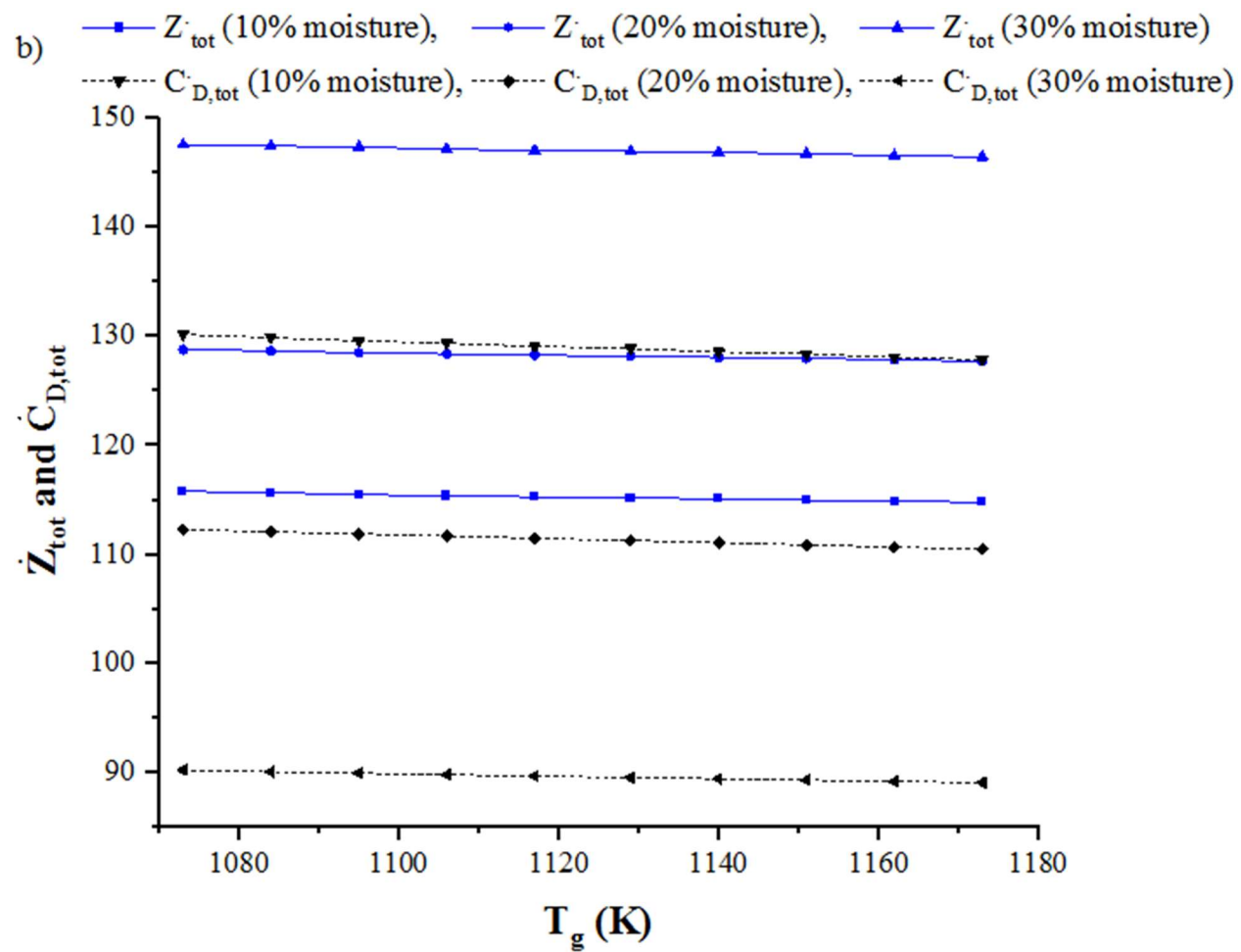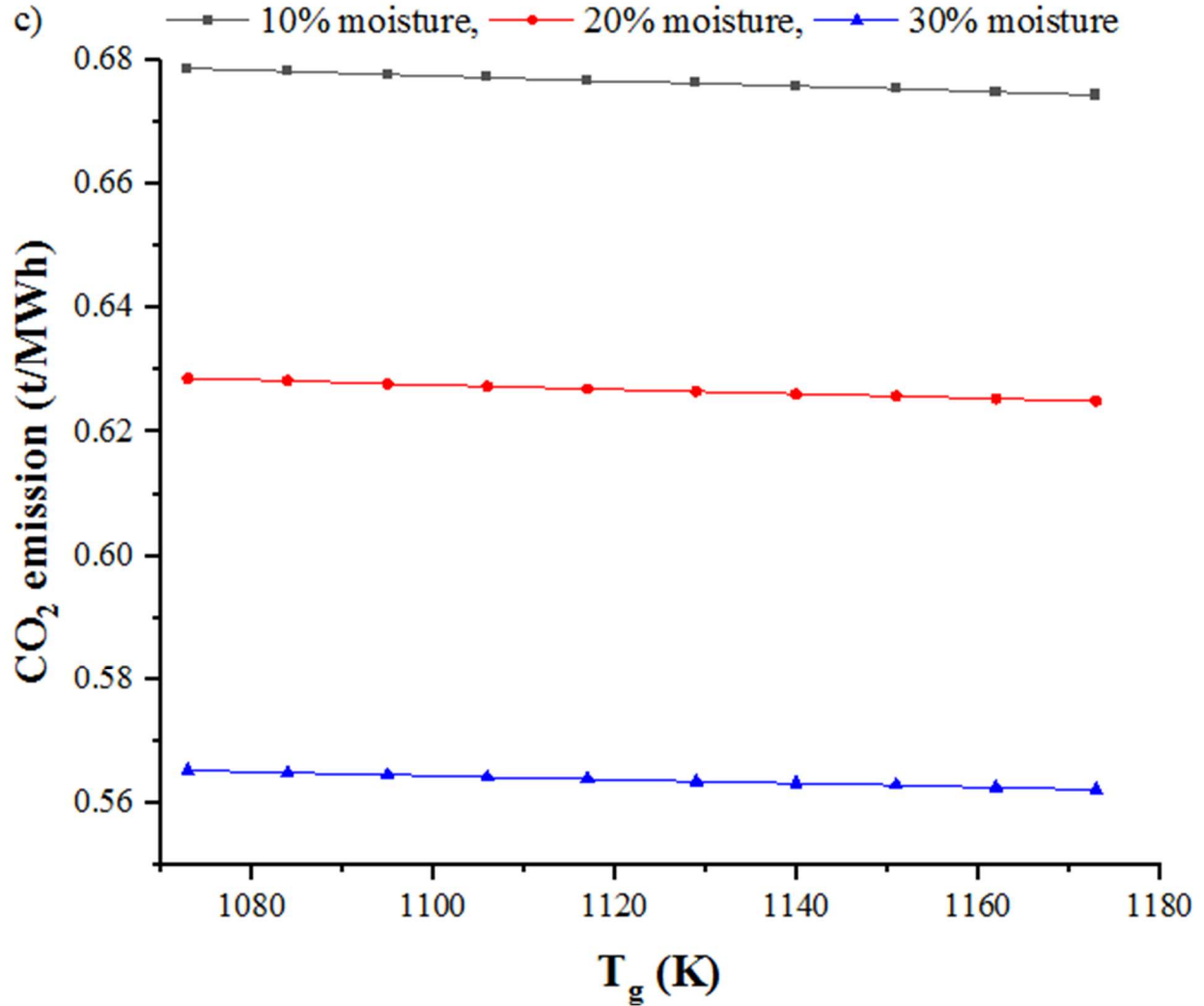
Fig. 12. Effect of varying biomass gasification temperature, for several percentages of biomass moisture content on: a) the system energy and exergy efficiencies, b) total investment cost rate and the cost rate associated with exergy destruction, c) CO_2 emission, for CHP cycle with steam injection to the CC and gasifier.

The impacts of varying mass flow rates of steam injection to CC on performance of second and fourth CHP cycles are shown in Fig. 13. Note that the steam injection rate to the gasifier remains constant for the fourth CHP cycle by changing $\dot{m}_{SteamInjection\_CC}$. As shown by Fig. 13, energy and exergy efficiencies of second and fourth CHP systems increase by 2.96% and 3.2% as $\dot{m}_{SteamInjection\_CC}$ rises from 0.032 kg/s to 0.072 kg/s. Due to the increase of $\dot{m}_{SteamInjection\_CC}$ and the

observation that the inlet heat to the cycles is constant, the net power generated by the CHP cycles raise. In addition, as the steam injection mass flow rate to combustion chamber increases, the CO_2 emitted for the CHP cycles decreases due to the lower production rate of CO_2 in the combustion chamber. By increasing $\dot{m}_{SteamInjection\_CC}$, the CO_2 emission declines from 0.7118 t/MWh to 0.6874 t/MWh for the second CHP cycle and from 0.6379 t/MWh to 0.6161 t/MWh for the fourth CHP cycle. Increasing $\dot{m}_{SteamInjection\_CC}$ reduces the total cost rate of exergy destruction for second and fourth CHP cycles (from 126.6 \$/h to 119.4 \$/h and 115.9 \$/h to 108.6 \$/h, respectively) by reducing the rates of exergy destruction of cycles, especially in combustion chamber and gas turbine components. However, by increasing $\dot{m}_{SteamInjection\_CC}$, total system investment costs have increased due to an increase in investment costs in components such as gas turbines and air compressors. Thus, when the $\dot{m}_{SteamInjection\_CC}$ increases from 0.032 kg/s to 0.072 kg/s, the second cycle investment costs increase from 113.3 \$/h to 117.2 \$/h and the fourth cycle investment costs increase from 125.9 \$/h to 129.8 \$/h.

a)

b)

Legend: $\dot{Z}_{tot}$ of 4th CHP, $\dot{Z}_{tot}$ of 2nd CHP, $\dot{C}_{D,tot}$ of 4th CHP, $\dot{C}_{D,tot}$ of 2nd CHP

Y-axis: $\dot{Z}_{tot}$ and $\dot{C}_{D,tot}$ ($/h)

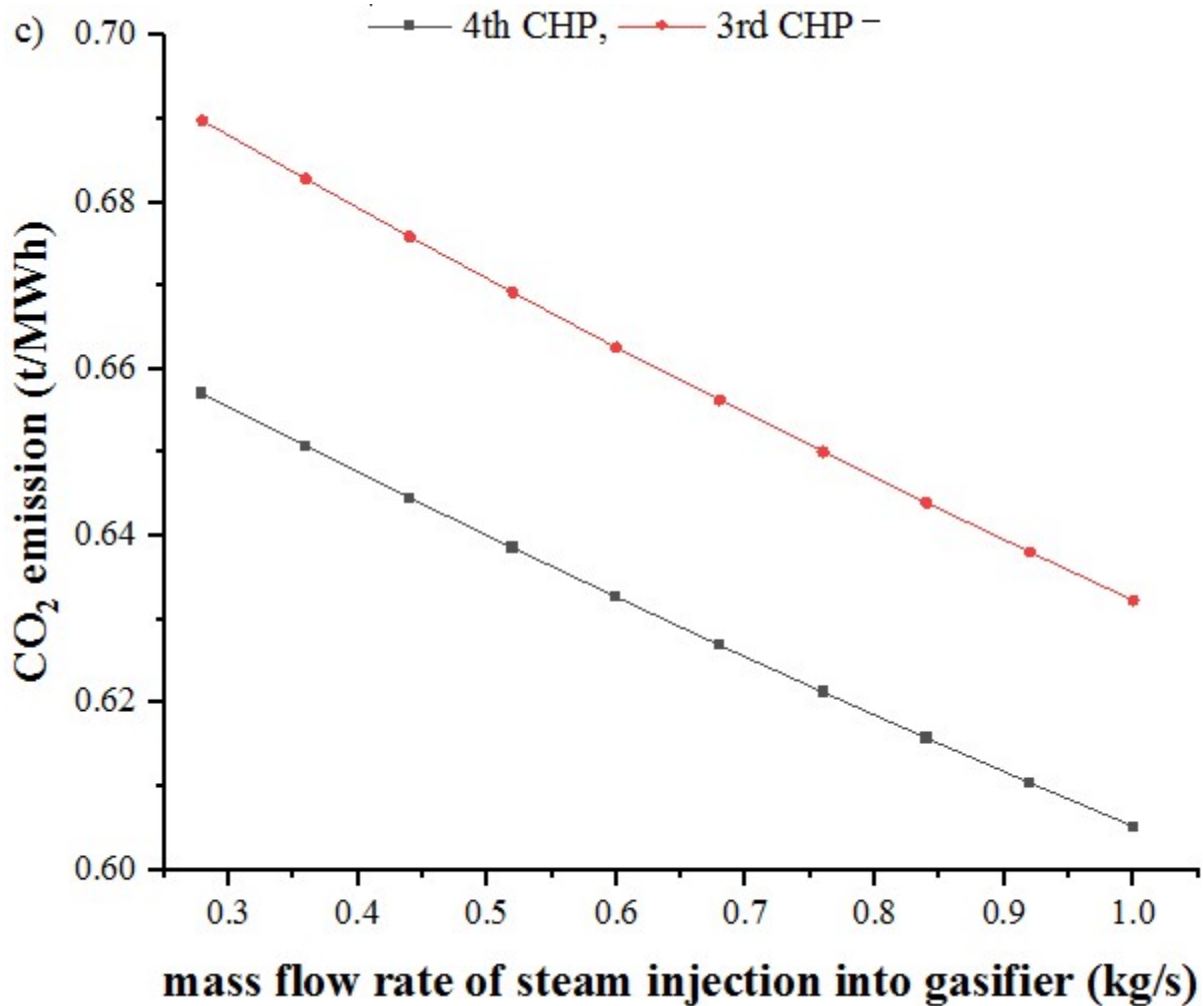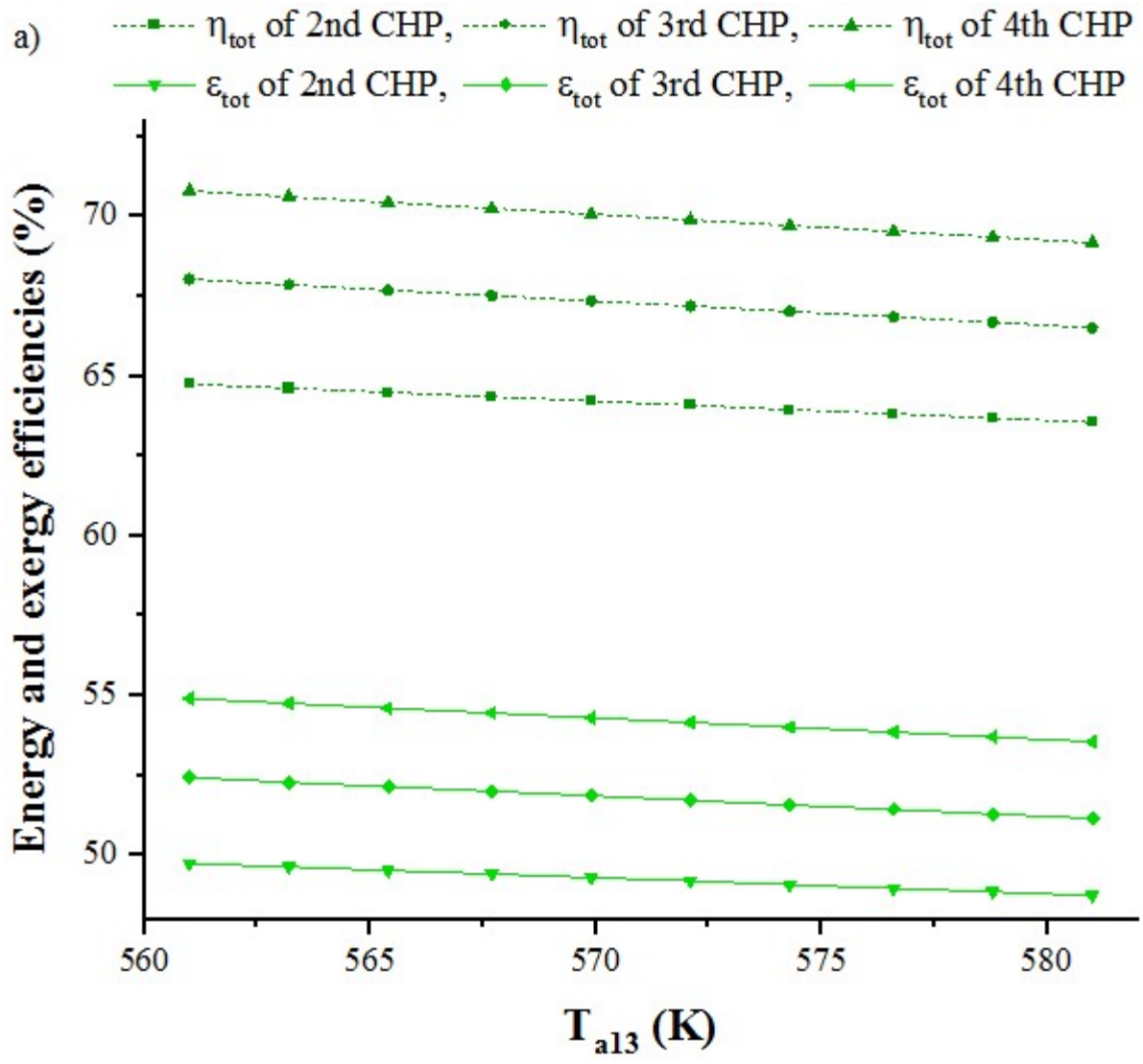X-axis: mass flow rate of steam injection into CC (kg/s)
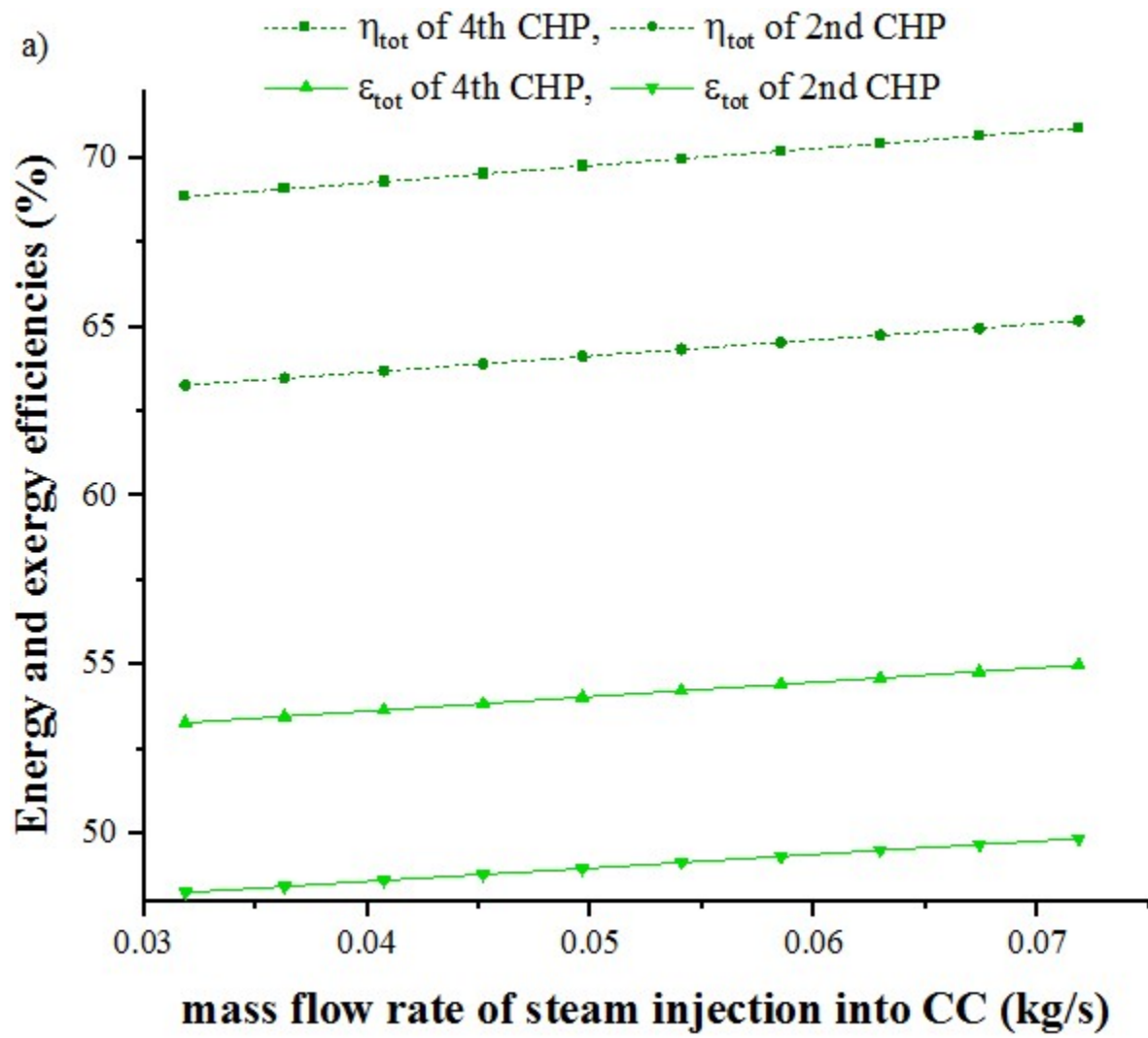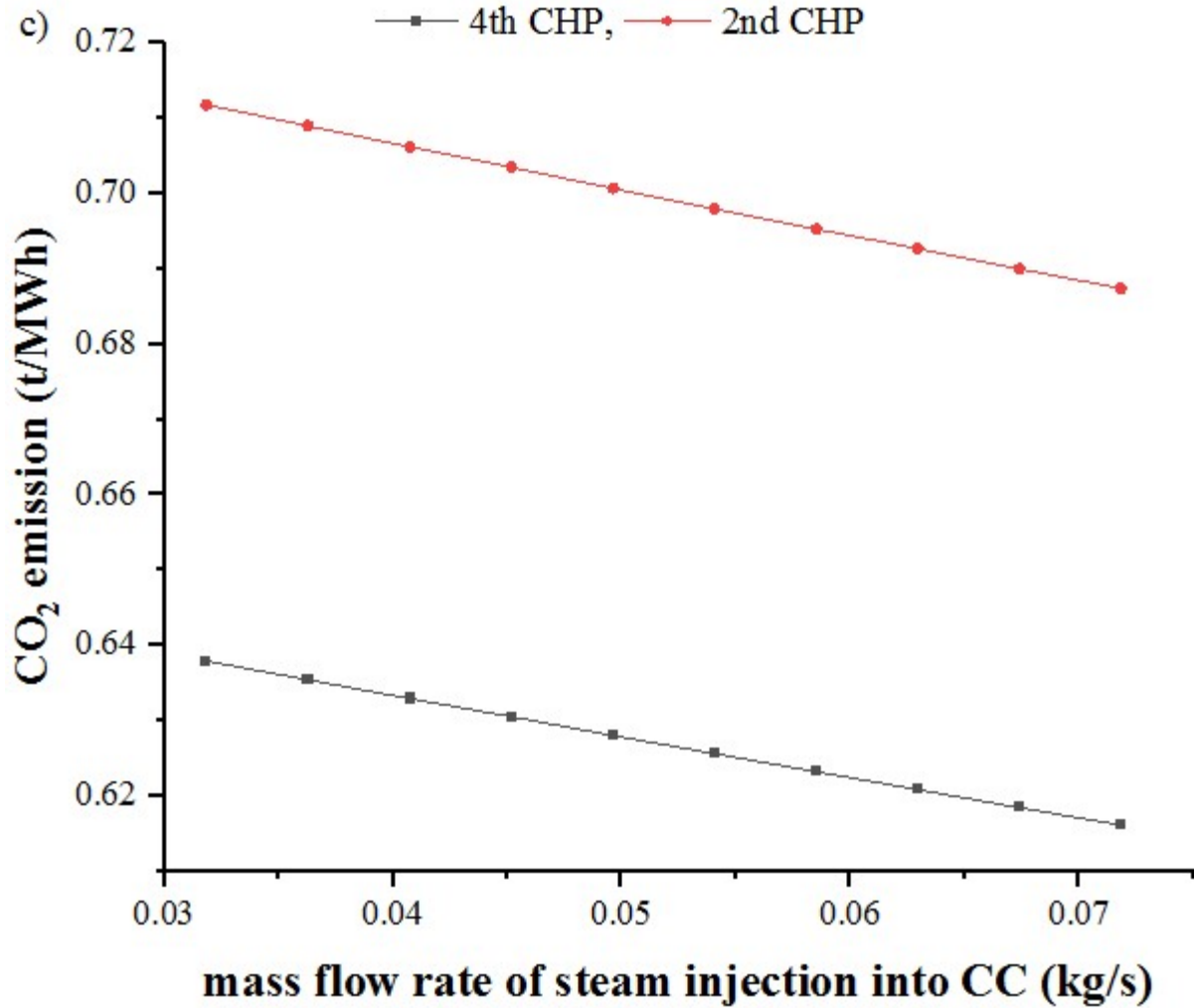
Fig. 13. The effect of varying the mass flow rate of the steam injection to CC on: a) energy and exergy efficiencies, b) total investment cost and the total cost associated by exergy destruction, c) CO_2 emission, for 2nd CHP cycle (CHP with steam injection to CC) and 4th CHP cycle (CHP with steam injection to CC and gasifier). Notable; mass flow rate of steam injection into gasifier at the 4th CHP is constant.

Fig. 14 demonstrates the effect of changing the mass flow rate of steam injection into gasifier on the performance of third and fourth CHP cycles. As $\dot{m}_{SteamInjection\_g}$ increases by 0.2796 kg/s to 1 kg/s, the efficiencies of the CHP cycles increase. For the fourth CHP cycle, the corresponding energy efficiency increase is from 67.12% to 71.97% and the corresponding exergy efficiency increase is from 51.78% to 55.84%. Increasing $\dot{m}_{SteamInjection\_g}$ increases the mass flow rate of hot gases produced in the combustion chamber, and because of this, the power output in the gas

51

turbine cycle is increased, resulting in improved efficiencies. Additionally, the CO_2 emission for the two investigated cycles in this figure decreases due to a reduction in the carbon dioxide generated in the combustion chamber. In both investigated CHP cycles in Fig. 14, investment costs rise as $\dot{m}_{SteamInjection\_g}$ increases; investment costs increase from 116 \$/h to 127.2 \$/h for the third CHP cycle and from 122.4 \$/h to 133.5 \$/h for the fourth CHP cycle. The increase in investment costs can also be justified by the fact that gas turbine components are more expensive due to an increase in power production by an increase in $\dot{m}_{SteamInjection\_g}$. However, for the fourth proposed CHP cycle, the costs of exergy destruction decrease slightly (from 110 \$/h to 109.4 \$/h), mainly because of reduction in exergy destruction at gasifier and combustion chamber. For the third cycle, however, the exergy destruction costs increase from 114.7 \$/h to 119.7 \$/h due to the increased exergy destruction rate in the gasifier and combustion chamber.
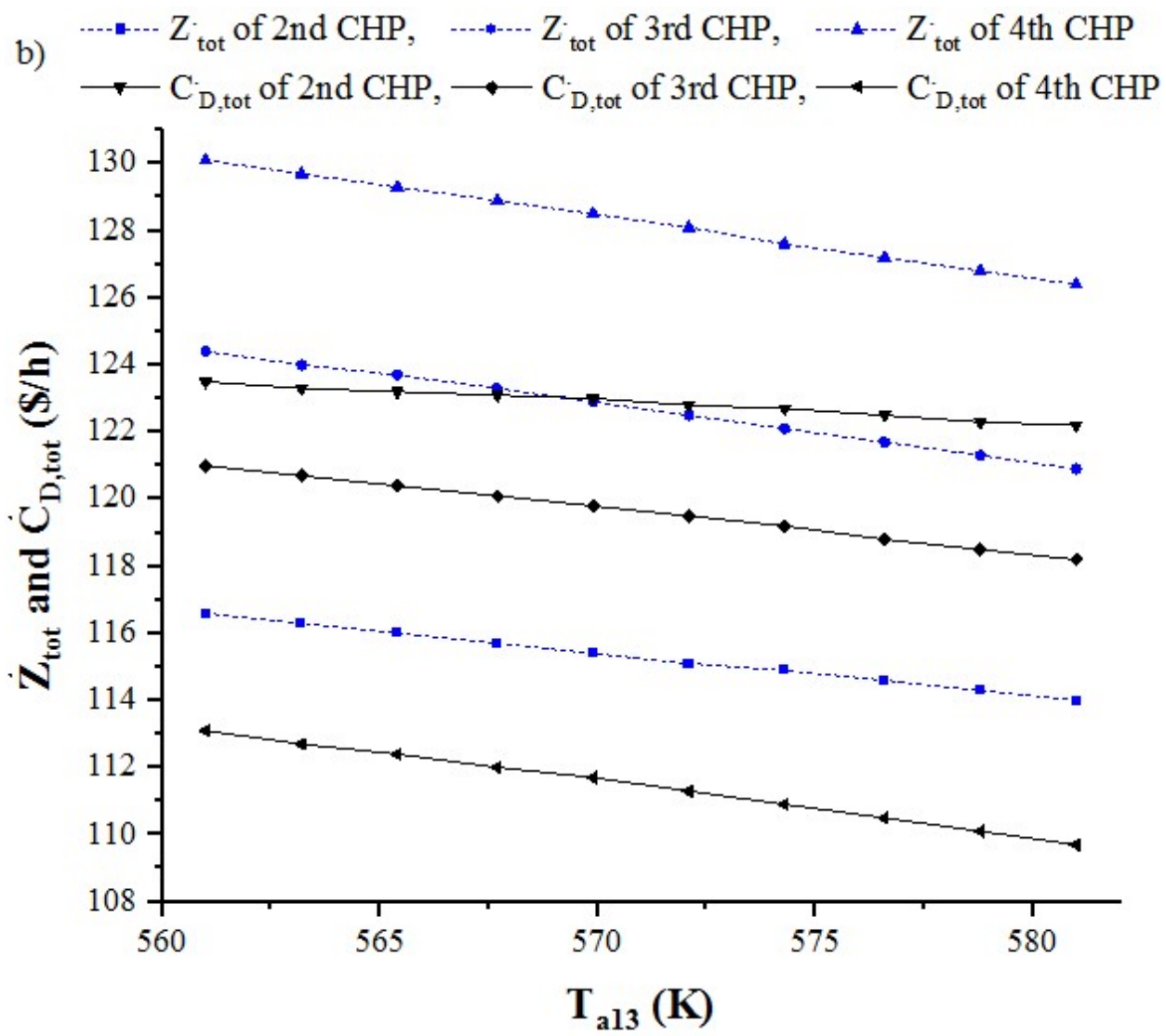
a)

b)

Legend:
- $\dot{Z}_{tot}$ of 4th CHP,
- $\dot{Z}_{tot}$ of 3rd CHP
- $\dot{C}_{D,tot}$ of 4th CHP,
- $\dot{C}_{D,tot}$ of 3rd CHP

Y-axis: $\dot{Z}_{tot}$ and $\dot{C}_{D,tot}$ ($/h)

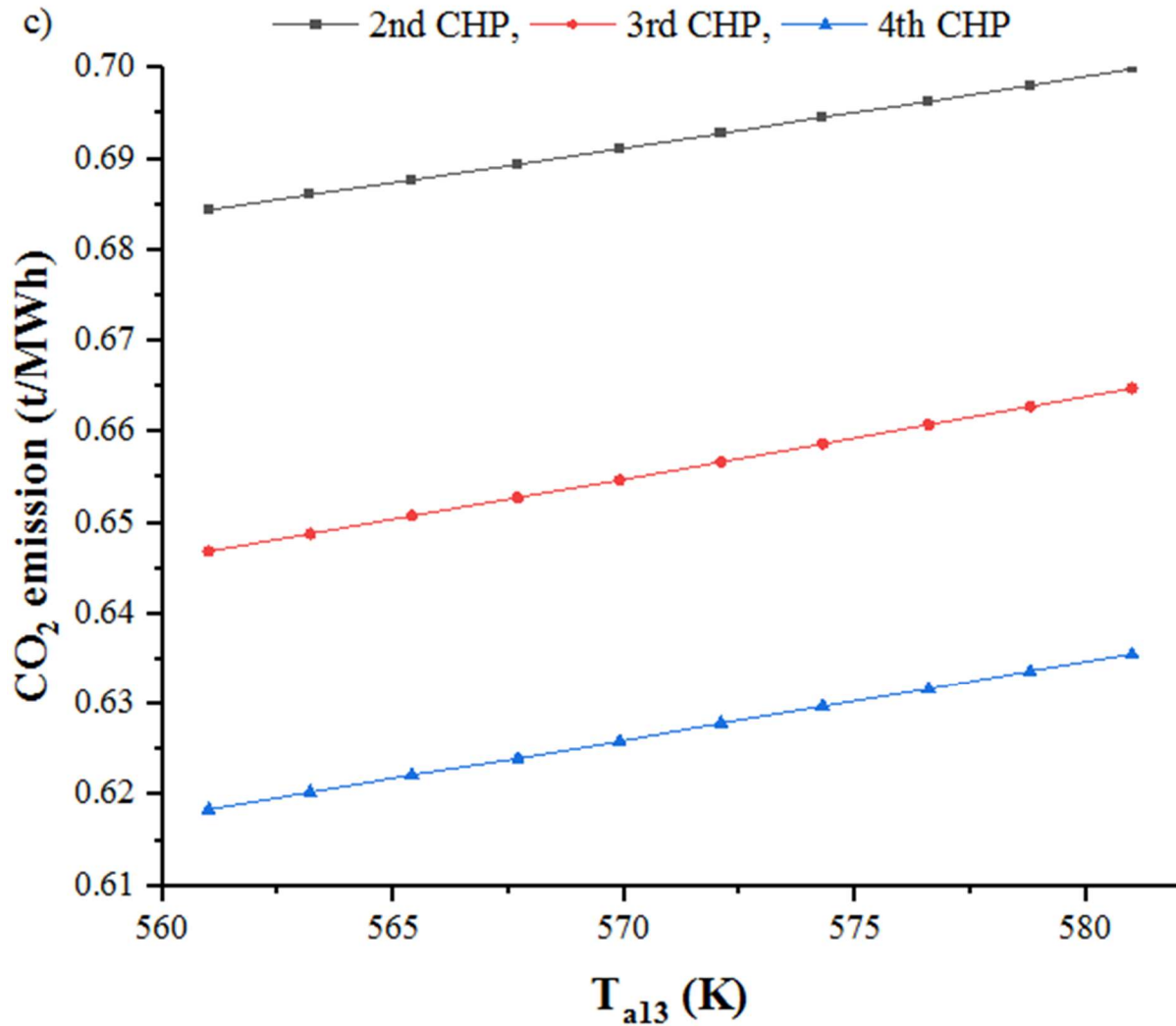X-axis: mass flow rate of steam injection into gasifier (kg/s)
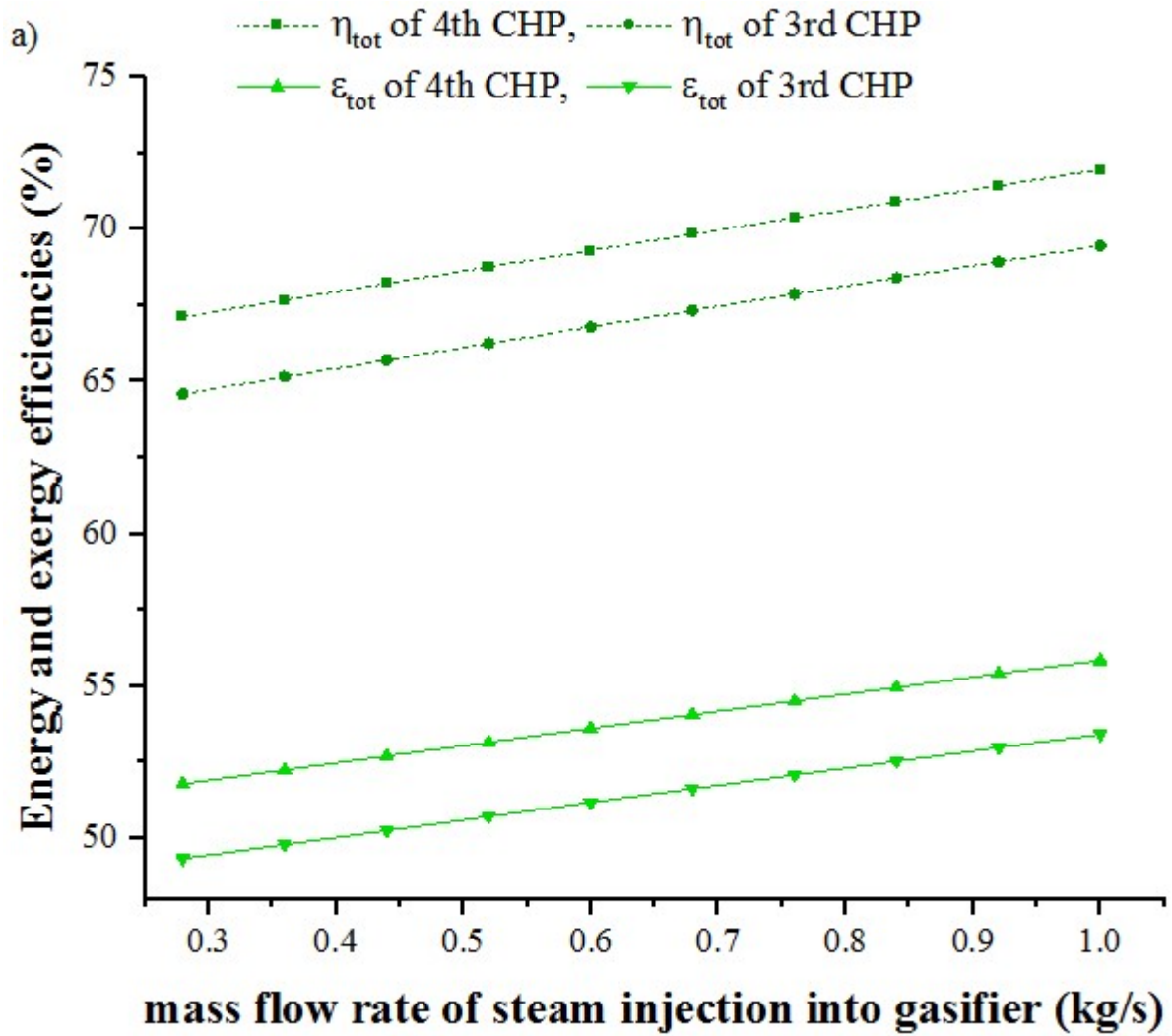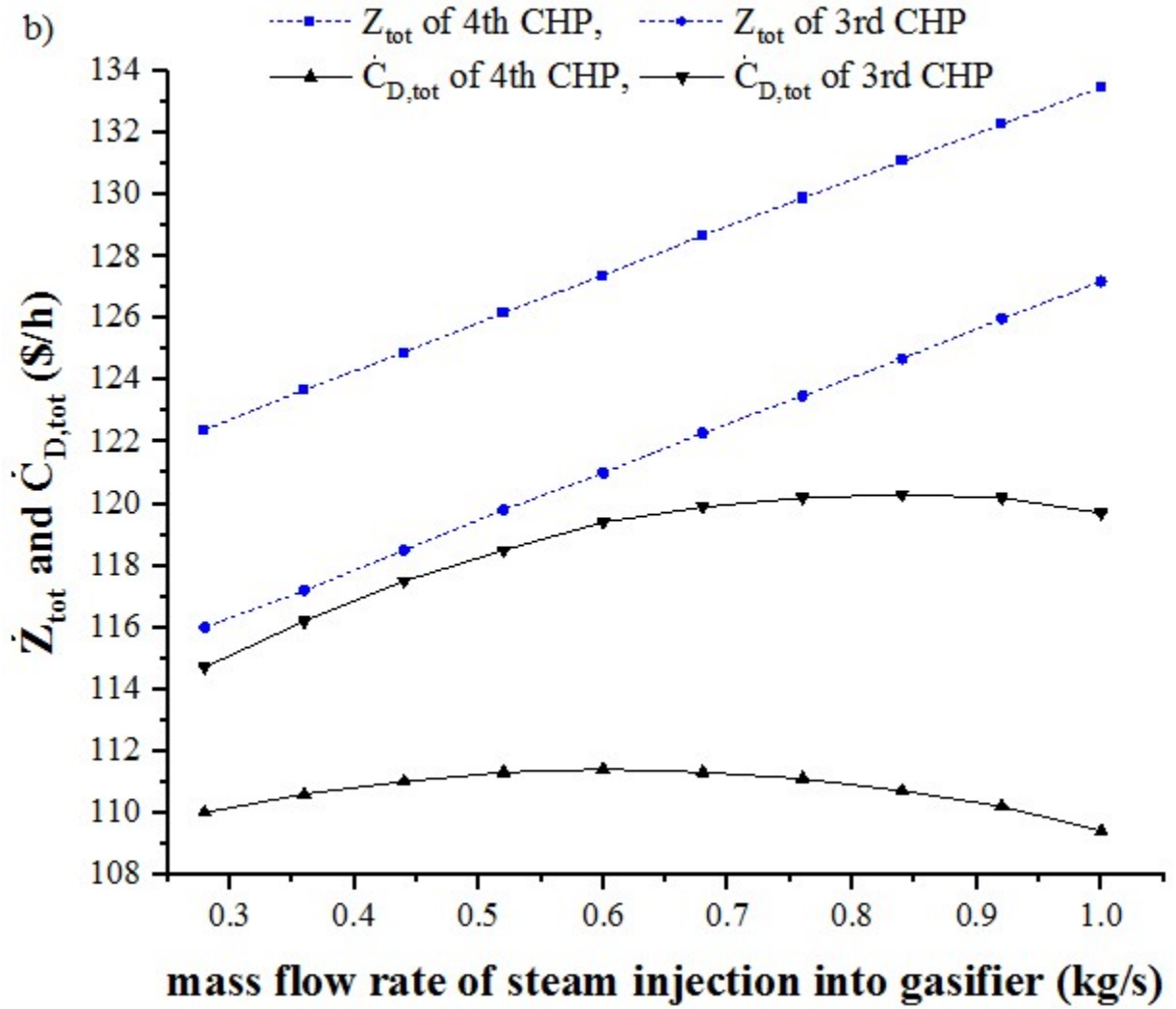
Fig. 14. The effect of changing mass flow rate of steam injection to gasifier on: a) energy and exergy efficiencies, b) total investment cost and the total cost associated by exergy destruction, c) CO_2 emission, for 3rd CHP cycle (CHP with steam injection to gasifier) and 4th CHP cycle (CHP with steam injection to CC and gasifier). Notable; mass flow rate of steam injection into CC at the 4th CHP is constant.

Fig. 15 illustrates the effect of changing the steam injection temperature on performance of the second, third and fourth CHP cycles. It can be determined that with raising T_{a13}, the efficiencies of the three CHP cycles decrease. When T_{a13} increases, the steam fluid mass flow rate in the steam turbine cycle decreases, causing a decrease in power output in this cycle and, consequently, a decrease in total CHP power output and efficiencies. As T_{a13} increases from 561

K to 581 K, the exergy efficiencies in the second, third and fourth CHP cycles decline from 49.75% to 48.74%, from 52.44% to 51.16%, and from 54.91% to 53.56% respectively.

Increasing T_{a13} also decreases the net power production by the CHP cycles, resulting in an increase in carbon dioxide emissions from 0.6844 t/MWh to 0.6999 t/MWh for the second CHP cycle, from 0.6469 t/MWh to 0.6648 t/MWh for the third CHP cycle and from 0.6184 t/MWh to 0.6356 t/MWh for the fourth CHP. The costs of exergy destruction rates and investment costs also decrease with increasing T_{a13} for each of the CHP cycles considered. The investment cost decreases from 130.1 $/h to 126.4 $/h for the fourth proposed CHP cycle as T_{a13} increases from 561 K to 581 K. A reduction in investment costs can be explained by the reduction in the investment costs of steam turbine components due to the production of less power in high-pressure steam turbine and low-pressure steam turbine components.

a)

Legend:
- η_{tot} of 2nd CHP,
- η_{tot} of 3rd CHP,
- η_{tot} of 4th CHP
- ε_{tot} of 2nd CHP,
- ε_{tot} of 3rd CHP,
- ε_{tot} of 4th CHP

Y-axis: Energy and exergy efficiencies (%)

X-axis: T_{a13} (K)

b)

Legend:
- $\dot{Z}_{tot}$ of 2nd CHP,
- $\dot{Z}_{tot}$ of 3rd CHP,
- $\dot{Z}_{tot}$ of 4th CHP
- $\dot{C}_{D,tot}$ of 2nd CHP,
- $\dot{C}_{D,tot}$ of 3rd CHP,
- $\dot{C}_{D,tot}$ of 4th CHP

Y-axis: $\dot{Z}_{tot}$ and $\dot{C}_{D,tot}$ ($/h)

X-axis: T_{a13} (K)

Fig. 15. Effect of varying temperature of steam injection into gasifier and CC on: a) energy and exergy efficiencies, b) total investment cost and the total cost associated by exergy destruction, c) CO_2 emission, for 2nd CHP cycle (CHP with steam injection to CC), 3rd CHP cycle (CHP with steam injection to gasifier) and 4th CHP cycle (CHP with steam injection to CC and gasifier).

It is important to determine how two thermodynamic parameters changing simultaneously affect the performance of the proposed CHP cycles through the parametric study. This is accomplished using three-dimensional diagrams. Figs. 16, 17 and 18 show the effects of modifying of two thermodynamic parameters on the exergy efficiency, CO_2 emissions and the total costs (sum of

the total investment costs, costs of the exergy destruction and fuel costs), for the fourth proposed CHP cycle.

Fig. 16 shows the effect of simultaneously varying $\dot{m}_{SteamInjection\_g}$ and $\dot{m}_{SteamInjection\_CC}$ on the performance of the fourth CHP cycle. It can be seen that, with raising mass flow rate of the steam injection to gasifier from 0.3196 kg/s to 1.04 kg/s and to combustion chamber from 0.03185 kg/s to 0.07185 kg/s, the exergy efficiency raises by about 11.1% and the CO_2 emission decreases from 0.6662 t/MWh to 0.5922 t/MWh. It is due to the increase in mass flow rate of steam injection into the system, hot gases exiting the combustion chamber have been moving at a higher mass flow rate. Therefore, the cycle has increased its output power, which has led to an increase in efficiency and a decrease in carbon dioxide emissions. Moreover, the total cycle costs raises by 3.4%, from 402.3 $/h to 416.2 $/h. The results demonstrate that the increase in steam injection to the proposed 4th CHP cycle, with only a slight increase in total costs, has significantly increased exergy efficiency and reduced pollutants. Due to this, simultaneously increasing these two parameters can increase the cycle's performance.

The effects of simultaneously varying the steam injection temperature and biomass gasification temperature on performance of the fourth CHP system are drawn in Fig. 17. A simultaneous increase of steam injection and biomass gasification temperatures, as well as decrease of the net power production of fourth CHP, cause the exergy efficiency of process to decline by 3%, from 54.01% to 55.6%. The carbon dioxide emission for the fourth CHP cycle also increases, by about 3.4%, as net power production decreases. Furthermore, due to a decreasing of both investment costs and the exergy destruction costs, the total cost of fourth CHP is decreased, by about 2.4%.

The effect of simultaneously varying the inlet temperature to gasifier T_g and the inlet temperature to gas turbine T_6 on performance of fourth CHP system is shown by Fig. 18. Due to the simultaneous increase T_g and T_6, the mass flow rate of the steam turbine cycle fluid increased, which increased the production power in high pressure and low pressure turbines. In this way, the exergy efficiency has increased by about 17.8% with the increase in the total production power of the 4th CHP cycle. In contrast, increasing the net power generation of the fourth CHP cycle reduces the carbon dioxide emission for the cycle, from 0.6984 t/MWh to 0.5824 t/MWh. As can be indicated in Fig. 18, the simultaneous increase in both T_g and T_6 has a positive impact on total cost of fourth CHP cycle, reducing it by about 7.3%. It can be explained by the reduction of investment costs and the reduction of exergy destruction costs in gas turbine cycle components.
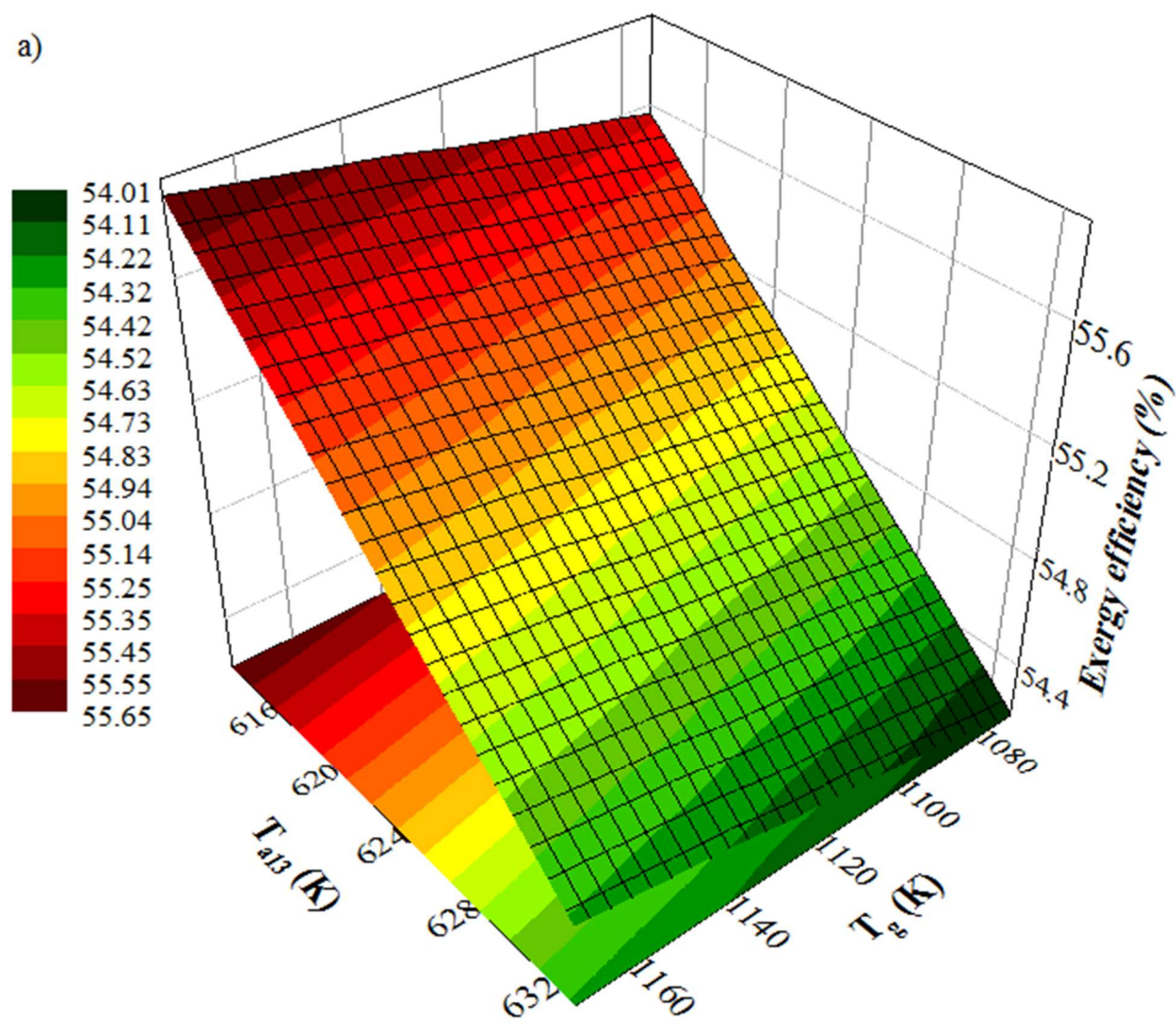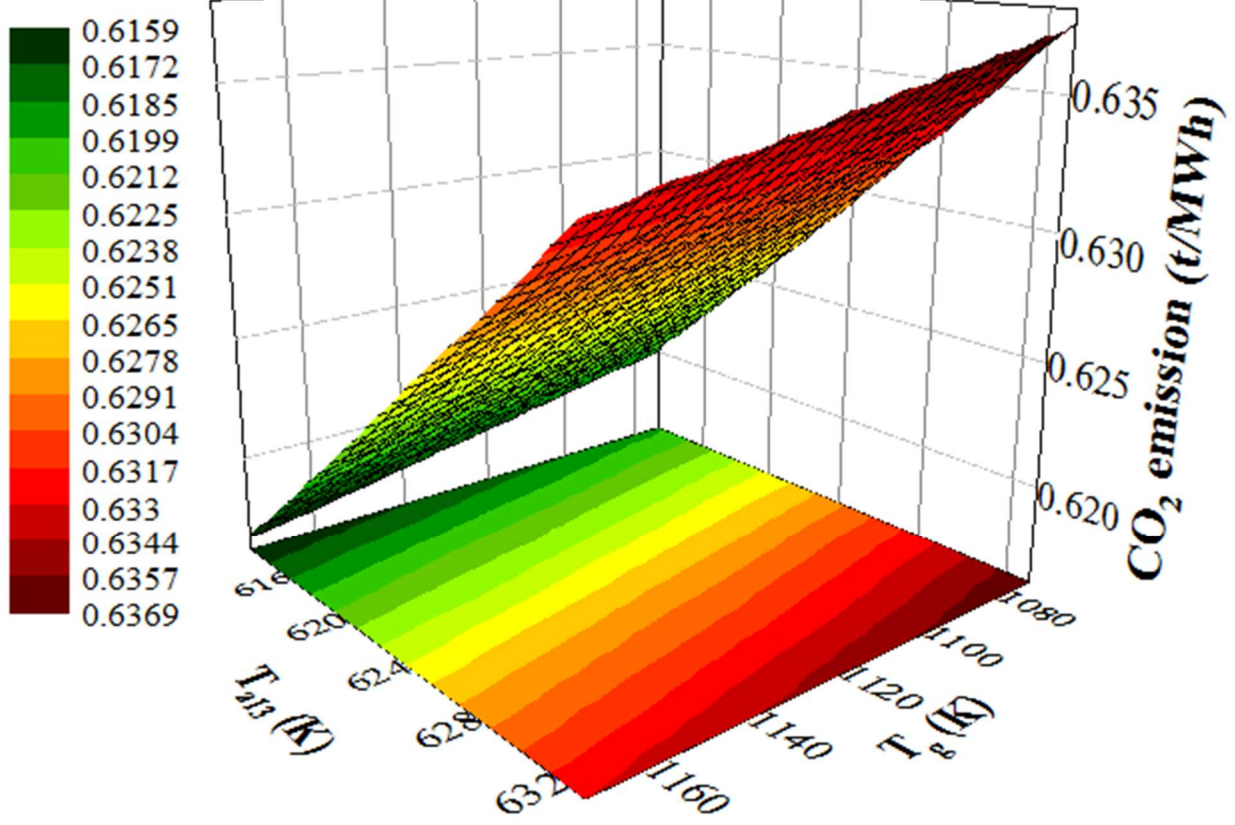
a)
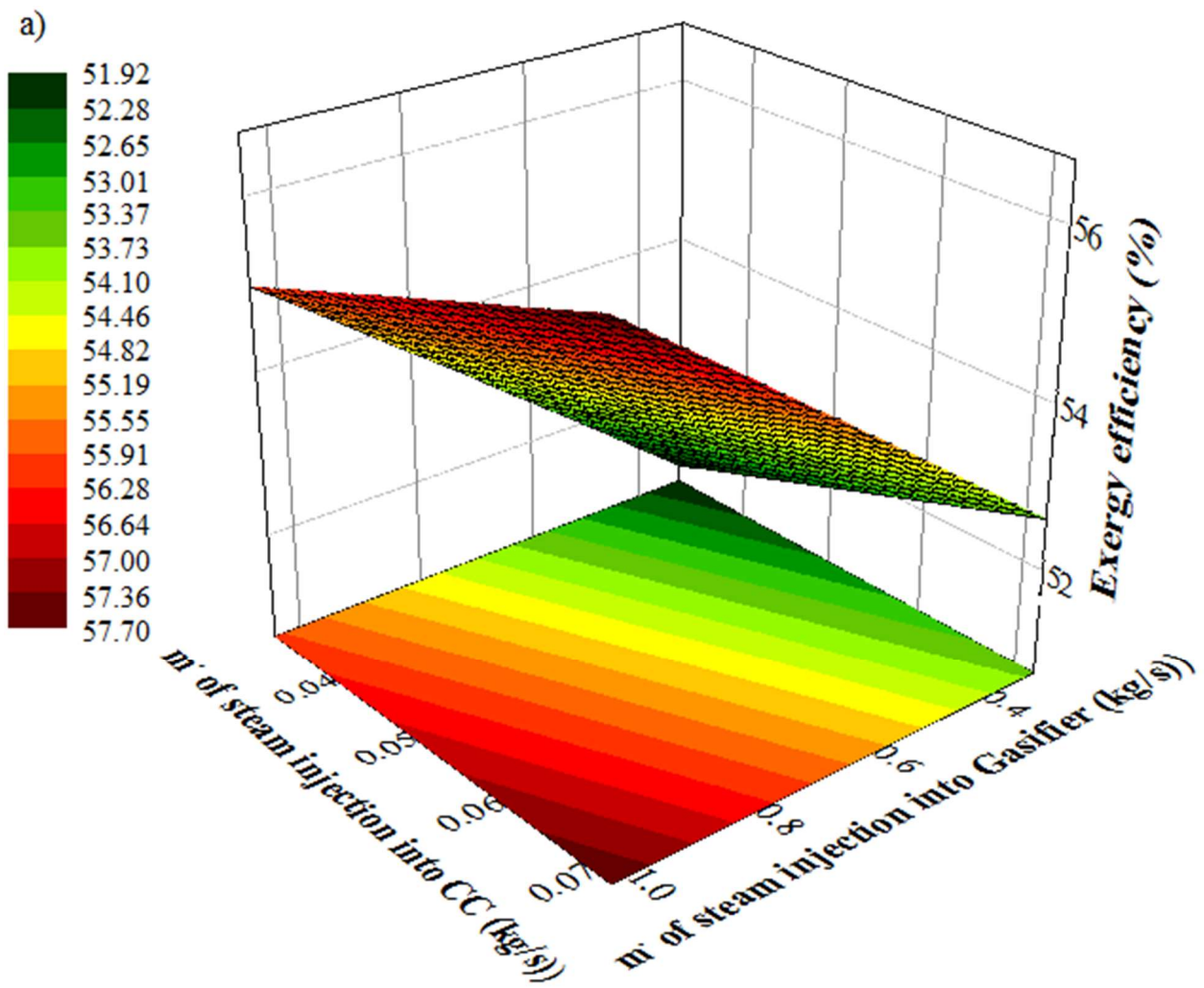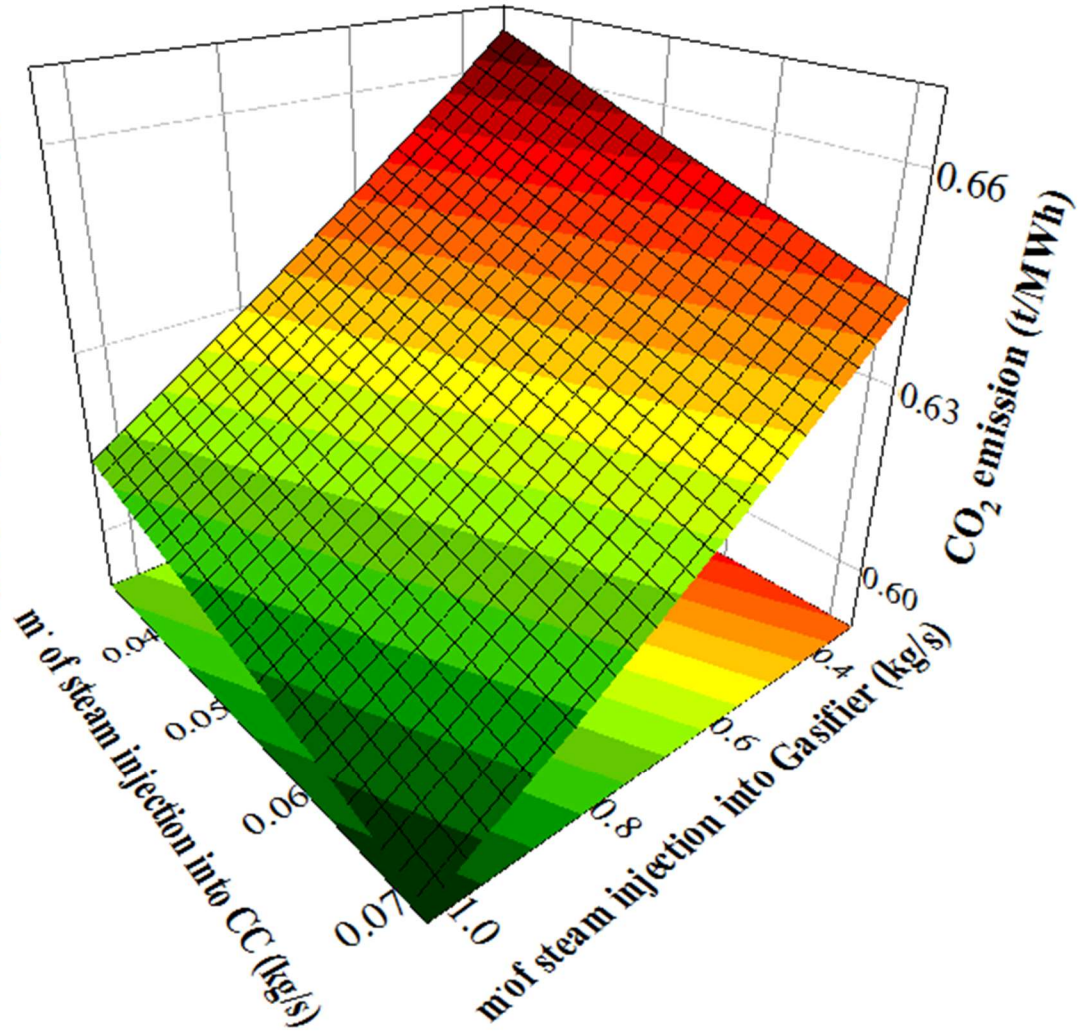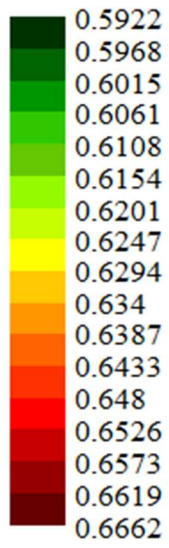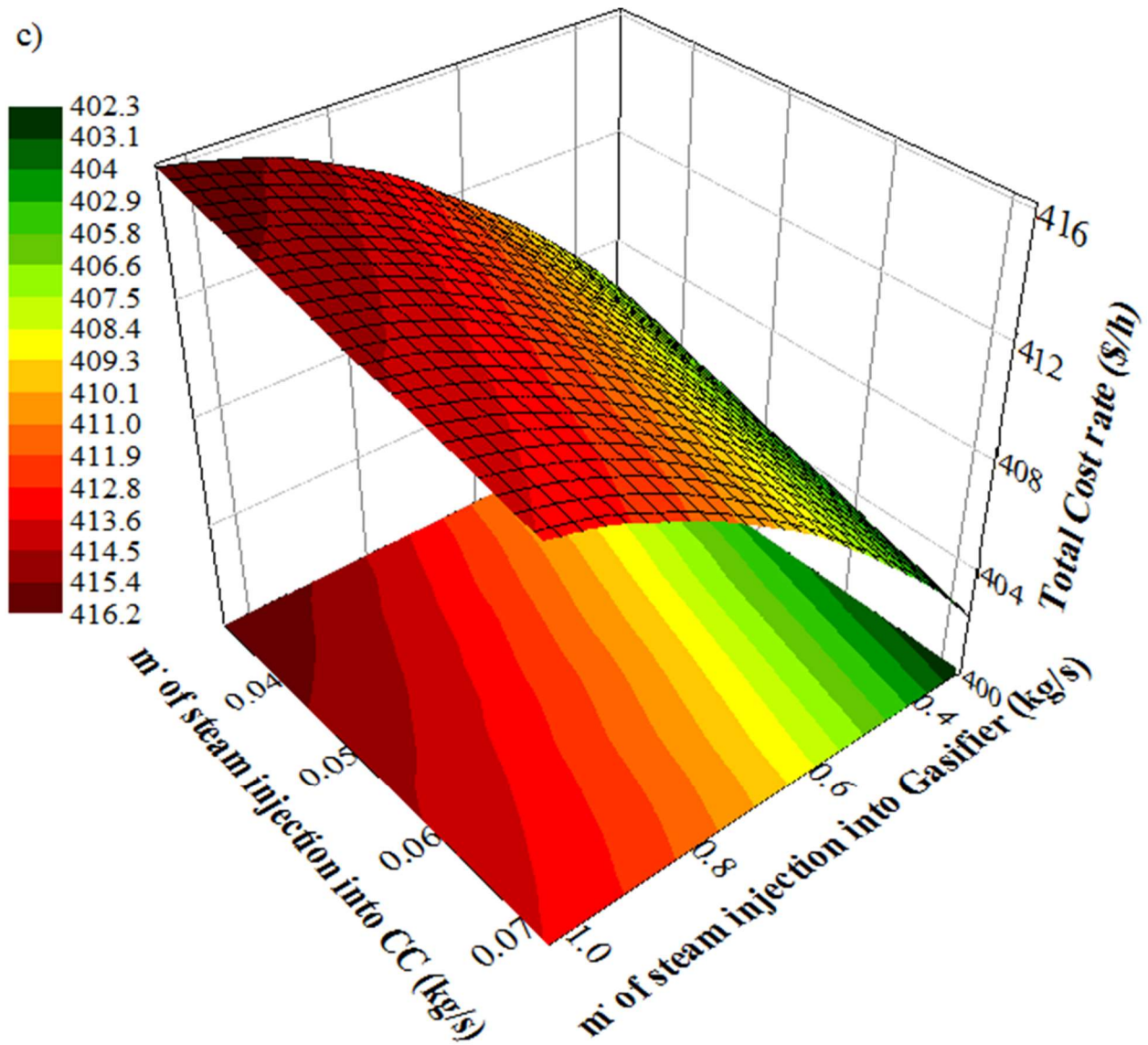
Fig. 16. Effect of varying mass flow rate of steam injection to combustion chamber and mass flow rate of steam injection to gasifier on: a) exergy efficiency, b) the CO_2 emission, and c) the total cost, for CHP cycle with the steam injection to the CC and gasifier.
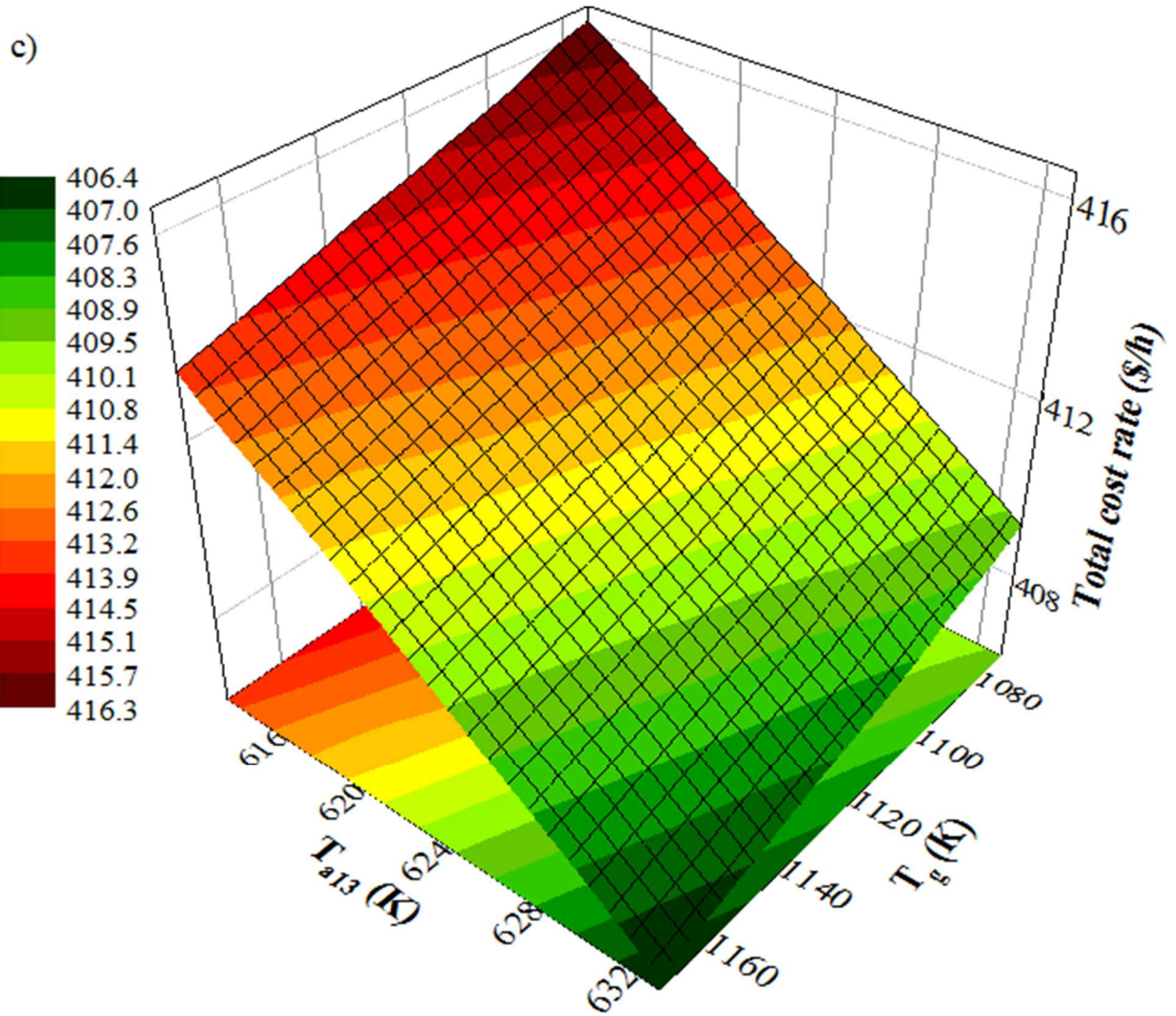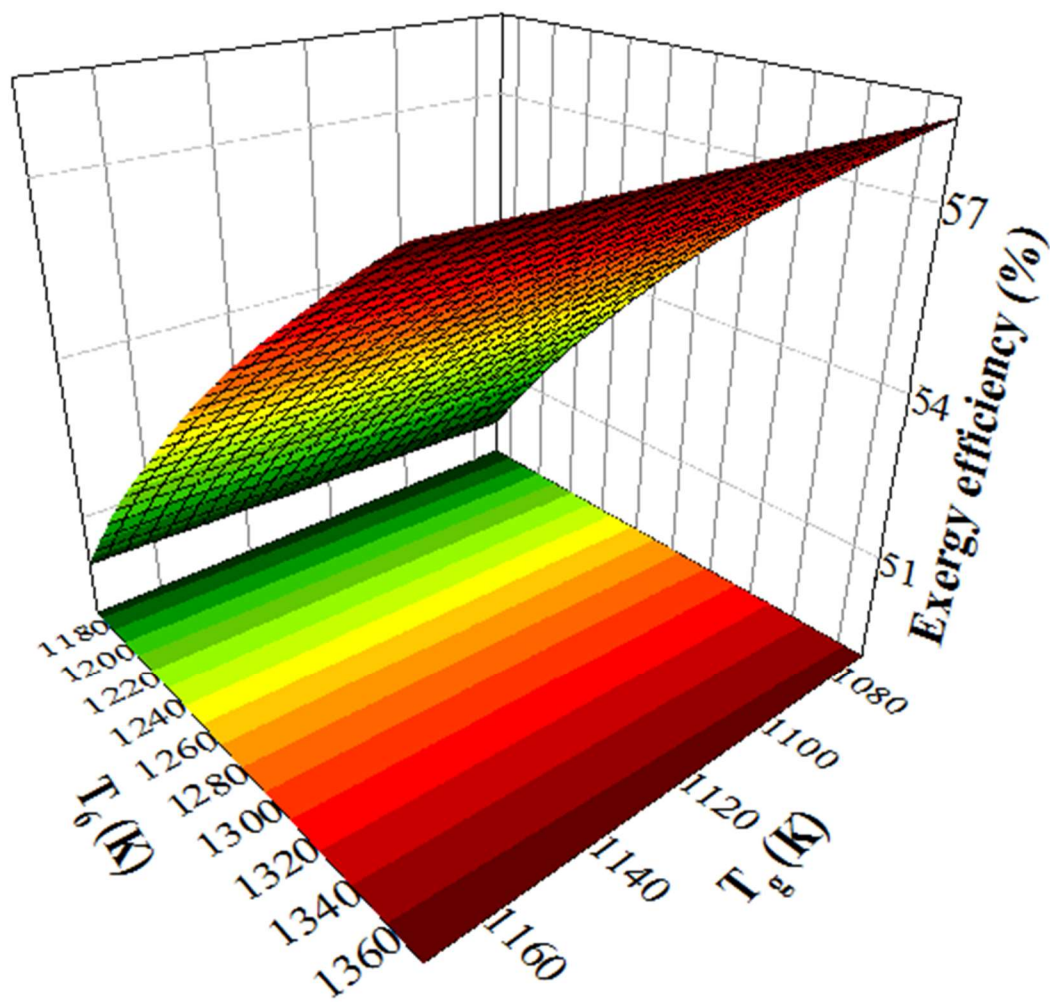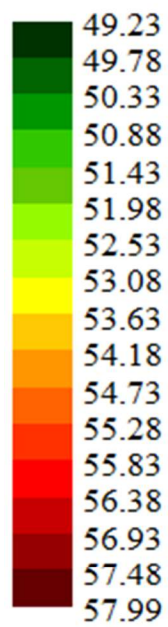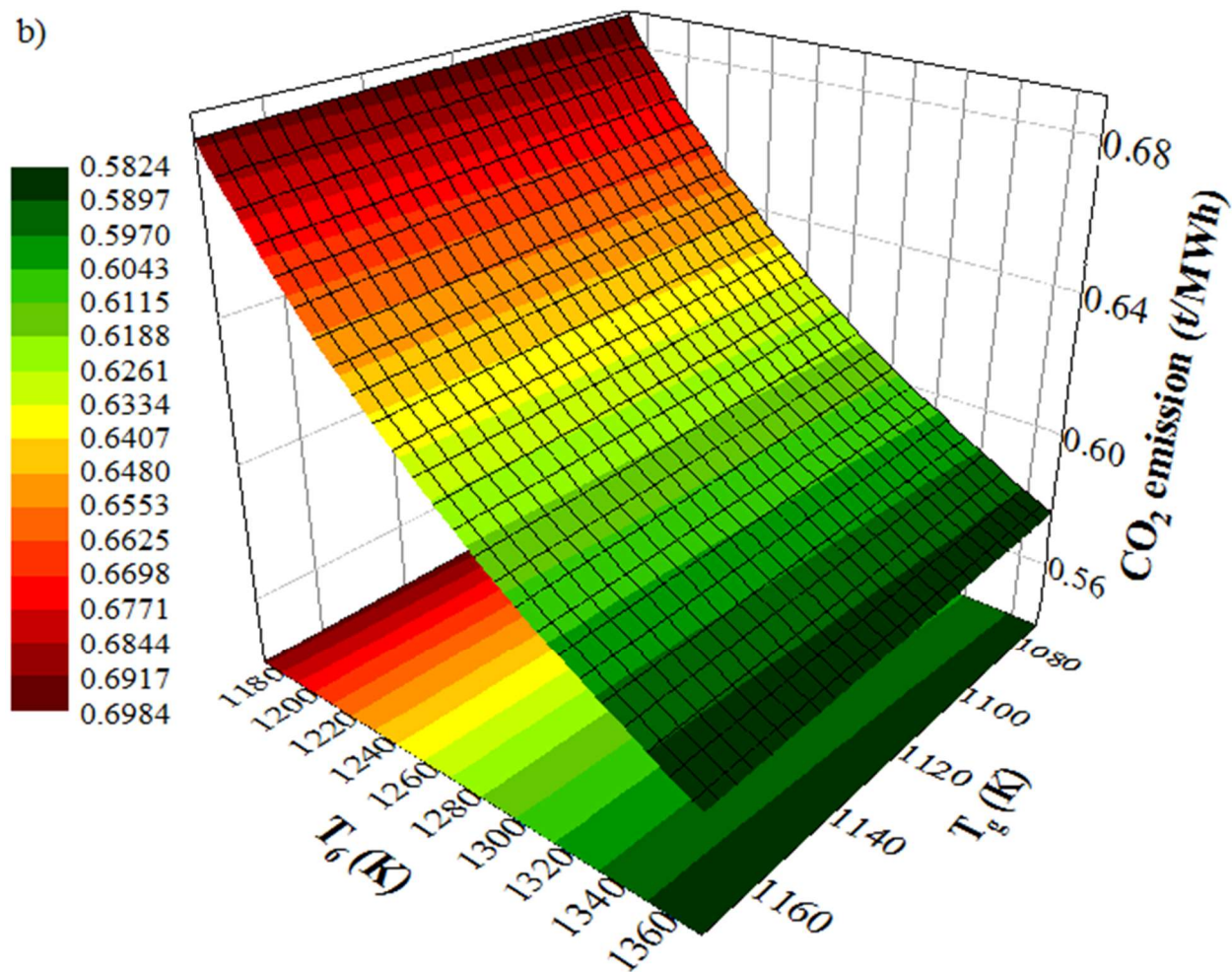
a)

b)

Fig. 17. Effect of varying biomass gasification temperature and the temperature of steam injection to gasifier and CC on: a) exergy efficiency, b) the CO_2 emission, and c) the total cost, for the CHP cycle with the steam injection to the CC and gasifier.
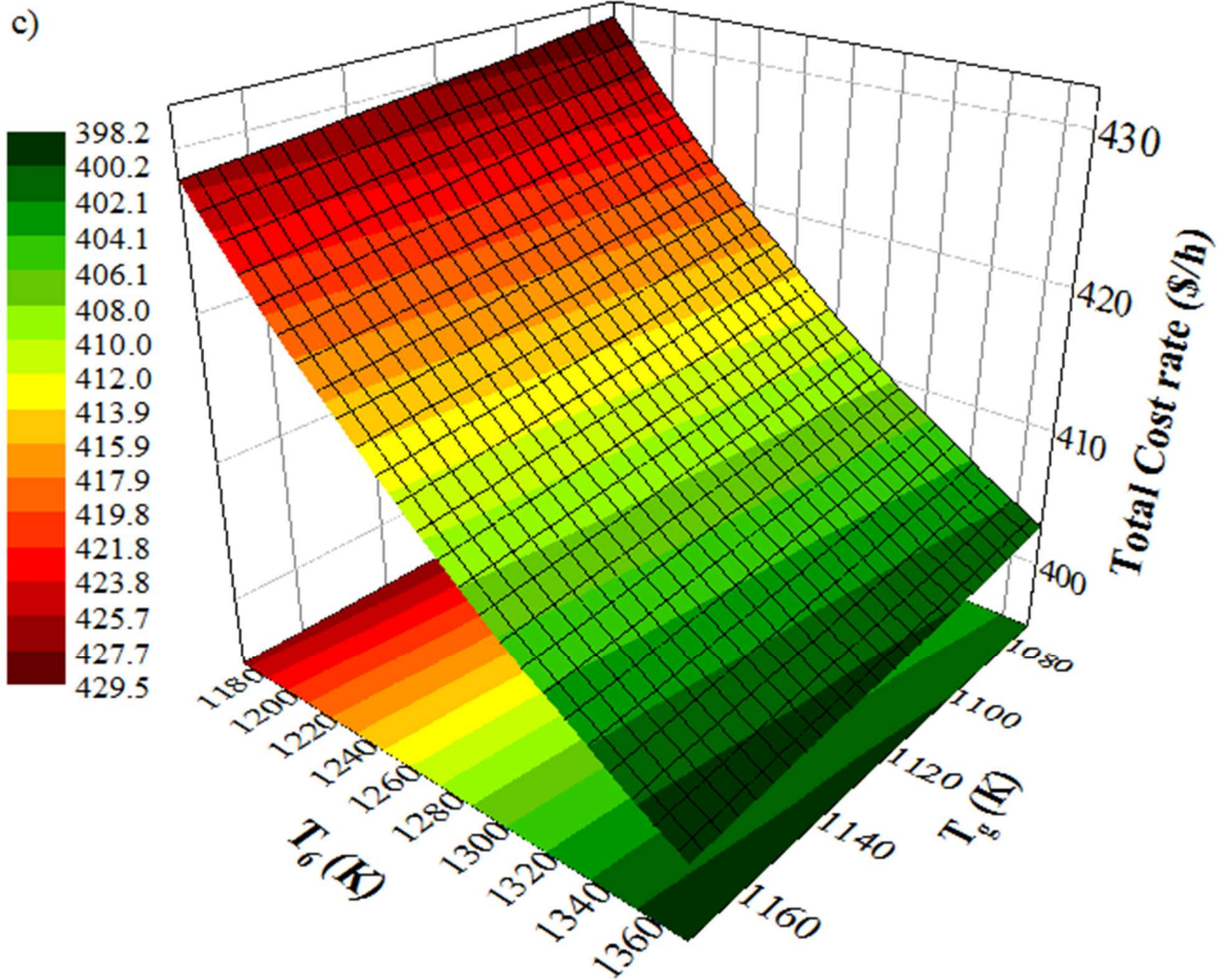
a)

b)

Fig. 18. Effect of varying biomass gasification temperature and inlet temperature to the gas turbine on: a) exergy efficiency, b) CO_2 emission, and c) total cost, for the CHP cycle with steam injection to the CC and gasifier.

7 Conclusion

Today, due to concerns regarding future scarcities of fossil fuels and climate change, the utilization of renewable sources in the power generation has gained lot attention. The biomass is a major source of renewable energy. Gasification of biomass is one of the methods for using biomass energy in power generation, and the resulting gas can be utilized in a Brayton power cycle. Alternatively, injecting steam into a Brayton cycle can improve its thermodynamic performance. This paper outlines a basic CHP cycle for power and cooling generation using biomass fuel gasification. Then, to improve the basic biomass-driven CHP cycle performance, several types of steam injection are proposed and investigated for the basic CHP cycle (steam injection to CC, steam injection to gasifier, steam injection into both of CC and gasifier). It is shown that injecting steam to the gasifier leads to a better performance than injecting steam to combustion chamber. For cycle with steam injection to the gasifier, an increase in investment cost of about 11.2% is observed compared to the basic CHP cycle, while the efficiency increases by 9.6%, CO_2 emissions decline by 8.8%, and costs of exergy destruction decline by 9.7%. Moreover, by simultaneously injecting steam to both the gasifier and the combustion chamber, the cycle efficiency increases by 11%, CO_2 emissions are decreased by 11.1%, and the total costs of cycle are increased by 3.4%. Therefore, here, the CHP cycle with a steam injection to combustion chamber and gasifier is chosen for further examination because of its better performance in the terms of thermodynamics, economics and environmental impact. Thermodynamic and exergo-economic analyses are checked out for the cycle. Then a parametric investigation is conducted using two-dimensional and three-dimensional diagrams to determine how the parameters interact with each other and how the parameters interact simultaneously on performance of the proposed CHP cycles.

The most important results of parametric study of the biomass-driven CHP cycle with the injected steam to the combustion chamber and gasifier follow:

- The Brayton cycle contributes 65% of total exergy destruction for fourth CHP cycle, followed by the steam turbine and absorption refrigeration cycles, at 31% and 4% respectively.

- When increasing T_g from 1073 to 1173 K, for input biomass moisture contents of 10%, 20%, and 30%, the cycle exergy efficiency increased from 48.56% to 48.84%, 54.29% to 54.58%, and 61.05% to 61.35%, respectively, and the CO_2 emission decreases from 0.6788 to 0.6745 t/MWh, 0.6287 to 0.625 t/MWh, and 0.5652 to 0.5621 t/MWh.

- As T_{a13} increases from 561 K to 581 K, the exergy efficiency in the second, third, and fourth CHP cycles is reduced by 2%, 2.4% and 2.5% the carbon dioxide emissions are increased by about 2.2%, 2.6% and 2.65% the investment costs are reduced by about 3%.

- Simultaneously increasing T_g and T_6, the cycle experiences an increase in exergy efficiency of about 17.8%, a reduction at carbon dioxide emission from 0.6984 t/MWh to 0.5824 t/MWh, and a decrease in costs of about 7.3%.

References

[1] Bilgen SE. Structure and environmental impact of global energy consumption. Renewable and Sustainable Energy Reviews, 2014;38:890-902.

[2] Basu P. Biomass gasification, pyrolysis, and torrefaction: practical design and theory. Academic Press; 2013.

[3] Anvari S, Desideri U, Taghavifar H. Design of a combined power, heating and cooling system at sized and undersized configurations for a reference building: Technoeconomic and topological considerations in Iran and Italy. Applied Energy, 2020;258:114105.

[4] Taghavifar H, Anvari S, Saray RK, Khalilarya S, Jafarmadar S, Taghavifar H. Towards modeling of combined cooling, heating and power system with artificial neural network for exergy destruction and exergy efficiency prognostication of tri-generation components. Applied Thermal Engineering, 2015;89:156-68.

[5] Wang T. (2016) The gas and steam turbines and combined cycle in IGCC systems. In: T Wang and G Stiegel (Eds), Integrated Gasification combined Cycle (IGCC) Technologies. Woodhead Publishing: 497- 640.

[6] Habibollahzade A, Ahmadi P, Rosen MA. Biomass gasification using various gasification agents: Optimum feedstock selection, detailed numerical analyses and tri-objective grey wolf optimization. Journal of Cleaner Production, 2021;284:124718.

[7] Fagbenle RL, Oguaka AB, Olakoyejo OT. A thermodynamic analysis of a biogas-fired integrated gasification steam injected gas turbine (BIG/STIG) plant. Applied Thermal Engineering, 2007;27(13):2220-5.

[8] Barreto D, Fajardo J, Caballero GC, Escorcia YC. Advanced exergy and exergoeconomic analysis of a gas power system with steam injection and air cooling with a compression refrigeration machine. Energy Technology, 2021;9(5):2000993.

[9] Shukla AK, Singh O. Performance evaluation of steam injected gas turbine based power plant with inlet evaporative cooling. Applied Thermal Engineering, 2016;102:454-64.

[10] Ziółkowski P, Kowalczyk T, Lemański M, Badur J. On energy, exergy, and environmental aspects of a combined gas-steam cycle for heat and power generation undergoing a process of retrofitting by steam injection. Energy Conversion and Management, 2019;192:374-84.

[11] Moradi R, Marcantonio V, Cioccolanti L, Bocci E. Integrating biomass gasification with a steam-injected micro gas turbine and an Organic Rankine Cycle unit for combined heat and power production. Energy Conversion and Management, 2020;205:112464.

[12] Kayadelen HK, Ust Y. Thermoenvironomic evaluation of simple, intercooled, STIG, and ISTIG cycles. International Journal of Energy Research, 2018;42(12):3780-802.

[13] Renzi M, Patuzzi F, Baratieri M. Syngas feed of micro gas turbines with steam injection: Effects on performance, combustion and pollutants formation. Applied Energy, 2017;206:697-707.

[14] Camporeale SM, Pantaleo AM, Ciliberti PD, Fortunato B. Cycle configuration analysis and techno-economic sensitivity of biomass externally fired gas turbine with bottoming ORC. Energy conversion and management, 2015;105:1239-50.

[15] Pio DT, Gomes HG, Tarelho LA, Vilas-Boas AC, Matos MA, Lemos FM. Superheated steam injection as primary measure to improve producer gas quality from biomass air gasification in an autothermal pilot-scale gasifier. Renewable Energy, 2022;181:1223-36.

[16] Reale F, Sannino R. Water and steam injection in micro gas turbine supplied by hydrogen enriched fuels: Numerical investigation and performance analysis. International Journal of Hydrogen Energy, 2021;46(47):24366-24381.

[17] Xiao G, Chen J, Ni M, Cen K. A solar micro gas turbine system combined with steam injection and ORC bottoming cycle. Energy Conversion and Management, 2021;243:114032.

[18] Karaali R, Öztürk IT. (2015), Thermoeconomic analyses of steam injected gas turbine cogeneration cycles. In: I Akkurt (Ed), Special issue of the International Conference on Computational and Experimental Science and Engineering (ICCESEN 2014). Acta Physica Polonica A; 128: B-279- B-281.

[19] Athari H, Soltani S, Rosen MA, Mahmoudi SM, Morosuk T. Gas turbine steam injection and combined power cycles using fog inlet cooling and biomass fuel: A thermodynamic assessment. Renewable Energy, 2016;92:95-103.

[20] Anvari S, Khalilarya S, Zare V. Exergoeconomic and environmental analysis of a novel configuration of solar-biomass hybrid power generation system. Energy, 2018;165:776-89.

[21] Anvari S, Taghavifar H, Parvishi A. Thermo-economical consideration of Regenerative organic Rankine cycle coupling with the absorption chiller systems incorporated in the trigeneration system. Energy Conversion and Management, 2017;148:317-29.

[22] Anvari S, Saray RK, Bahlouli K. Conventional and advanced exergetic and exergoeconomic analyses applied to a tri-generation cycle for heat, cold and power production, Energy 2015;91:925-39.

[23] Gholamian E, Mahmoudi SM, Zare V. Proposal, exergy analysis and optimization of a new biomass-based cogeneration system. Applied Thermal Engineering, 2016;93:223-35.

[24] Hosseini M, Dincer I, Rosen MA. Steam and air fed biomass gasification: comparisons based on energy and exergy. International Journal of Hydrogen Energy, 2012;37(21):16446-52.

[25] Anvari S, Khalilarya S, Zare V. Power generation enhancement in a biomass-based combined cycle using solar energy: Thermodynamic and environmental analysis. Applied Thermal Engineering, 2019;153:128-41.

[26] Sanaye S, Amani M, Amani P. 4E modeling and multi-criteria optimization of CCHPW gas turbine plant with inlet air cooling and steam injection. Sustainable Energy Technologies and Assessments, 2018;29:70-81.

[27] Zainal ZA, Ali R, Lean CH, Seetharamu KN. Prediction of performance of a downdraft gasifier using equilibrium modeling for different biomass materials. Energy Conversion and Management, 2001;42(12):1499-515.

[28] Bejan A, Tsatsaronis G, Moran M. Thermal design and optimization. New York: John Wiley; 1996.

[29] Hassan R, Barua H, Das BK. Energy, exergy, exergo-environmental, and exergetic sustainability analyses of a gas engine-based CHP system. Energy Science & Engineering, 2021;9(12):2232-51.

[30] Zare V. Performance improvement of biomass-fueled closed cycle gas turbine via compressor inlet cooling using absorption refrigeration; thermoeconomic analysis and multi-objective optimization. Energy Conversion and Management, 2020;215:112946.

[31] Anvari S, Mahian O, Solomin E, Wongwises S, Desideri U. Multi-objective optimization of a proposed multi-generation cycle based on Pareto diagrams: Performance improvement, cost reduction, and CO_2 emissions. Sustainable Energy Technologies and Assessments, 2021; 45: 101197.

[32] Anvari S, Saray RK, Bahlouli K. Employing a new optimization strategy based on advanced exergy concept for improvement of a tri-generation system. Applied Thermal Engineering, 2017; 113:1452-63.

[33] Spring CR, Cirella GT. (2022) Fostering Sustainable Development: Green Energy Policy in the European Union and the United States. In: GT Cirella (Eds) Human Settlements. Advances in 21st Century Human Settlements. Springer; 101- 137.

Appendix A. Equations for energy rate balance for each component of the first biomass-driven CHP cycle

- Air compressor (AC):

$$\dot{E}_{D,AC} = \dot{E}_1 + \dot{W}_{AC} - \dot{E}_2 \qquad (A.1)$$

- Gasifier:

$$\dot{E}_{D,gasifier} = \dot{E}_4 - \dot{E}_5 + \dot{E}_3 \qquad (A.2)$$

- Combustion chamber (CC):

$$\dot{E}_{D,CC} = \dot{E}_5 + \dot{E}_2 - \dot{E}_6 \qquad (A.3)$$

- Gas turbine (GT):

$$\dot{E}_{D,GT} = \dot{E}_6 - \dot{W}_{GT} - \dot{E}_7 \qquad (A.4)$$

- Heat recovery steam generator 1 (HRSG1):

$$\dot{E}_{D,HRSG1} = \dot{E}_7 - \dot{E}_{a13} + \dot{E}_{a12} - \dot{E}_8 \qquad (A.5)$$

- Heat recovery steam generator 2 (HRSG2):

$$\dot{E}_{D,HRSG2} = \dot{E}_8 - \dot{E}_{a17} + \dot{E}_{a16} - \dot{E}_9 \qquad (A.6)$$

- High pressure steam turbine (HPST):

$$\dot{E}_{D,HPST} = \dot{E}_{a13} - \dot{W}_{HPST} - \dot{E}_{a16} - \dot{E}_{a14} - \dot{E}_{a15} \qquad (A.7)$$

- Low pressure steam turbine (LPST):

$$\dot{E}_{D,LPST} = \dot{E}_{a17} - \dot{E}_{a18} - \dot{E}_{a19} - \dot{W}_{LPST} \qquad (A.8)$$

- Condenser (Con_ST):

$$\dot{E}_{D,Con\_ST} = \dot{E}_{a19} + \dot{E}_{a20} - \dot{E}_{a1} - \dot{E}_{a21} \qquad (A.9)$$

- Open feed water heater (OFW):

$$\dot{E}_{D,OFW} = \dot{E}_{a2} + \dot{E}_{a18} - \dot{E}_{a3} \qquad\qquad (A.10)$$

- Close feed water 1 heater (CFW1):

$$\dot{E}_{D,CFW1} = \dot{E}_{a8} - \dot{E}_{a11} + \dot{E}_{a14} - \dot{E}_{a9} \qquad\qquad (A.11)$$

- Close feed water heater 2 (CFW2):

$$\dot{E}_{D,CFW2} = \dot{E}_{a4} - \dot{E}_{a7} + \dot{E}_{a15} - \dot{E}_{a5} \qquad\qquad (A.12)$$

- Pump 1 (PI):

$$\dot{E}_{D,PI} = \dot{E}_{a1} - \dot{E}_{a2} + \dot{W}_{PI} \qquad\qquad (A.13)$$

- Pump 2 (PII):

$$\dot{E}_{D,PII} = \dot{E}_{a3} - \dot{E}_{a4} + \dot{W}_{PII} \qquad\qquad (A.14)$$

- Pump 3 (PIII):

$$\dot{E}_{D,PIII} = \dot{E}_{a5} - \dot{E}_{a6} + \dot{W}_{PIII} \qquad\qquad (A.15)$$

- Pump 4 (P4):

$$\dot{E}_{D,P4} = \dot{E}_{a9} - \dot{E}_{a10} + \dot{W}_{P4} \qquad\qquad (A.16)$$

- Generator (Gen):

$$\dot{E}_{D,Gen} = \dot{E}_{13} - \dot{E}_{14} + \dot{E}_{9} - \dot{E}_{17} \qquad\qquad (A.17)$$

- Condenser (Con_ABS):

$$\dot{E}_{D,Con\_ABS} = -\dot{E}_{26} - \dot{E}_{18} + \dot{E}_{17} + \dot{E}_{25} \qquad\qquad (A.18)$$

- Evaporator (Eva):

$$\dot{E}_{D,Eva} = -\dot{E}_{20} - \dot{E}_{28} + \dot{E}_{19} + \dot{E}_{27} \qquad\qquad (A.19)$$

- Absorber (Abs):

$$\dot{E}_{D,ABS} = -\dot{E}_{11} + \dot{E}_{23} + \dot{E}_{20} - \dot{E}_{24} + \dot{E}_{16} \tag{A.20}$$

- Heat exchanger (SEX):

$$\dot{E}_{D,SHE} = \dot{E}_{14} + \dot{E}_{15} - \dot{E}_{13} + \dot{E}_{12} \tag{A.21}$$

Appendix B. Equations for exergoconomic rate balance for the each component of the first biomass-driven CHP cycle

- Air compressor (AC):

$$\dot{C}_2 - \dot{Z}_{AC} - \dot{C}_1 - \dot{C}_{d0} = 0 \ , \ \dot{C}_1 = 0 \tag{B.1}$$

- Gasifier:

$$\dot{C}_3 - \dot{C}_5 + \dot{Z}_{Gasifier} + \dot{C}_4 = 0 \ , \ \dot{C}_4 = 0 \tag{B.2}$$

- Combustion chamber (CC):

$$\dot{C}_2 + \dot{C}_5 + \dot{Z}_{CC} = \dot{C}_6 \tag{B.3}$$

- Gas turbine (GT):

$$\dot{C}_7 + \dot{C}_{24} - \dot{C}_6 + \dot{C}_{d0} - \dot{Z}_{GT} = 0 \ , \ \left(\dot{C}_6/\dot{E}_6\right) = \left(\dot{C}_7/\dot{E}_7\right), \ \left(\dot{C}_{d0}/\dot{W}_{AC}\right) = \left(\dot{C}_{d1}/\dot{W}_{GT}\right) \tag{B.4}$$

- Heat recovery steam generator 1 (HRSG1):

$$\dot{C}_7 + \dot{C}_{a12} + \dot{Z}_{HRSG} - \dot{C}_8 = \dot{C}_{a13} \ , \ \left(\dot{C}_7/\dot{E}_7\right) = \left(\dot{C}_8/\dot{E}_8\right) \tag{B.5}$$

- Heat recovery steam generator 2 (HRSG2):

$$\dot{C}_{a16} + \dot{Z}_{HRSG2} + \dot{C}_8 - \dot{C}_{a17} - \dot{C}_9 - \dot{C}_{Gen} = 0 \ , \ \left(\dot{C}_9/\dot{E}_9\right) = \left(\dot{C}_8/\dot{E}_8\right) \tag{B.6}$$

- High pressure steam turbine (HPST):

$$\dot{C}_{a13} + \dot{Z}_{HPST} = \dot{C}_{a16} + \dot{C}_{a15} + \dot{C}_{a14} + \dot{C}_{d2}$$, (B.7)

$$\left(\dot{C}_{a13}/\dot{E}_{a13}\right) = \left(\dot{C}_{a14}/\dot{E}_{a14}\right) = \left(\dot{C}_{a15}/\dot{E}_{a15}\right) = \left(\dot{C}_{a16}/\dot{E}_{a16}\right)$$

- Low pressure steam turbine (LPST):

$$\dot{Z}_{LPST} - \dot{C}_{a19} + \dot{C}_{a17} = \dot{C}_{a18} + \dot{C}_{d3}, \ \left(\dot{C}_{a17}/\dot{E}_{a17}\right) = \left(\dot{C}_{a18}/\dot{E}_{a18}\right) = \left(\dot{C}_{a19}/\dot{E}_{a19}\right)$$ (B.8)

- Condenser (Con_ST):

$$\dot{C}_{a19} + \dot{C}_{a20} + \dot{Z}_{Con\_ST} = \dot{C}_{a1} + \dot{C}_{a21}, \ \dot{C}_{a20} = 0$$ (B.9)

- Open feed water heater (OFW):

$$\dot{C}_{a18} + \dot{C}_{a2} + \dot{Z}_{OFW} = \dot{C}_{a3}$$ (B.10)

- Close feed water heater 1 (CFW1):

$$\dot{C}_{a14} + \dot{C}_{a8} + \dot{Z}_{CFW1} = \dot{C}_{a9} + \dot{C}_{a11}, \ \left(\dot{C}_{a14}/\dot{E}_{a14}\right) = \left(\dot{C}_{a9}/\dot{E}_{a9}\right)$$ (B.11)

- Close feed water heater 2 (CFW2):

$$\dot{C}_{a4} + \dot{C}_{a15} + \dot{Z}_{CFW2} = \dot{C}_{a5} + \dot{C}_{a7}, \ \left(\dot{C}_{a15}/\dot{E}_{a15}\right) = \left(\dot{C}_{a5}/\dot{E}_{a5}\right)$$ (B.12)

- Pump 1 (PI):

$$\dot{C}_{a1} + \dot{C}_{d4} + \dot{Z}_{PI} = \dot{C}_{a2}, \ \left(\dot{C}_{d4}/\dot{W}_{PI}\right) = \left(\dot{C}_{d3}/\dot{W}_{LPST}\right)$$ (B.13)

- Pump 2 (PII):

$$\dot{C}_{a3} + \dot{C}_{d5} + \dot{Z}_{PII} = \dot{C}_{a4}, \ \left(\dot{C}_{d5}/\dot{W}_{PII}\right) = \left(\dot{C}_{d2}/\dot{W}_{HPST}\right)$$ (B.14)

- Pump 3 (PIII):

$$\dot{C}_{a5} + \dot{C}_{d6} + \dot{Z}_{PIII} = \dot{C}_{a6}, \ \left(\dot{C}_{d5}/\dot{W}_{PII}\right) = \left(\dot{C}_{d6}/\dot{W}_{PIII}\right)$$ (B.15)

- Pump 4 (P4):

$$\dot{C}_{a9} + \dot{C}_{d7} + \dot{Z}_{P4} = \dot{C}_{a10}, \left(\dot{C}_{d4} / \dot{W}_{PI} \right) = \left(\dot{C}_{d7} / \dot{W}_{P4} \right) \tag{B.16}$$

- Generator (Gen):

$$\dot{C}_{13} + \dot{C}_{Gen} - \dot{C}_{17} + +\dot{Z}_{Gen} - \dot{C}_{14} = 0, \quad \frac{\dot{C}_{14} - \dot{C}_{13} \times \left(\dfrac{\dot{m}_{14}}{\dot{m}_{13}} \right)}{\dot{E}_{14} - \dot{E}_{13} \times \left(\dfrac{\dot{m}_{14}}{\dot{m}_{13}} \right)} - \frac{\dot{C}_{17} - \dot{C}_{13} \times \left(\dfrac{\dot{m}_{17}}{\dot{m}_{13}} \right)}{\dot{E}_{17} - \dot{E}_{13} \times \left(\dfrac{\dot{m}_{17}}{\dot{m}_{13}} \right)} = 0 \tag{B.17}$$

- Condenser (Con_ABS):

$$\dot{C}_{17} + \dot{C}_{Con\_ABS} - \dot{C}_{18} + \dot{Z}_{Con\_ABS} = 0, \left(\dot{C}_{18} / \dot{E}_{18} \right) = \left(\dot{C}_{17} / \dot{E}_{17} \right) \tag{B.18}$$

- Evaporator (Eva):

$$\dot{C}_{19} - \dot{C}_{Eva} + \dot{Z}_{Eva} = \dot{C}_{20}, \left(\dot{C}_{20} / \dot{E}_{20} \right) = \left(\dot{C}_{19} / \dot{E}_{19} \right) \tag{B.19}$$

- Absorber (Abs):

$$\dot{C}_{20} - \dot{C}_{Abs} + \dot{C}_{16} - \dot{C}_{11} + \dot{Z}_{Abs} = 0, \left(\left(\dot{C}_{20} + \dot{C}_{16} \right) / \left(\dot{E}_{16} + \dot{E}_{20} \right) \right) = \left(\dot{C}_{11} / \dot{E}_{11} \right) \tag{B.20}$$

- Heat exchanger (SEX):

$$\dot{C}_{12} - \dot{C}_{15} + \dot{Z}_{SHX} + \dot{C}_{14} - \dot{C}_{13} = 0, \left(\dot{C}_{15} / \dot{E}_{15} \right) = \left(\dot{C}_{14} / \dot{E}_{14} \right) \tag{B.21}$$